NBSIR 80-1999

Models for the Migration of Additives in Polyolefins

L. E. Smith, S. S. Chang, F. L. McCrackin,
I. C. Sanchez and G. A. Senich

Polymer Science and Standards Division
Center for Materials Science
National Bureau of Standards
U.S. Department of Commerce
Washington, D.C. 20234

Annual Report for the Period
October 1, 1978 - September 30, 1979

Issued February 1980

Prepared for

of Foods
nd Drug Administration
gton, D.C. 20201

NBSIR 80-1999

MODELS FOR THE MIGRATION OF ADDITIVES IN POLYOLEFINS

L. E. Smith, S. S. Chang, F. L. McCrackin,
I. C. Sanchez and G. A. Senich

Polymer Science and Standards Division
Center for Materials Science
National Bureau of Standards
U.S. Department of Commerce
Washington, D.C. 20234

Annual Report for the Period
October 1, 1978 - September 30, 1979

Issued February 1980

Prepared for
Bureau of Foods
Food and Drug Administration
Washington, D.C. 20201

U.S. DEPARTMENT OF COMMERCE, Philip M. Klutznick, *Secretary*

Luther H. Hodges, Jr., *Deputy Secretary*
Jordan J. Baruch, *Assistant Secretary for Productivity, Technology, and Innovation*

NATIONAL BUREAU OF STANDARDS, Ernest Ambler, *Director*

TABLE OF CONTENTS

Migration Decision Tree

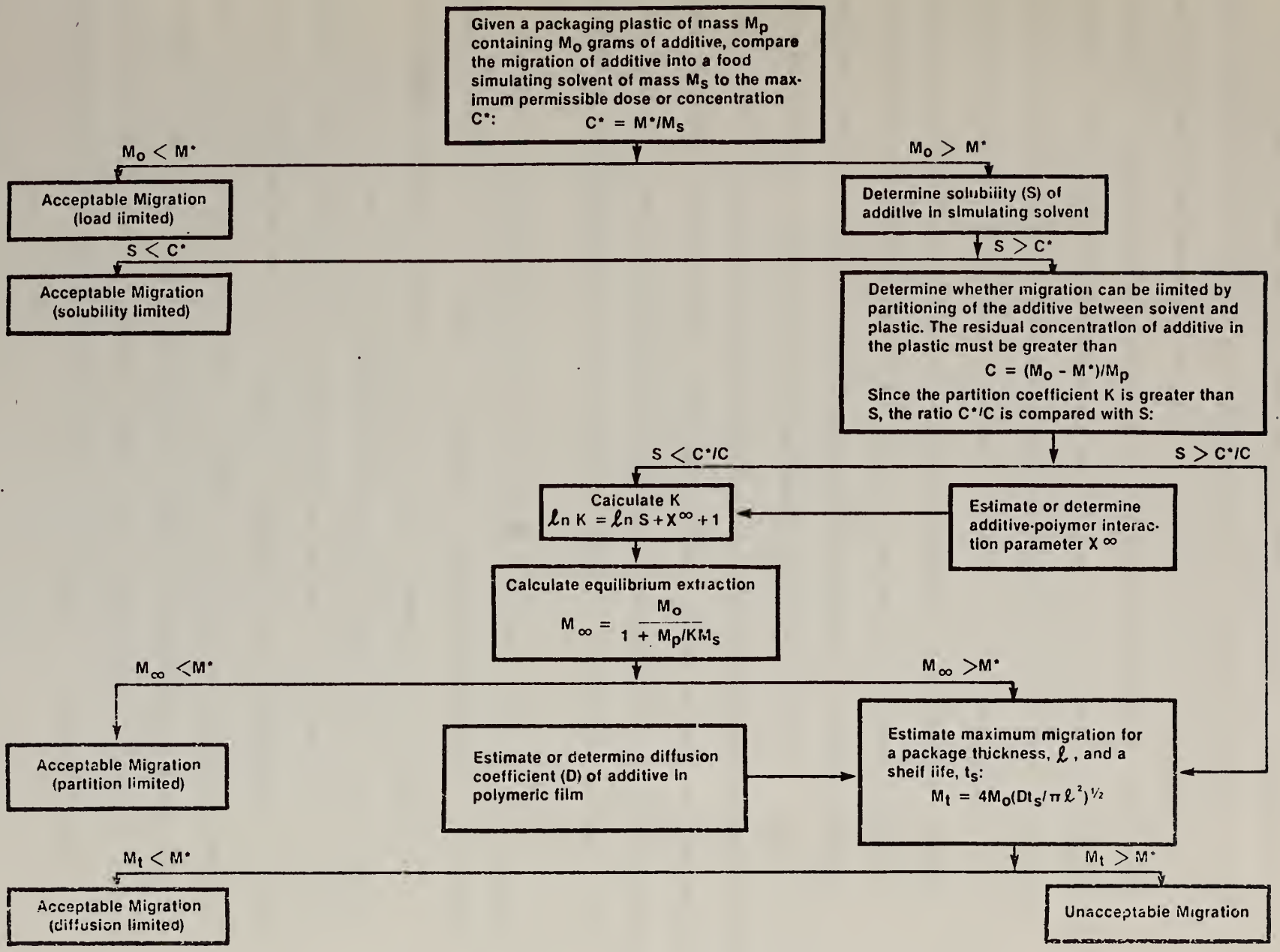

Introduction

The Bureau of Foods of The Food and Drug Administration has regulatory responsibility for the use of packaging materials in contact with food. Their regulatory decisions demand an estimate of the amount of material that can reasonably be expected to migrate from the package into the food. Worst-case estimates are generally needed and may be obtained from analysis of packaged food, laboratory migration data, extrapolation from closely related data, or by calculation using some theoretical framework. Clearly, direct analysis or laboratory migration measurements are less efficient and therefore less desirable than extrapolation or estimation methods. This program at the National Bureau of Standards aims to provide technical suggestions and data to the Food and Drug Administration that can be useful in increasing the applicability of more efficient estimation and extrapolation methods to this challenging regulatory problem. This report, however, represents only technical opinions of the authors as representatives of the National Bureau of Standards and should not be taken in any way as regulatory decisions or recommendations of the Bureau of Foods, the principal sponsor of this work.

In order to organize the specific technical questions involved in regulating packaging materials, it is useful to consider a formal decision tree. A general, but incomplete example of such a decision tree is shown on the facing page.

In this chart and in all acompanying discussion several facts are presumed as given, either because they can reasonably be assumed to be generally available or because their determination is beyond the scope of our considerations. Specifically, the basic geometry and size of package is assumed to be known as well as the range of food stuffs to be contained. Further, an appropriate simulating solvent or solvents are to have been chosen. The comparison of simulating solvent extraction with that found in actual food is the subject of current work by the

Arthur D. Little Corp., under contract to the Bureau of Foods. Worst-case limits of shelf life and use temperatures for the package are also needed in some cases. Finally, to simplify the discussion we assume that a critical amount or concentration of additive exists. This critical value must be based on toxicological considerations and might represent points between different tiers of required testing or an action level that determines an allowed or a disallowed application.

There are four general phenomena that can limit the amount of an additive that will migrate into a food, or a food simulating solvent. First, migration is obviously limited to the total amount of additive present in the packaging material. This is called load limited migration. Secondly, migration may be limited by insufficient solubility of the additive in the simulating solvent. Third, the additive partitions between the polymer and solvent phases. Finally, the total additive migration may be limited by the diffusion of the additive during the estimated shelf life. The limiting transport rate may occur in diffusion through the polymer or, in some cases, in diffusion through the solvent phase. A more detailed description of these possible diffusion processes is given in the following section. Other sections of this annual report present some estimation methods as well as experimental results on laboratory measurements of migration in polyethylene.

I. Migration Models

A large number of mathematical models of diffusion have been derived to cover conditions having various boundary conditions or simplifying relationships among some of the pertinent variables. Although many of these equations are available in the literature, it is valuable to derive a relatively complete set here using consistent arguments and notation. The following sections organize and collect such equations and derive some new experessions for a few special cases.

Boundary Layer Limited Migration

In migration experiments with solvent agitation, diffusion of the additive in the polymer is usually rate determining. This is not the only possibility. For example, if the solubility of the additive in the food simulating solvent is limited, diffusion through a relatively stagnant boundary layer of solvent may become rate determining. The concentration profile for strong boundary layer limited diffusion is schematically shown below:

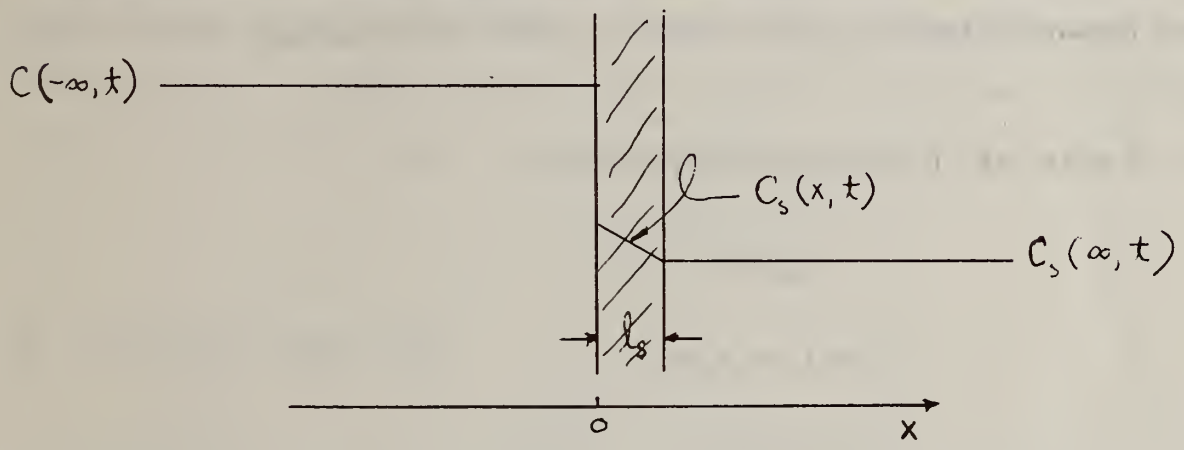

ℓ_s is the thickness of the stagnant solvent layer (ℓ_s is determined by the degree of solvent agitation), C_s is the additive concentration in the solvent phase and C is the additive concentration in the polymer sheet.

At the boundary between polymer and solvent, we assume equilibrium; i.e.,

$$C_s(0,t) = KC(0,t) \qquad (1)^*$$

where K is the partition coefficient.

A necessary but not sufficient condition for the above concentration profile to prevail is for the difference in additive concentration between polymer and solvent, $C - C_s(\infty,t)$, to be very large compared to the concentration difference across the boundary layer $KC - C_s(\infty,t)$. Thus, this condition prevails when $K \ll 1$ and we can approximate the concentration gradient across the boundary as a linear gradient (a quasi-stationary approximation):

---

*All numbers for equations, figures, references and tables are local reference numbers for each section of the report.

$$\frac{\partial C_s}{\partial x} = \left[KC(t) - C_s(\infty,t)\right] / \ell_s \qquad (2)$$

By Fick's first law (flux is proportional to the concentration gradient), the rate at which additive migrates to the solvent is given by

$$\frac{dM_t}{dt} = \frac{2AD_s}{\ell_s}\left[KC - C_s(\infty,t)\right] \qquad (3)$$

where D_s is the diffusion coefficient of the additive in the solvent boundary layer and A is the cross-sectional area of the polymer sheet. The factor of 2 appears because diffusion occurs from both sides of the polymer sheet of thickness ℓ.

We now make use of the following relations:

$$C = (M_o - M_t)/V_p$$

$$C_s(\infty,t) = M_t/V_s$$

$$\alpha = (V_s/V_p)K$$

$$M_\infty/M_o = \frac{\alpha}{1+\alpha}$$

where V_s and V_p are the volumes of solvent and polymer, respectively, M_o is the amount of additive in the polymer at t=0 and M_∞ is the equilibrium amount of additive extracted as $t\to\infty$. Now Eq. (3) can be rewritten as

$$\frac{d(M_t/M_\infty)}{dt} = \frac{2D_sK}{\ell\ell_s}\left(\frac{M_o}{M_\infty}\right)\left[1 - M_t/M_\infty\right] \qquad (4)$$

which has the solution

$$\boxed{M_t/M_\infty = 1 - e^{-st}} \qquad (5)$$

$$s = \frac{2D_sK}{\ell\ell_s}\left(\frac{M_o}{M_\infty}\right) \qquad (6)$$

At short times where $st \ll 1$, we have to a good approximation

$$M_t/M_\infty = st$$

or

$$M_t/M_o = \left(\frac{2D_s K}{\ell \ell_s}\right) t \qquad (7)$$

That is, M_t is initially linear in time.

A good procedure for determining s in Eq. (5) is to plot ln $(1-M_t/M_\infty)$ against t. The slope of this plot is equal to -s. In Fig. 1, migration data of $n\text{-}C_{18}H_{38}$ from linear polyethylene (LPE) into a 50/50 ethanol/water mixture at 60°C (E50B60L) are plotted in this manner. Data for M_t/M_∞ values greater than 0.9 were omitted from the plot because small errors in M_t/M_∞ in this range yield large errors in calculated s values. From the slope, we obtain

$$s = 2 \times 10^{-4} \text{ sec}^{-1}$$

For this system we know that

$$K \simeq 10^{-3}$$

$$\ell = 0.07 \text{ cm}$$

$$M_\infty/M_o = 0.18$$

$$D_s = 9 \times 10^{-6} \text{ cm}^2/\text{sec}$$

and thus we find from Eq. (6) that

$$\ell_s = .007 \text{ cm or } 70 \text{ microns}$$

The diffusion coefficient D_s of n-octadecane in the 50/50 ethanol/water mixture was estimaced from the Wilke-Chang correlation[1].

The idea of diffusion through a relatively stagnant boundary layer is not novel. For example, similar ideas have been invoked in theories of dissolution rates of crystals[2a] and electrode overvoltage[2b]. Estimates of the thickness of

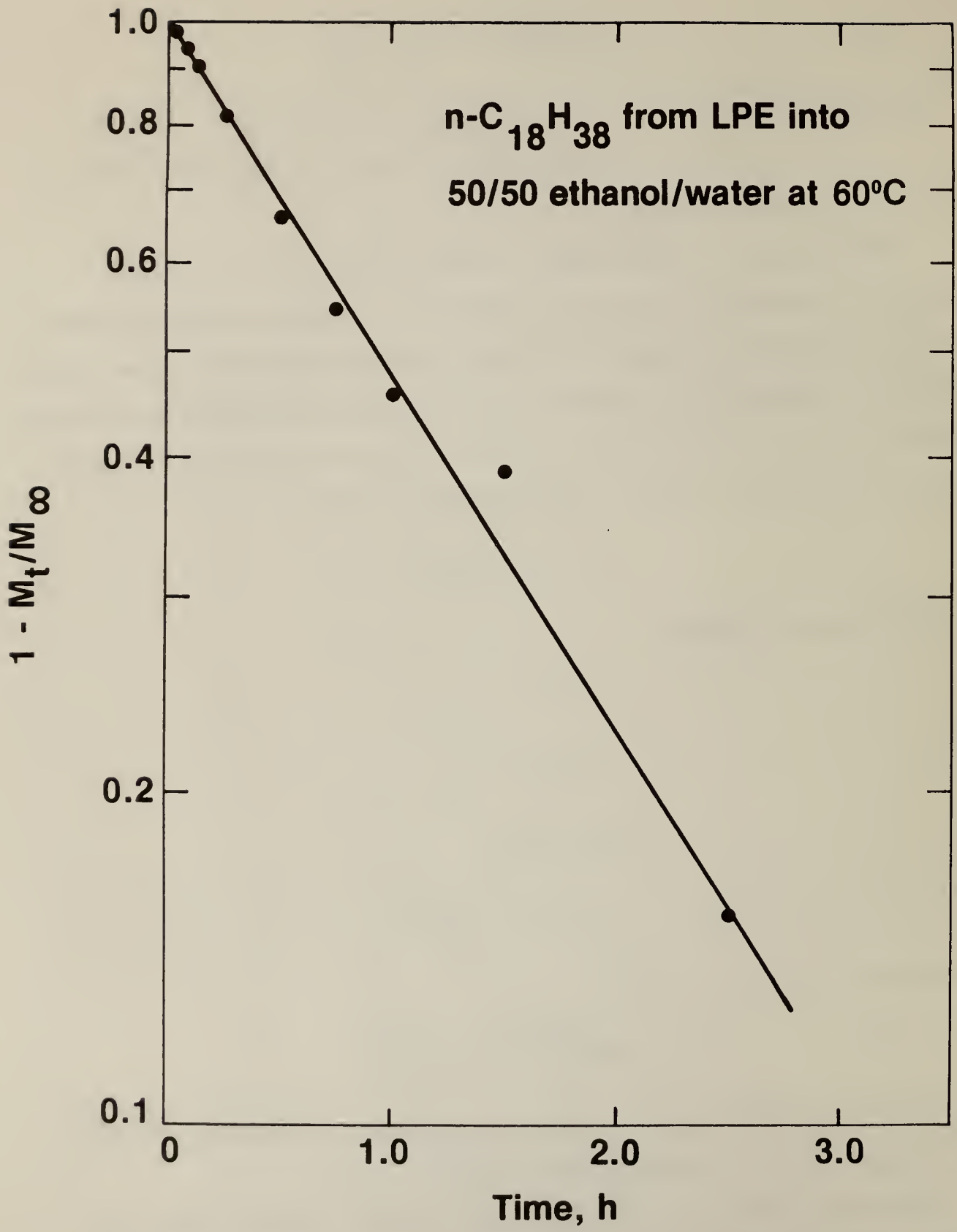
1.0
0.8
0.6
0.4
0.2
0.1
0
1.0
2.0
3.0
Time, h
1 - M_t/M_∞
n-$C_{18}H_{38}$ from LPE into
50/50 ethanol/water at 60°C

Fig. I-1

the boundary layer for turbulent flow typically are in the 10 micron range[2b].

To illustrate that Eq. (5) cannot describe migration when diffusion in the polymer is rate determining, a plot of $\ln(1-M_t/M_\infty)$ against t for the migration of radiolabeled $C_{18}H_{38}$ from LPE into non-labeled $C_{18}H_{38}$ used as a solvent (OE30) is shown in Fig. 2. Notice the strong deviation from linearity for these data.

Quiescent Migration

We now address the situation where diffusion through the solvent phase is rate determining. This type of migration will be important in an unstirred solvent or when the food stuff is a solid or viscous liquid.

Consider an ideal system of an infinitely thick polymer in contact with an infinite solvent reservoir. There is only one polymer-solvent interface located at x=0. The following conditions hold:

$$\frac{\partial C}{\partial t} = D \frac{\partial^2 C}{\partial x^2} \qquad x<0 \tag{8}$$

$$\frac{\partial C_s}{\partial t} = D_s \frac{\partial^2 C_s}{\partial x^2} \qquad x>0 \tag{9}$$

$$C=C_o \quad x<0 \quad \text{and} \quad C_s=0 \quad x>0 \quad \text{at} \quad t=0 \tag{10}$$

$$C_s(0,t)/C(0,t) = K \tag{11}$$

$$J(0,t) = D\left(\frac{\partial C}{\partial x}\right)_{x=0} = D_s\left(\frac{\partial C_s}{\partial x}\right)_{x=0} \tag{12}$$

Equation (11) indicates that we have assumed that equilibrium holds at the interface (x=0). Equation (12) indicates that the flux, J, on either side of the plane at x=0 is the same (an equation of continuity).

A general solution of this problem is

$$C = C_o \left\{1 - \left[\frac{\mu}{\mu+1}\right] \left[1 + \operatorname{erf}\left(\frac{x}{2\sqrt{Dt}}\right)\right]\right\} \tag{13}$$

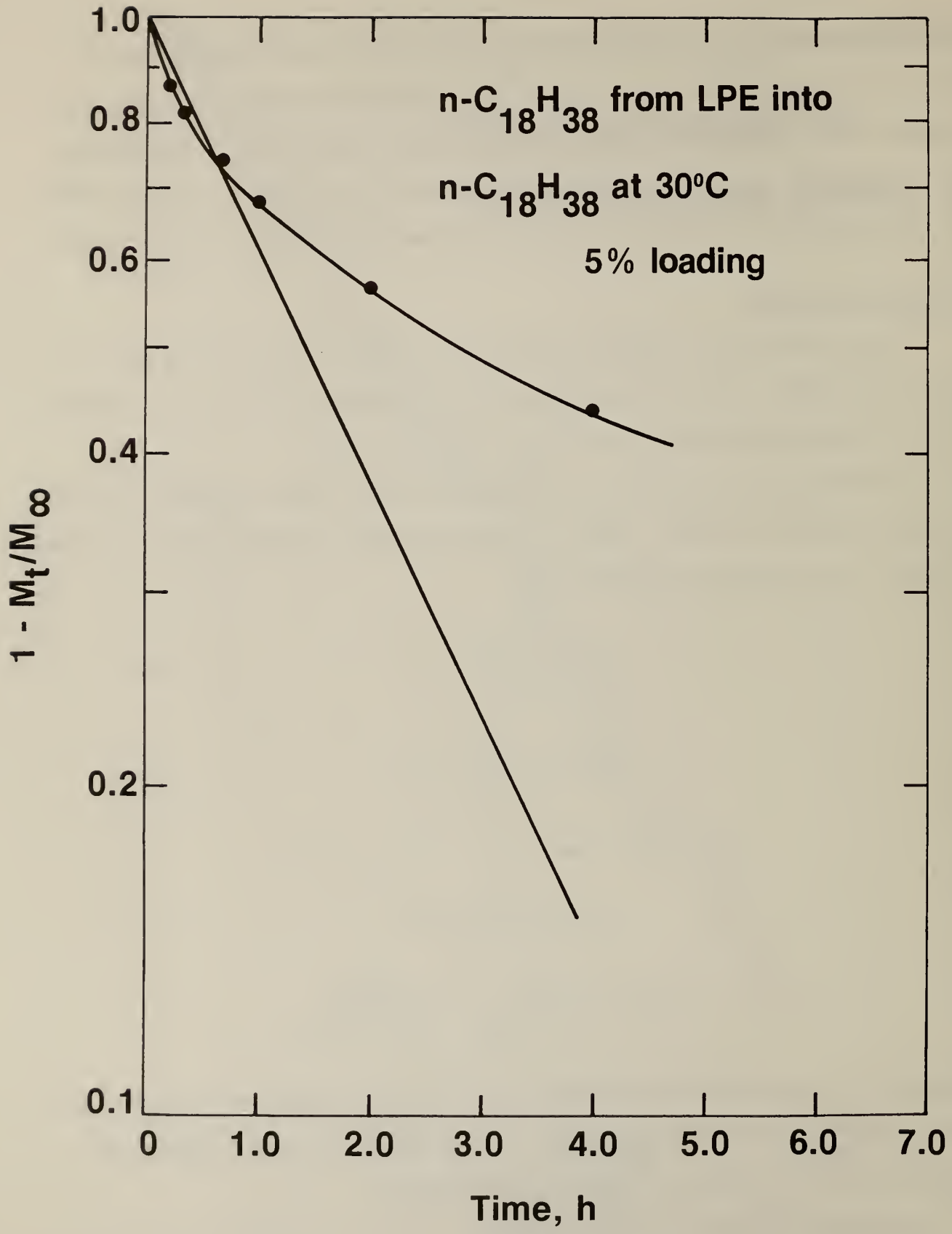
n-C18H38 from LPE into
n-C18H38 at 30°C
5% loading
1 - Mt/M∞
Time, h
1.0
0.8
0.6
0.4
0.2
0.1
0
1.0
2.0
3.0
4.0
5.0
6.0
7.0

Fig. I-2

$$C_s = C_o \left[\frac{\mu}{\mu + 1}\right] \left[1 - \text{erf}\left(\frac{x}{2\sqrt{D_s t}}\right)\right] \tag{14}$$

$$\mu \equiv K(D_s/D)^{1/2} \tag{15}$$

and where erf(z) is the error function. From Eqs. (12) and (13) it is easy to show that the flux across the plane at x=0 is

$$J(0,t) = -\frac{\mu}{\mu + 1} \frac{C_o}{\sqrt{\pi t}} \tag{16}$$

At time t the amount of additive, M_t, that will have crossed the plane at x=0 and of cross-sectional area A is

$$M_t = -2A\int_o^t J(0,t')dt' = \frac{4AC_o\mu}{1 + \mu} \left(\frac{Dt}{\pi}\right)^{1/2} \tag{17}$$

Now

$$C_o = M_o/A\ell \tag{18}$$

where ℓ is the polymer sheet thickness. An additional factor of 2 appears because we assume that both sides of the polymer sheet are in contact with the solvent. Although we assumed that the polymer is infinitely thick, all that is really required is for $\ell >> \sqrt{Dt}$. Therefore, for sufficiently thick polymer sheets Eq. (17) is valid and with the help of Eq. (18) it can be rewritten as

$$\boxed{M_t/M_o = \frac{4\mu}{\mu + 1} \left(\frac{Dt}{\pi\ell^2}\right)^{1/2}} \tag{19}$$

For finite sheets for which $\ell < \sqrt{Dt}$ and/or finite solvent amounts, Eq. (19) will slightly <u>overestimate</u> the amount of migration; thus, Eq. (19) is always a conservative measure of quiescent migration.

Notice that

$$M_t/M_o = 4 \begin{cases} (Dt/\pi\ell^2)^{1/2} & \text{if } \mu>>1 \\ K(D_s t/\pi\ell^2)^{1/2} & \text{if } \mu<<1 \end{cases} \qquad (20)$$

The result for $\mu>>1$ is the familiar one for polymer limited migration with strong solvent agitation.

The above analysis of quiescent migration as well as boundary layer limited migration clearly shows that partition coefficients can have a strong influence on migration rates.

A General Migration Model

(a) Exact Analysis

Polymer limited migration as well as the boundary layer and quiescent migration models represent particular extremes of migration behavior. What is needed is a more general model which can span the total range of migration behavior. The most general model that we might consider is diffusion from a polymer sheet of thickness ℓ through a stagnant solvent layer of thickness ℓ_s to a solvent reservoir of volume V_s. We can simplify the analysis considerably by allowing ℓ to be very large. Our results for an infinitely thick polymer will always accurately represent migration from a finite polymer sheet for times less than about 0.1 t_ℓ:

$$t_\ell \equiv \ell^2/D \qquad (21)$$

The characteristic time t_ℓ is approximately equal to the time required for a molecule to diffuse a distance ℓ in the polymer sheet. Therefore, for $t<t_\ell$ only molecules within a distance ℓ of the polymer surface will significantly contribute to migration. A more careful analysis of this "thick polymer approximation" will be given later in Section II.

Locating the polymer-solvent interface at x=0, we wish to solve the following two diffusion equations:

$$\frac{\partial C}{\partial t} = D \frac{\partial^2 C}{\partial x^2} \qquad x<0 \tag{22}$$

$$\frac{\partial C_s}{\partial t} = D_s \frac{\partial^2 C_s}{\partial x^2} \qquad x>0 \tag{23}$$

subject to the following initial conditions:

$$C(x,0) = C_o \quad \text{and} \quad C_s(x,0) = 0 \tag{24}$$

and boundary conditions:

$$C_s(0,t) = K\, C(0,t) \tag{25}$$

$$D \left(\frac{\partial C}{\partial x}\right)_{x=0} = D_s \left(\frac{\partial C_s}{\partial x}\right)_{x=0} \equiv J(0,t) \tag{26}$$

$$\left.\frac{\partial C}{\partial x}\right|_{x \to -\infty} = 0 \tag{27}$$

$$\left.\frac{\partial C_s}{\partial t}\right|_{x \geq \ell_s} = -\frac{2A}{V_s} J(0,t) \tag{28}$$

Boundary condition (27) is the thick polymer approximation. Boundary condition (28) reflects the condition that the solvent reservoir is finite and is being agitated. It also implicitly assumes that the volume of the boundary layer, $2A\ell_s$, is very much smaller than the total solvent volume V_s.

The above diffusion problem can be solved by the Laplace transform method. The solution is outlined in Appendix B. The Laplace transform of the flux $J(0,t)$ is given by

$$-A\, \bar{J}(0,p) = \frac{\alpha M_o \cosh(t_s p)^{1/2}}{2 + \alpha (t_\ell p)^{1/2} \left[\cosh(t_s p)^{1/2} + \mu^{-1} \sinh(t_s p)^{1/2}\right]} \tag{29}$$

where

$$\alpha \equiv KV_s/V_p \equiv KV_s/A\ell \tag{30}$$

$$\mu^2 \equiv K^2 D_s/D \tag{31}$$

$$t_s \equiv \ell_s^2/D_s \tag{32}$$

and p is the transform variable. The Laplace transform of a variable, such as J, is denoted as $\bar{J}$. The characteristic time t_s is approximately the average time required for a molecule to diffuse a distance ℓ_s in the solvent phase. Under normal conditions of solvent agitation $t_\ell >> t_s$ since $\ell >> \ell_s$ and $D << D_s$.

The amount of additive that migrates to the solvent is given by (two sided migration):

$$M_t = -2A \int_0^t \bar{J}(0,t')dt' \tag{33}$$

and its Laplace transform is

$$\bar{M}_p = -2A\, \bar{J}(0,p)/p \tag{34}$$

Thus, to obtain M_t, we must invert $\bar{J}/p$. To date we have been unable to carry out this inversion except for some special cases which we now consider.

Case I <u>Zero Boundary Layer and Finite Solvent Reservoir</u>

$$\lim_{\ell_s \to 0} -A\, \bar{J}(0,p) = \frac{\alpha M_o}{2 + \alpha(t_\ell p)^{1/2}} \tag{35}$$

The inverse of $\bar{J}/p$ is tabulated[3] and the result is

$$\boxed{M_t/M_o = \alpha\left[1 - e^{4\tilde{t}/\alpha^2}\,\mathrm{erfc}(2\tilde{t}^{1/2}/\alpha)\right]} \tag{36}$$

where $\tilde{t}$ is a dimensionless time variable defined by

$$\tilde{t} \equiv t/t_\ell \tag{37}$$

This is the same thick polymer approximation given by Crank for a plane sheet[4].

Case II Zero Boundary Layer and Infinite Solvent Reservoir

For an infinite solvent reservoir, we obtain from Eq. 36

$$\lim_{\alpha\to\infty} M_t/M_o = \lim_{\alpha\to\infty} \alpha\left[1 - \left(1 - \frac{4}{\sqrt{\pi}}\frac{\tilde{t}^{1/2}}{\alpha} + \ldots\right)\right]$$

$$\boxed{M_t/M_o = \frac{4}{\sqrt{\pi}}\tilde{t}^{1/2} = 4\left(\frac{Dt}{\pi\ell^2}\right)^{1/2}} \tag{38}$$

which is the familiar result for polymer limited migration.

Case III Infinite Boundary Layer

$$\lim_{\ell_s\to\infty} -A\bar{J}(0,p) = \frac{M_o}{(t_\ell p)^{1/2}(1+\mu^{-1})} \tag{39}$$

The inverse of $\bar{J}/p$ is tabulated[3] and the result is

$$\boxed{M_t/M_o = \frac{4\mu}{1+\mu}\left(\frac{Dt}{\pi\ell^2}\right)^{1/2}} \tag{40}$$

which is the result previously obtained, Eq. (19), for quiescent migration.

Case IV $\mu<<1$ (Boundary Layer Limited Migration)

When $\mu<<1$ we can approximate $\bar{J}$ by (expand cosh x and sinh x):

$$-A\bar{J}(0,p) \simeq \frac{\alpha M_o}{2 + \alpha\mu^{-1}(t_\ell t_s)^{1/2}p} \tag{41}$$

In making this approximation we assumed that

$$(t_s p)^{1/2} << 1$$

and

$$\mu^{-1}(t_s p)^{1/2} >> 1 \tag{42}$$

These conditions on the reciprocal time variable p are equivalent to restricting

the validity of this approximation to the following time interval:

$$t_s << t << \mu^{-2} t_s \tag{43}$$

Again the inverse of $\bar{J}/p$ is tabulated[3] and the result is

$$M_t/M_o = \alpha \left[1 - \left(\exp - \frac{2\mu t}{\alpha (t_s t_\ell)^{1/2}} \right) \right] \tag{44a}$$

$$\boxed{M_t/M_o = \frac{2\mu t}{(t_\ell t_s)^{1/2}} - \ldots} \tag{44b}$$

Equation 44b is identical to Eq. (7), the short time linear "t law" for boundary layer limited migration. Notice that the leading term in Eq. (44b) is the only non-zero one in the infinite solvent reservoir limit ($\alpha \to \infty$). What the above result tells us is that t law type migration can only be expected in the time interval defined by relationship (43).

(b) Approximate Analysis

Because we have in general been unable to invert $\bar{J}/p$ with $\bar{J}$ defined by Eq. (29), we present here an approximate analytical solution to this problem. At time t the concentration profile will look similar to the one shown below.

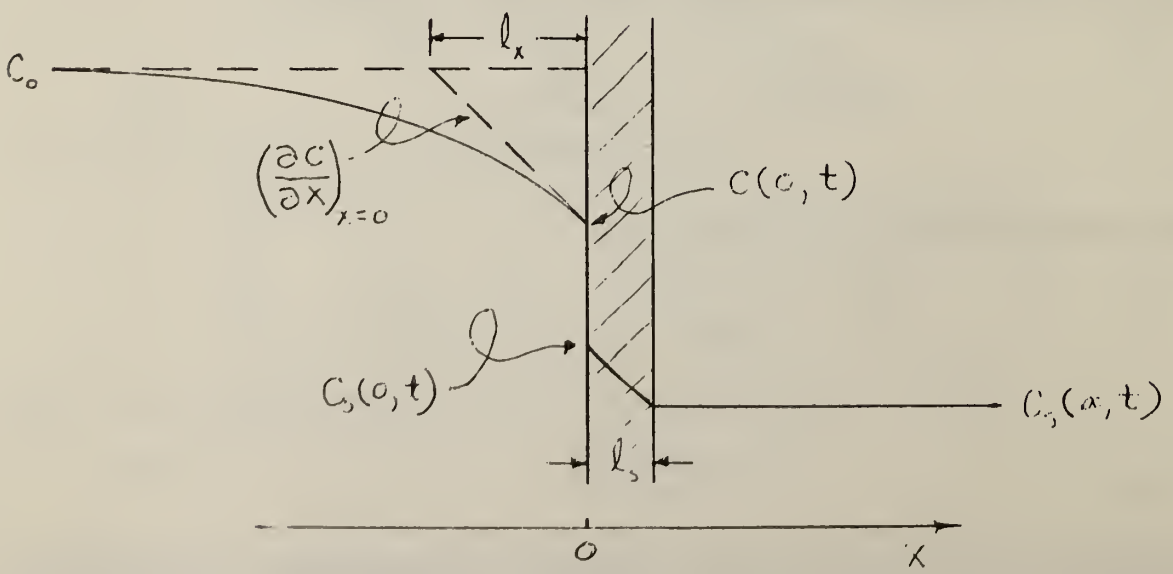

We approximate the concentration gradients at the polymer-solvent interface by

$$\left(\frac{\partial C}{\partial x}\right)_{x=0} \simeq \frac{C_o - C(0,t)}{\ell_x} \tag{45}$$

$$\left(\frac{\partial C_s}{\partial x}\right)_{x=0} \simeq \frac{KC(0,t) - C_s(\infty,t)}{\ell_s} \tag{46}$$

where ℓ_x is given by

$$\ell_x = \sqrt{\pi D t} \tag{47}$$

Equation (45) would be exact if ℓ_x where known exactly as a function of time. Our choice of Eq. (47) for ℓ_x is the exact value for polymer limited migration and quiescent migration. For example, from Eq. (13) we have

$$C(0,t) = C_o\left[\frac{1}{1+\mu}\right] \tag{48}$$

and

$$\left(\frac{\partial C}{\partial x}\right)_{x=0} = \frac{C_o}{\sqrt{\pi D t}}\left[\frac{\mu}{1+\mu}\right] \tag{49}$$

Combining Eqs. (45), (48) and (49) we obtain Eq. (47). Thus, we know Eq. (47) is exact in certain extremes and should be a good approximation for intermediate cases.

Equation (46) is an excellent approximation for small ℓ_s, but a poor one if ℓ_s is large. Thus, our approximate calculation is limited to small ℓ_s.

Notice in Eqs. (45) and (46) that C(0,t) is unknown. However, from the continuity condition Eq. (26), we can solve for C(0,t):

$$C(0,t) = \frac{C_o + C_s(\infty,t)(D_s/D)(\ell_x/\ell_s)}{1 + (KD_s/D)(\ell_x/\ell_s)} \tag{50}$$

where

$$C_s(\infty,t) = M_t/V_s \tag{51}$$

The flux across the polymer-solvent interface is given by Eq. (26). For two-sided migration, we multiply this result by two and then integrate to obtain

$$\alpha\, \ell n\left[1 - \frac{M_t}{\alpha M_o}\right] = 4(\tilde{t}/\pi)^{1/2}\left\{\ell n\left[1+\mu(\pi t/t_s)^{1/2}\right]\Big/\mu(\pi t/t_s)^{1/2}-1\right\} \tag{52}$$

We now look at the special cases as before:

Case I Zero Boundary Layer and Finite Solvent Reservoir

As $\ell_s \to 0$, or equivalently as $t_s \to 0$, Eq. (52) becomes

$$\boxed{M_t/M_o = \alpha\left\{1 - \exp[-4(\tilde{t}/\pi\alpha^2)^{1/2}]\right\}} \tag{53}$$

This approximate solution (two-sided migration) is compared with the exact solution Eq. (36) in the Table below:

	$M_t/\alpha M_o$	
$\tilde{t}^{1/2}/\alpha$	Eq. (36)	Eq. (53)
0.00	0.00	0.00
0.05	0.104	0.107
0.10	0.191	0.202
0.20	0.329	0.363
0.30	0.432	0.492
0.40	0.511	0.594
0.50	0.572	0.676
1.0	0.745	0.895
∞	1.00	1.00

As $\alpha \to \infty$ (see below) or as $t \to 0$ the two solutions become identical. The small t limit for both equations is

$$M_t/M_\infty = 4\left(\frac{1+\alpha}{\alpha}\right)\left(\frac{Dt}{\pi\ell^2}\right)^{1/2} \tag{54}$$

Since $M_t \leq M_\infty$, Eq. (36) or (53) is only applicable for $M_t/\alpha M_o$ values $\leq (1+\alpha)^{-1}$.

Case II Zero Boundary Layer and Infinite Solvent Reservoir

As $\alpha \to \infty$ Eq. (53) reduces to Eq. (38), the correct result for polymer limited migration.

Case III Infinite Boundary Layer

Our approximate solution is invalid in this limit because of our assumption of a linear concentration gradient, Eq. (46), becomes invalid.

Case IV $\mu << 1$ (Boundary Layer Limited Migration)

If μ is very small and we restrict ourselves to times such that

$$\mu(\pi t/t_s)^{1/2} << 1 \quad \text{or} \quad t << \mu^{-2} t_s \tag{55}$$

we can expand Eq. (53) to recover Eqs. (7) and (44b). Notice that the time restrictions (43) and (55) are for practical purposes identical.

Case V Finite Boundary Layer and Infinite Solvent Reservoir

This is an especially useful result that is obtained from Eq. (52) by letting $\alpha \to \infty$:

$$M_t/M_o = 4(\tilde{t}/\pi)^{1/2} \left\{ 1 - \left[\ln \; 1+\mu(\pi t/t_s)^{1/2} \right] \Big/ \left[\mu(\pi t/t_s)^{1/2} \right] \right\} \tag{56a}$$

which can also be written as

$$\boxed{M_t/M_o = 4(\tilde{t}/\pi)^{1/2} \left\{ 1 - \ln(1+\beta \tilde{t}^{1/2}) \Big/ (\beta \tilde{t})^{1/2} \right\}} \tag{56b}$$

where

$$\beta \equiv \mu(\pi t_\ell/t_s)^{1/2} \tag{57}$$

When $\beta \tilde{t}^{1/2}$ is small, Eq. (56) reduces to Eqs. (7) or (44b) and when $\beta \tilde{t}^{1/2} >> 1$, it

reduces to Eq. (38); i.e., initially M_t obeys a t law (pure boundary layer limited migration), but at longer times it follows a $t^{1/2}$ law (polymer limited migration). Evidence of the transition from t to $t^{1/2}$ behavior has been observed for the migration of n-octadecane from high density PE to ethanol, corn oil and trioctanoin as shown in Fig. E-3 in the experimental section VI.

Figure 3 illustrates the general effects of boundary layer limited migration according to Eq. (56).

(c) Migration Bounds

Assuming that the additive is uniformly distributed throughout the polymer and is not supersaturated, we can place meaningful upper and lower bounds on migration. The upper bound is Case II or polymer limited migration and the lower bound is Case III or quiescent migration. These bounds, of course, are not the best ones, but in both cases we err on the safe or conservative side. Thus

$$\frac{4\mu}{1+\mu}\left(\tilde{t}/\pi\right)^{1/2} \leq M_t/M_o \leq 4\left(\tilde{t}/\pi\right)^{1/2} \qquad (58)$$

For one-sided migration the above factors of 4 become factors of 2.

Boundary layer limited migration, Case V, as calculated from Eq. (56) will always be less than or equal to Case II and greater than Case III for $t>4t_s$.

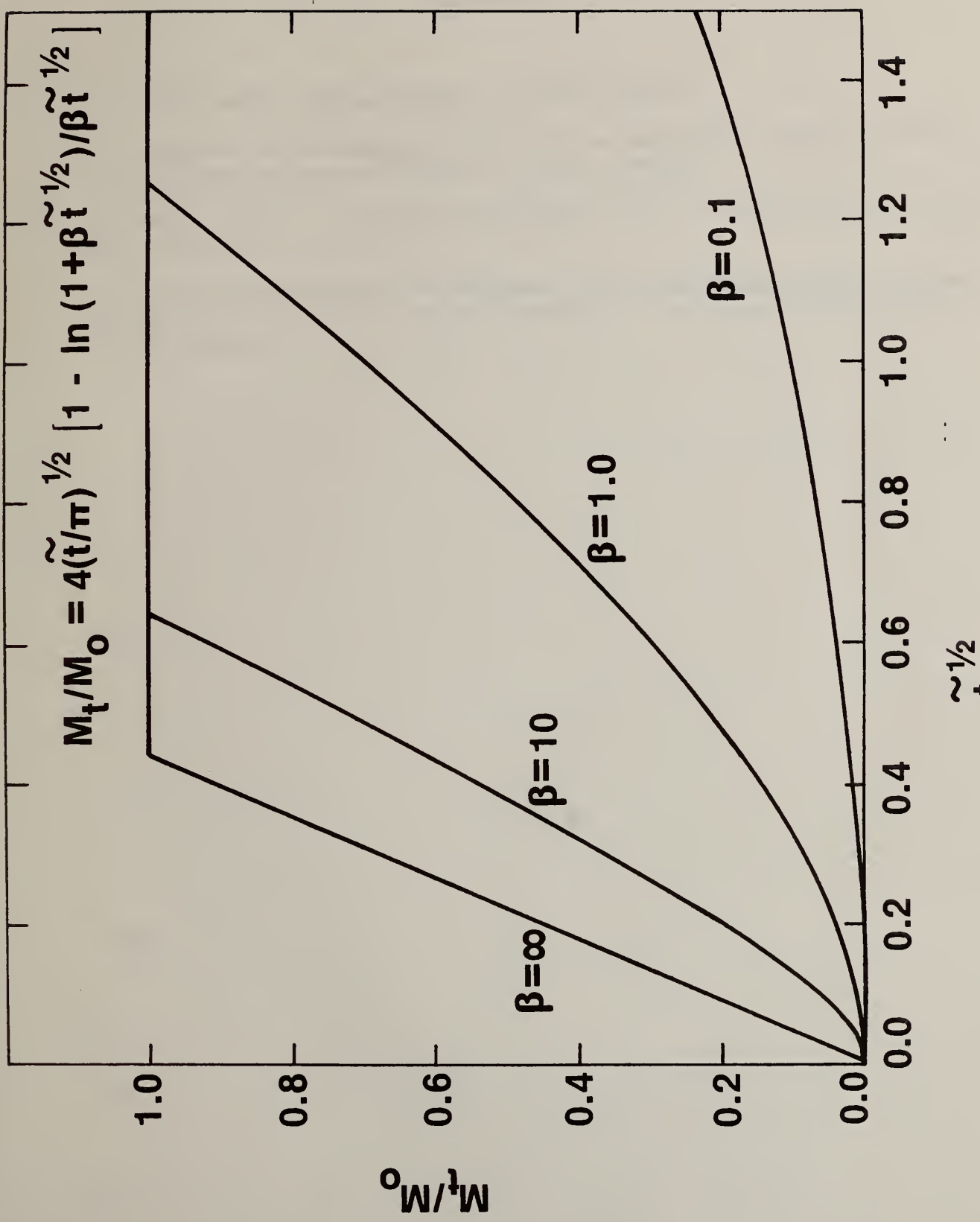
$M_t/M_o = 4(\tilde{t}/\pi)^{1/2} [1 - \ln(1+\beta\tilde{t}^{1/2})/\beta\tilde{t}^{1/2}]$
β=∞
β=10
β=1.0
β=0.1
M_t/M_o
$\tilde{t}^{1/2}$
0.0
0.2
0.4
0.6
0.8
1.0
1.2
1.4

Fig. I-3

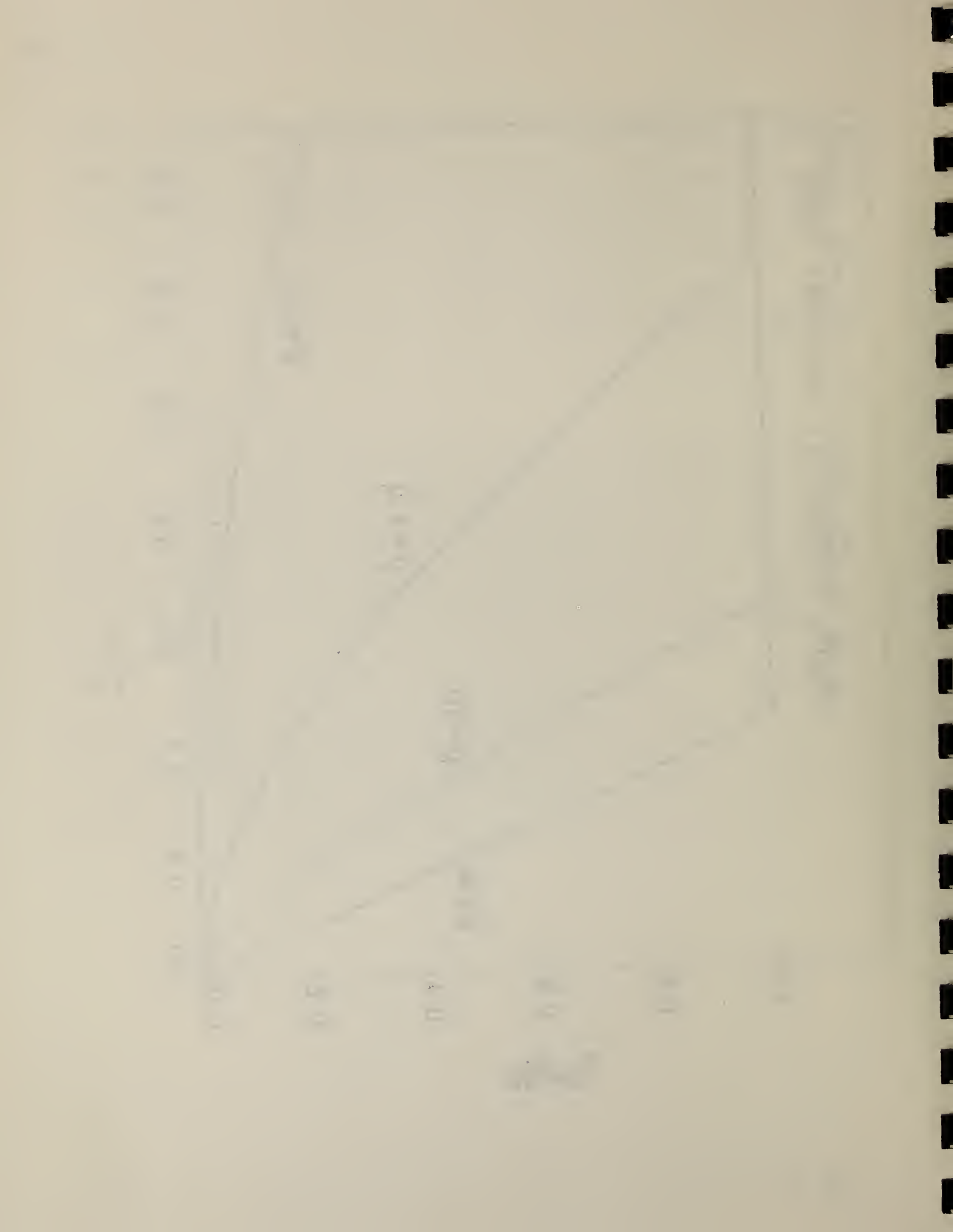

References

1. C. R. Wilke and P. Chang, AIChE J., 1, 264 (1955).

2. K. J. Vetter, "Electrochemical Kinetics", Academic Press, New York, 1967. (a) p. 160 and references therein. (b) pp. 188-193.

3. H. Bateman, "Tables of Integral Transforms", Vol. I, McGraw-Hill, New York, 1954, Ch. V.

4. J. Crank, "The Mathematics of Diffusion", Clarendon Press, Oxford, England, 2nd Ed., 1975. Ch. 4. In Crank's treatment, ℓ is the half-thickness of the plane sheet.

II. Effect of Sample Thickness on Migration

We have asserted, without proof, that for times less than 0.1 t_ℓ (or $\tilde{t}<0.1$) we can accurately treat migration from a polymer sheet of thickness ℓ as if it were infinitely thick. We have called this procedure the "thick polymer approximation". The utility of this approximation is especially transparent for Case II or polymer limited migration. The exact solution of this problem is

$$M_t/M_o = 1 - \sum_{n=0}^{\infty} \frac{8}{(2n+1)^2\pi^2} \exp[-(2n+1)^2\pi^2\tilde{t}] \qquad (1)$$

whereas the thick polymer approximation is

$$M_t/M_o = \begin{cases} 4(\tilde{t}/\pi)^{1/2} & \tilde{t} \leq \pi/16 \\ 1 & \tilde{t} > \pi/16 \end{cases} \qquad (2)$$

The series in Eq. (1) converges very slowly for small values of $\tilde{t}$ and is awkward to use.

Equations (1), dashed line, (2), solid line, are compared in Figure 1. As can be seen, for M_t/M_o values less than or equal to 0.6, the thick polymer approximation is very accurate. This corresponds to times

$$\tilde{t} \leq 0.07 \qquad (3)$$

The maximum error occurs at $\tilde{t} = \pi/16 \simeq 0.2$ and even here it is acceptable (1.0 versus 0.87). Besides it convenience, use of the thick polymer approximation always yields a conservative estimate (i.e., an overestimate) of migration.

A corollary of the above result is that for times $\tilde{t}\leq 0.07$, the migration per unit area will be independent of polymer thickness. By using Eq. (I.18), ℓ can be eliminated from Eq. (2) and we obtain

$$M_t/A = 4C_o\left(\frac{Dt}{\pi}\right)^{1/2} \qquad (4)$$

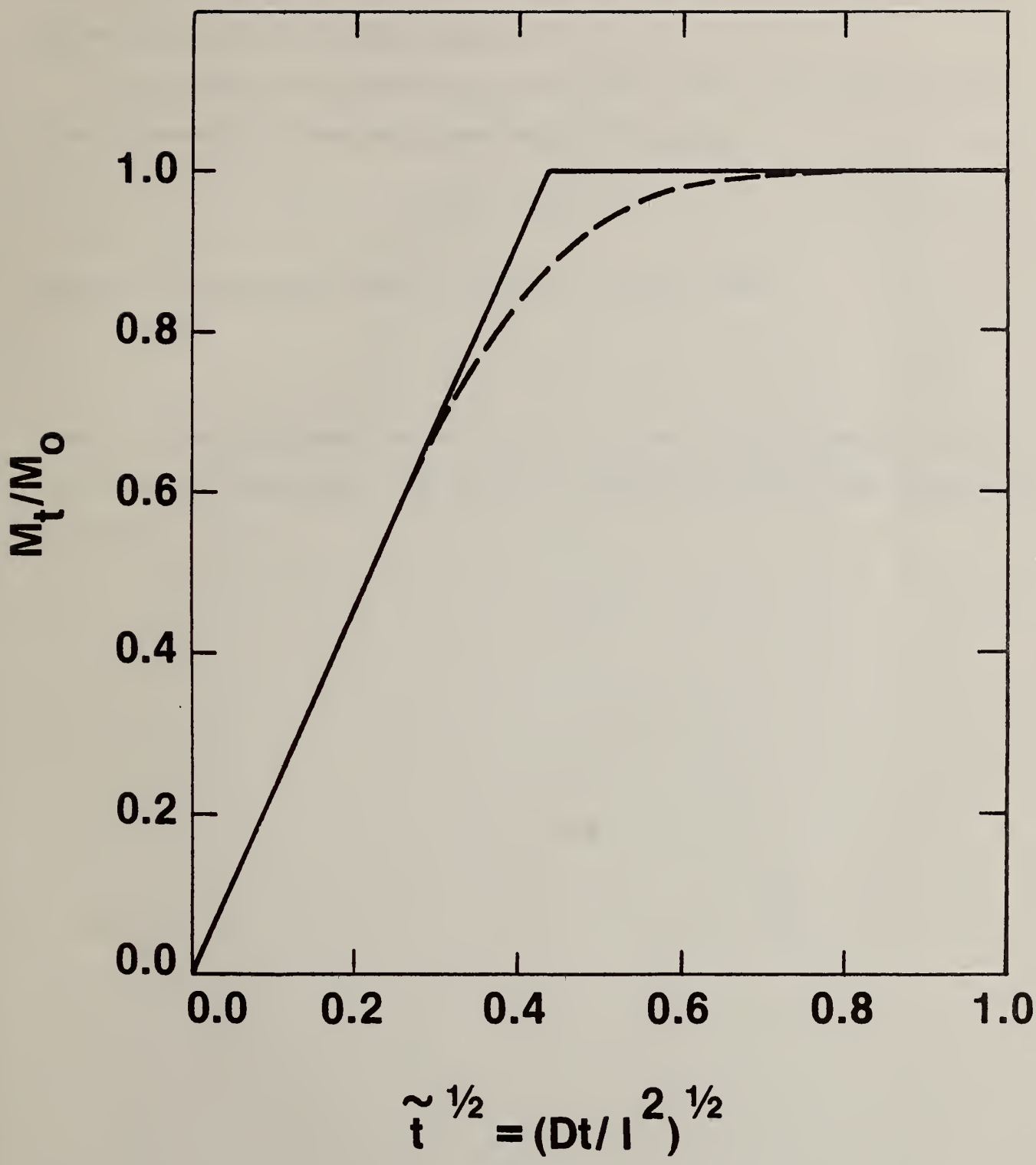

Fig. I-4

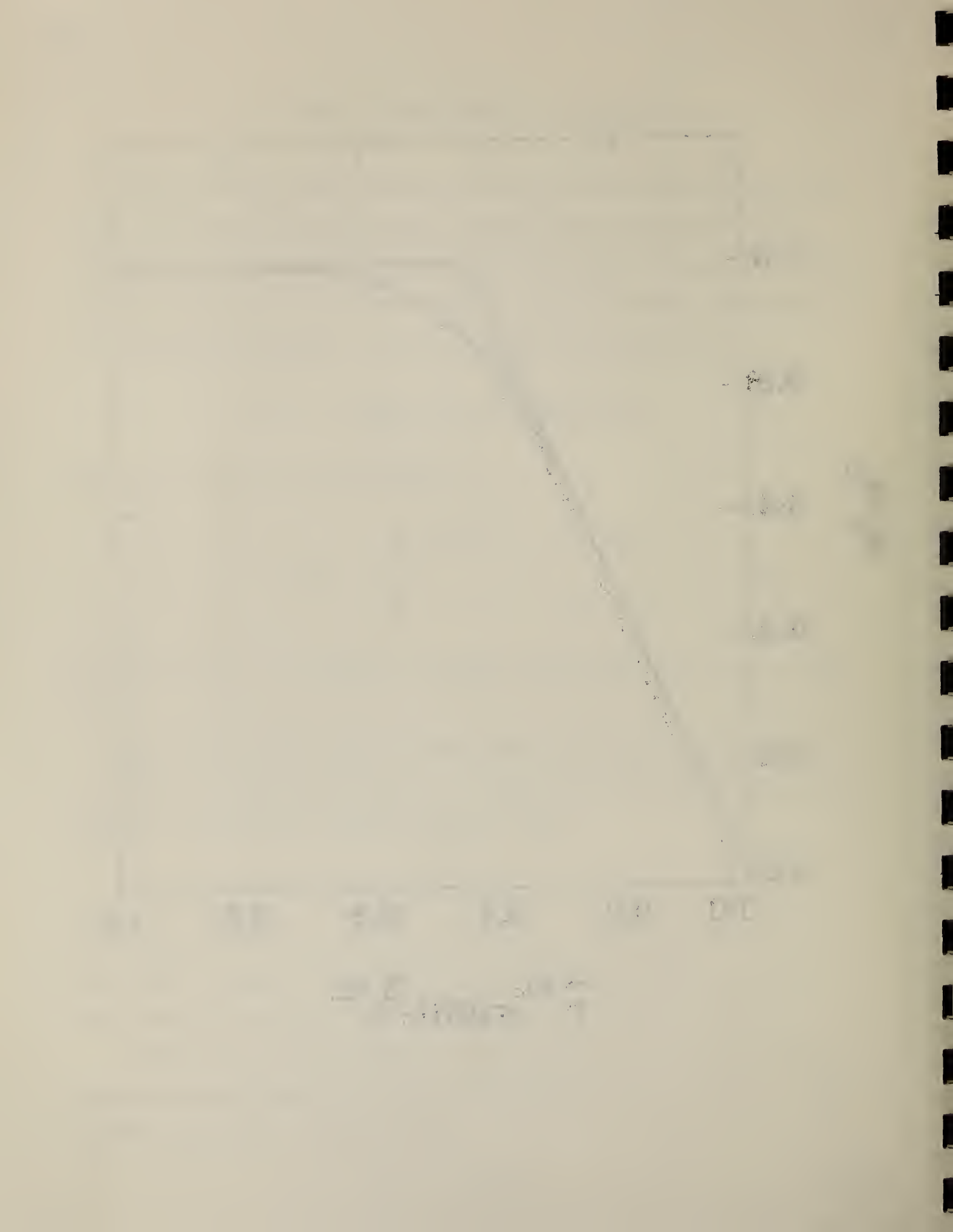

Thus, if inequality (3) is satisfied, migration measured at one sheet thickness can be safely used for thicker samples.

On the other hand, migration per unit area at sufficiently long times becomes independent of time and proportional to thickness:

$$M_t/A \simeq M_o/A = \ell C_o \tag{5}$$

Equation (5) will apply within an accuracy of 1% for times

$$\tilde{t} > 0.44 \tag{6}$$

Figure 2 illustrates migration per unit area plotted versus the square root of time for three thicknesses. The initial concentrations in all three samples were identical.

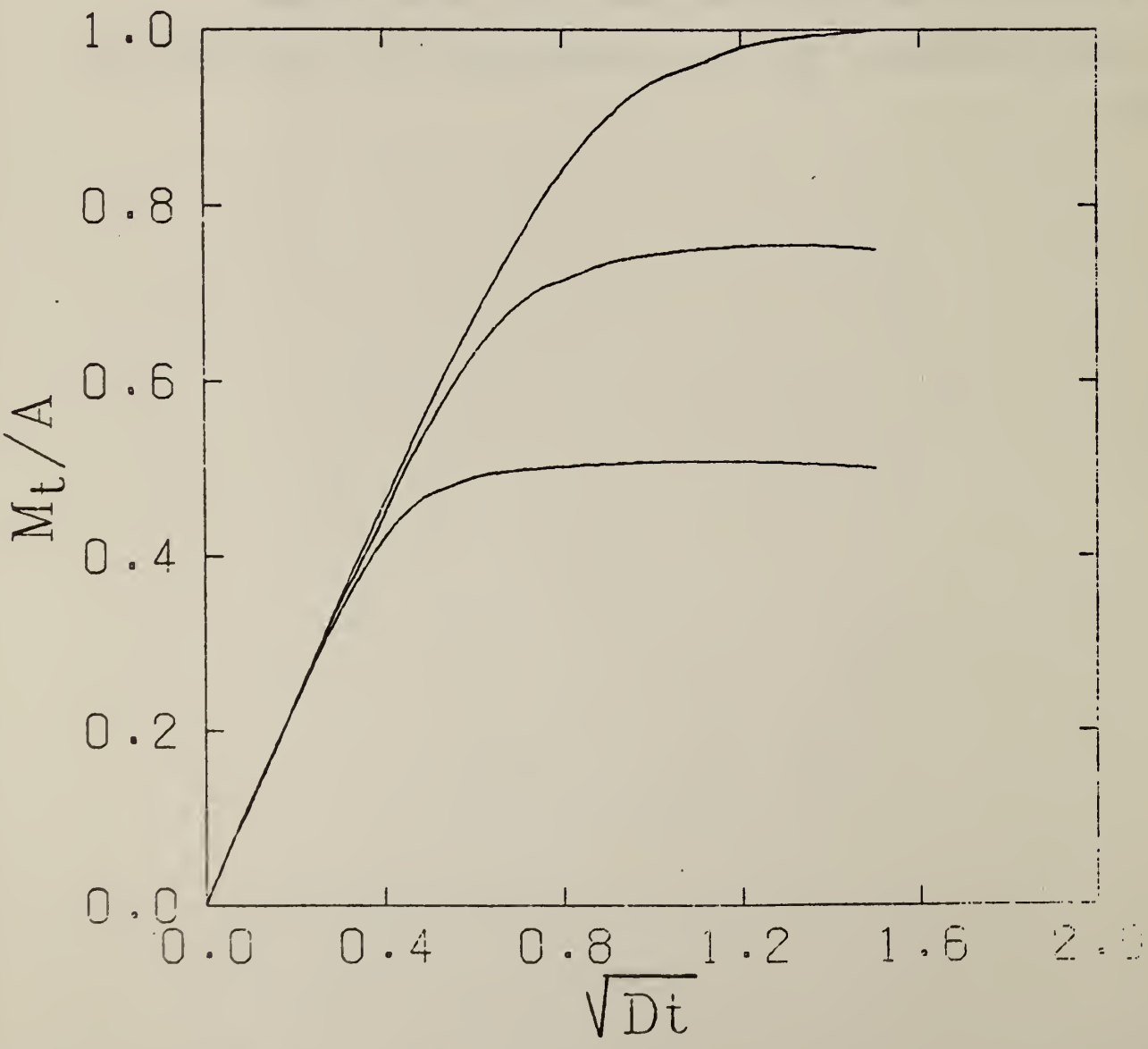

Fig. II-2. Migration curves of films of three thicknesses.

III. Errors in Temperature Extrapolations

Let the diffusion coefficient of a migrant in a polymer be D_1 at a temperature T_1 with an activation energy E. Then the diffusion coefficient at a temperature T_2 may be extrapolated to be:

$$D_2 = D_1 \exp[E/R(1/T_1 - 1/T_2)] \qquad (1)$$

Let an estimated activation energy $E + \Delta E$ in error by ΔE be used instead of the true activation energy E. Then the error in the predicted diffusion coefficient D_2' at temperature T_2, expressed in percent, is:

$$100 \frac{D_2' - D_2}{D_2} = 100 \exp\left[\frac{\Delta E}{R}\left(\frac{1}{T_1} - \frac{1}{T_2}\right)\right] - 100$$

where R is the gas constant and the temperature T_1 and T_2 are in degrees Kelvin. Notice that the extrapolation error, when expressed in percent, depends only on the error in the activation energy and on the temperatures; the percent error does not depend on the activation energy or the diffusion coefficient. Table 1 gives percent errors of the extrapolated diffusion coefficient for extrapolations from 80°C to 60, 40 and 20°C for errors ΔE in the estimated activation energy of 2, 5, 10 and 15 kcal/mole.

Table 1 shows that accurate values of the activation energy are required for temperature extrapolation. Thus, if the activation energy is estimated to within 2 kcal/mole, the diffusion coefficient may be extrapolated for 80 to 20°C with less than 50% error. However, if the activation energy is only known to within 10 kcal/mole, the diffusion coefficient may not be extrapolated from 80°C to even 60°C with less than 50% error.

Table 1

Percent Error in Diffusion Coefficients Extrapolated

From 80°C to Given Temperature

Error in activation energy, kcal/mole	20°C	40°C	60°C
2	44	31	16
5	77	60	35
10	95	84	58
15	98	93	72

IV. An Empirical Formula for Migration in Polyolefins

A selected compilation of literature values of diffusion coefficients for migrants in polyolefins reported[1] in a preceding progress report was extended. Values for which the same migrant was tested in several polyolefins at 25°C or 80°C were selected from this compilation. For comparison purposes, values of the diffusion coefficients of gases in polyolefins at 25°C were selected from other sources[2]. These diffusion coefficients were fit to the empirical equation

$$D = PM^F \qquad (1)$$

where the value of M depends only on the migrant and temperature while the values of P and F depend only on the polyolefin. This approach is similar to the simple functional relationships developed by Stannett and Szwarc[3], Rogers et al[4], and Frisch[5] to correlate permeabilities and diffusion coefficients of gases through polymer films. Values of M are given in Table 1 and the values of P and F are given in Table 2. In the correlation discussed here, M is the diffusion constant of the migrant in low density polyethylene. The units of D is cm^2/sec.

Eq. 1 may be written

$$\ln D = \ln P + F \ln M \qquad (2)$$

so that a log-log plot of D for a polyolefin versus the M values of migrants is a straight line. Eq. 2 is plotted in Figures 1 to 6 for the nine polyolefins and compared with the experimental values of D. The experimental values of the diffusion coefficients are seen to agree with the line predicted by Eq. 2 to within a factor of 2 in almost all cases. These figures also illustrate the paucity of data available for fitting some of the polymers. Values of P and F for these polymers should be considered very tentative.

The diffusion coefficients of hydrogen, helium and benzene did not fit Eq. 1 so were eliminated from the fitting. Hydrogen and helium are very small mole-

cules, so that their rate of diffusion is probably overly sensitive to features of the structure of the polyolefins that do not affect the diffusion of larger molecules. Benzene is strongly absorbed by polyolefins and the diffusion coefficients measured for benzene are probably not representative of the pure polyolefin but of the polymer swollen with benzene.

The application of Eq. 1 can best be illustrated by the following examples:

Example 1. Estimate the diffusion coefficient of Didodecyl,3,3-thio Dipropinate in Isotactic Polypropylene at 80°C.

From Table 1, $M = 4.18 \times 10^{-8}$

From Table 2, $P = 500$ and $F = 1.523$

By Eq. 1, $D = 500 \times (4.18 \times 10^{-8})^{1.523}$

$= 2.9 \times 10^{-9}$ cm^2/sec.

Example 2. The diffusion coefficient of Thiodiphenylamine in isotactic polypropylene at 80°C is 2.1×10^{-9} cm^2/s. Estimate is diffusion coefficient at 80°C in low and high density polyethylene.

From Table 2, for isotactic polypropylene, $P = 500$ and $F = 1.523$. Substituting in Eq. 1,

$$2.1 \times 10^{-9} = 500\ M^{1.523}$$

Solving, the M value for Thiodiphenylamine

$$M = (2.1 \times 10^{-9}/500)^{1/1.523}$$

$$= 3.4 \times 10^{-8}$$

For low density polyethylene, $P = F = 1$ so the diffusion coefficient is

$$D = M = 3.4 \times 10^{-8} \text{ cm}^2/\text{s}$$

The diffusion coefficient in high density polyethylene is by Eq. 1,

$$D = 915\ (3.4 \times 10^{-8})^{1.509} = 5 \times 10^{-9} \text{ cm}^2/\text{s}.$$

This empirical formula, Eq. 1, is not expected to predict highly accurate values of diffusion coefficients. Some of the limitations in its derivation are:

1. The form of Eq. 1 is purely correlative and has no intrinsic physical basis.
2. The polyolefins have been grouped into general classes. For example, different samples of low density polyethylene differ in crystallinity, morphology, etc. so will have different diffusion coefficients. Ideally, the variation of diffusion coefficients with at least the crystallinity of the polyolefins should be taken into account.
3. The data of Table 1 is incomplete. Only a few migrants other than gases are included. Also, only a few diffusion coefficients are available for some of the polyolefins.
4. The experimental accuracy of some of the diffusion coefficients is low, especially some of the measurements by radioactive analysis.
5. Small errors were introduced by temperature extrapolation of some of the diffusion coefficients.
6. This formula does not apply to solvent extraction of the migrant. For example, if a polyolefin is immersed in pentane, the effective diffusion coefficient may be an order of magnitude greater than that given by the formula.

In spite of these limitations, it is hoped that the empirical formula will be of value in estimating diffusion coefficients in polyolefins when no other method is available.

Physical Interpretation of the Empirical Formula

For diffusion of a migrant in low density polyethylene (LDPE), P=F=1, so D=M

by Eq. 1. That is, the value of M for a migrant is simply its diffusion coefficient in low density polyethylene.

If F=1 for a polyolefin, Eq. 1 becomes

$$D = PM \qquad (3)$$

so that the diffusion coefficient in the polyolefin is P times its diffusion coefficient in LDPE by Table 5, P=4 and F=1 for ET-C-PR. Therefore, the diffusion coefficient of a migrant in Hydrogenated Butadiene is 3.25 times its diffusion coefficient in LDPE. If F is not 1 for a Polyolefin, a constant ratio between the diffusion coefficient of a migrant in the Polyolefin and in LDPE does not exist.

The compilation of diffusion coefficients in Polyolefins is being extended and an empirical fit of the diffusion coefficients based on more data will be given in a later report. Also, an empirical fit of the activation energies will be attempted. The correlation of the M values with the molecular weight, size or other properties of the migrants will be investigated. This will allow the estimation of the diffusion coefficient of a migrant prior to any measurements using the migrant.

References

1. NBSIR 79-1779, Progress report for period Jan. 1 to Mar. 31, 1979.

2. Polymer Handbook, edited by J. Brandrup and E. H. Immergut, John Wiley & Sons, Inc. (1975).

3. V. Stannett and M. Szwarc, J. Polym. Sci., 16, 89 (1955).

4. C. Rogers, J. A. Meyer, V. Stannett and M. Szwarc, Tappi, 39, 741 (1956).

5. H. L. Frisch, Polymer Letters, 1, 581 (1963).

Table 1

Values of M

Migrant	Temperature, °C	M x 10^8
Oxygen	25	40.2
Carbon Dioxide	25	33.4
Carbon Monoxide	25	25.7
Nitrogen	25	30.1
Argon	25	29.3
C_3H_4	25	18.8
Sulfur Tetrafluoride	25	1.73
Methane	25	17.2
Ethane	25	7.15
Allene	25	9.96
Propene	25	6.00
Propane	25	3.64
n-Pentane	25	1.69
n-Octane	25	.895
n-Decane	25	.346
2-4 Dihydroxy Benzophenone	80	5.19
2-5-Di-Tert-Butyl-4-Hydroxy Toluene	80	9.21
2-Hydroxy-4-Methoxy Benzophenone	80	4.50
2-Hydroxy-4-Butoxy Benzophenone	80	2.71
2-Hydroxy-4-Octoxy Benzophenone	80	3.29
N-Octadecyl-Diethanol Amine	80	12.0
2-Hydroxy-4-Dodecoxy Benzophenone	80	2.61
Di(2-Ethyl-1-Hexyl)Pthalate	80	.392
2-Hydroxy-4-Octadecoxy Benzophenone	80	1.34
Didodecyl,3,3-thio Dipropionate	80	4.18
n-Butane	25	2.22
Cyclohexane	25	.677
Methylene Chloride	25	7.23
n-Hexane	25	1.51

Table 2

Values of P and F

Polyolefin	P	F
Low density polyethylene	1	1
High density polyethylene	915	1.509
Isotactic Polypropylene 60-64% Crystallization	500	1.523
Stereblock Polypropylene 24% Crystallization	5.45×10^{-3}	0.694
Poly(isobutene-co-isoprene) 98/2 (Butyl Rubber)	7.1×10^{-4}	0.623
Poly(4-methylpentent-1)	2.13	1
Poly(ethylene-co-propylene) 49/51	8.0	1.053
Hydrogenated Butadiene	3.25	1
Polyisobutylene	.093	1

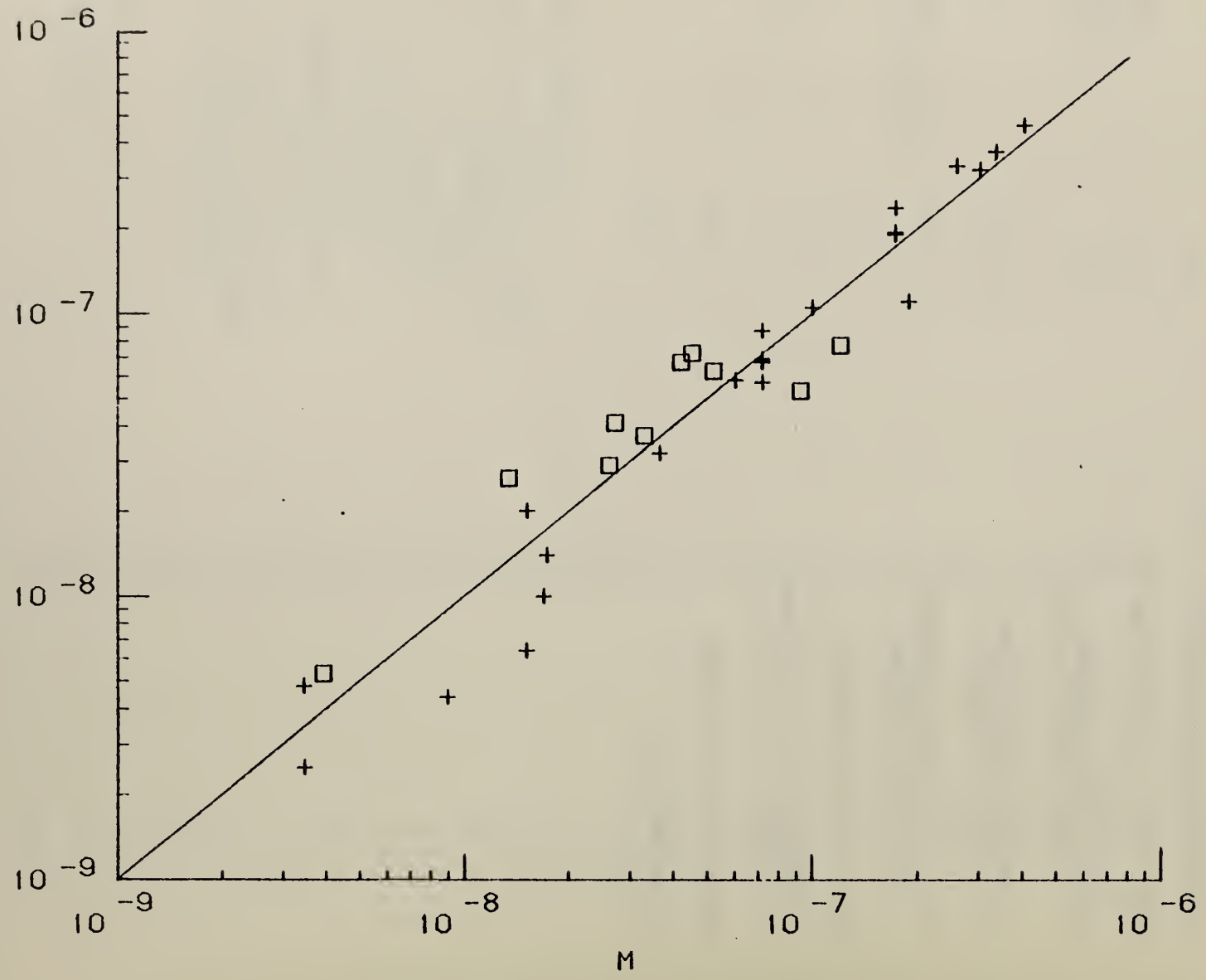

Figure IV-1. Low density polyethylene + 25°C □ 80°C

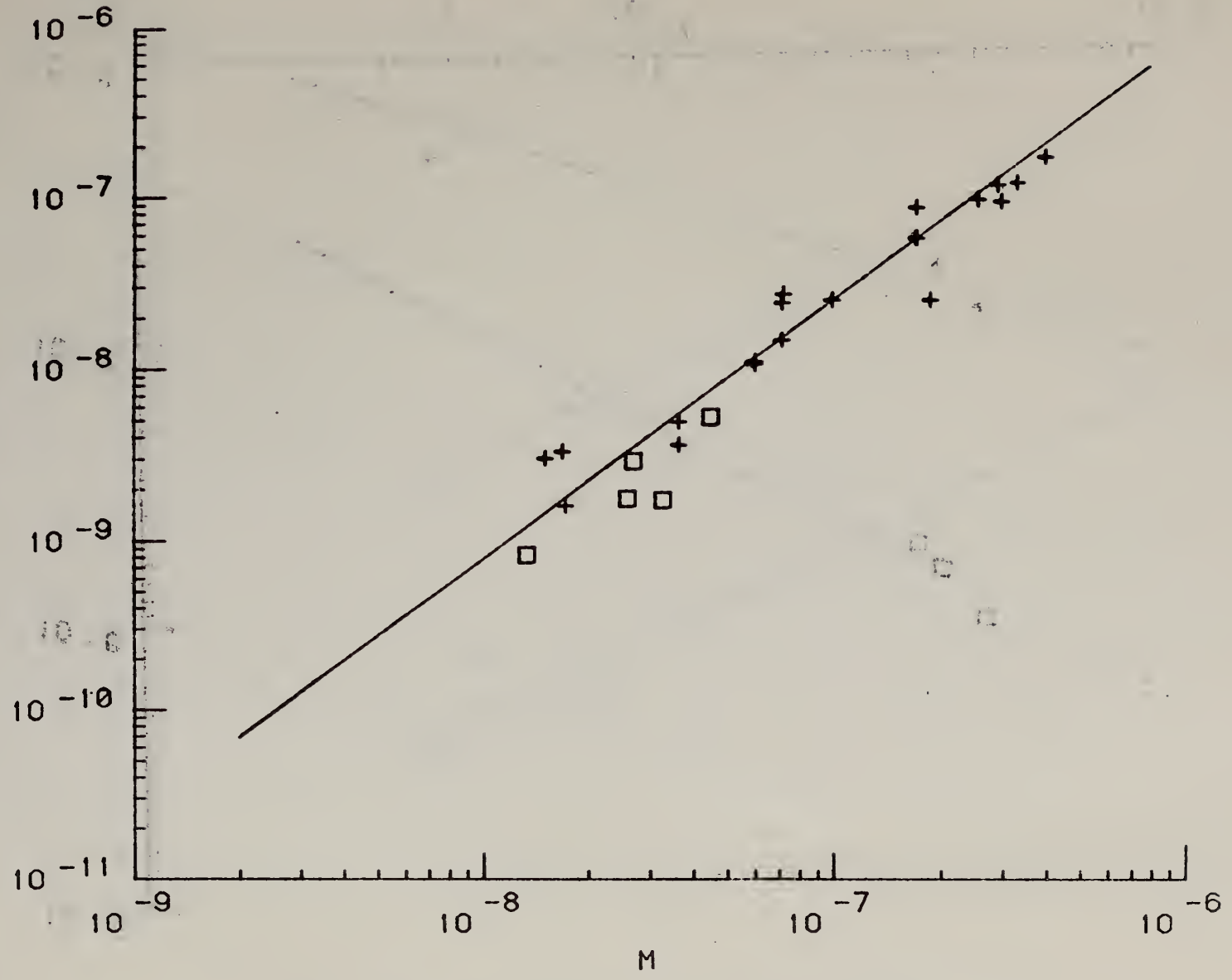

Figure IV-2. High density polyethylene. + 25°C □ 80°C

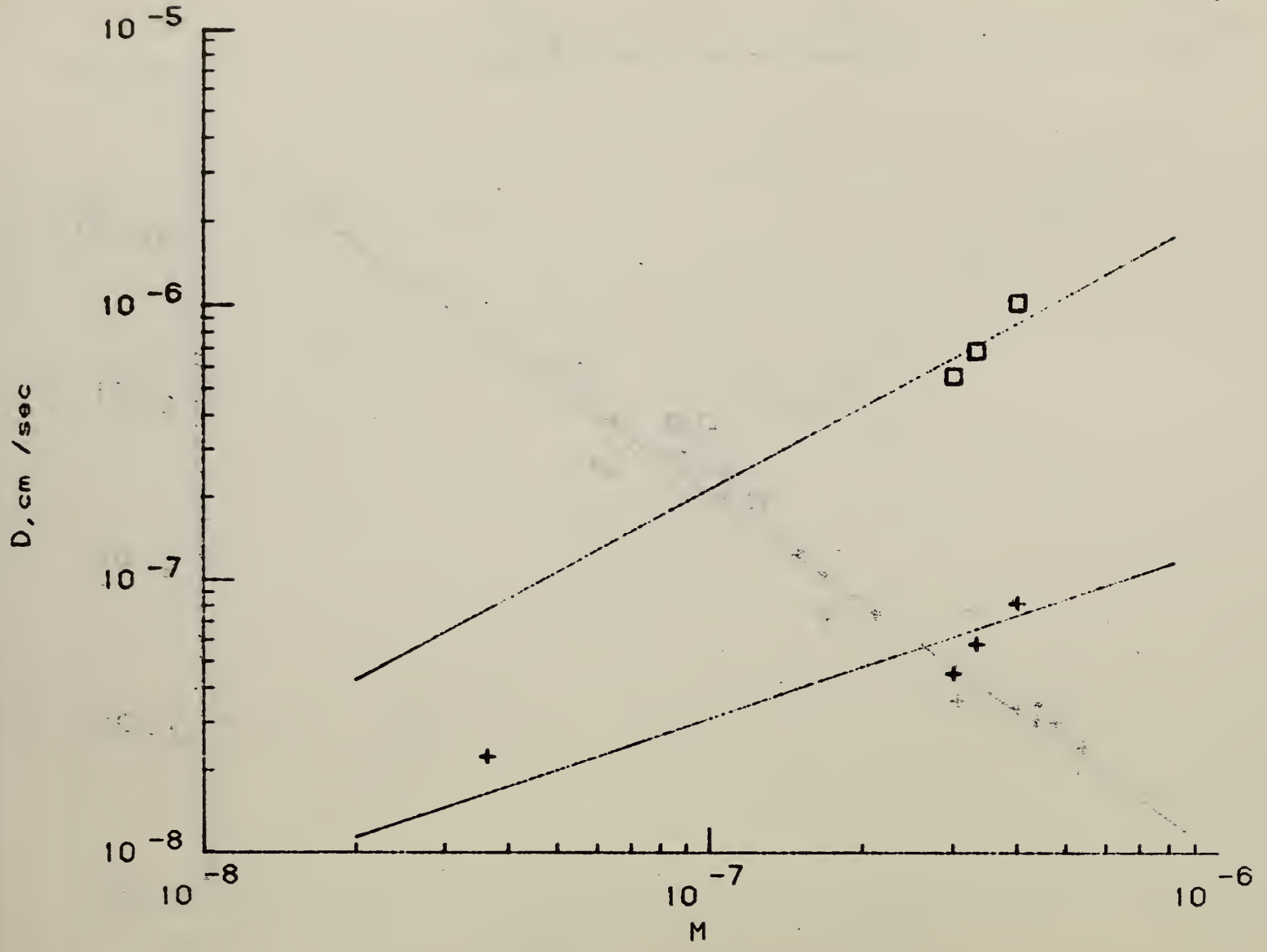

Figure IV-3. + Poly(isobutene-co-isoprene) 98/2 (Butyl Rubber)

□ Poly(4-methylpentene-1)

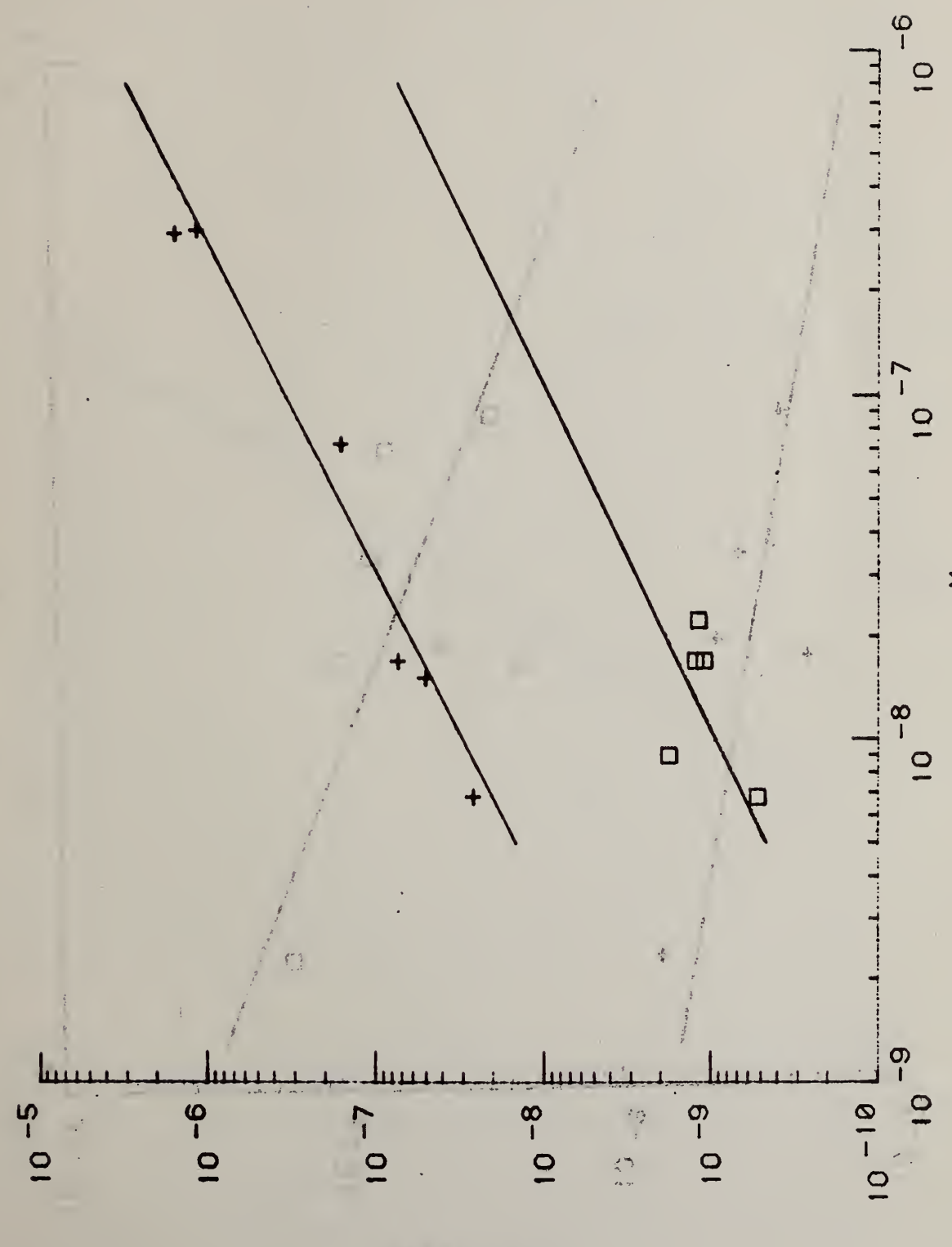

Figure IV-4. + Poly(ethylene-co-propylene) 49/51

□ Polyisobutylene

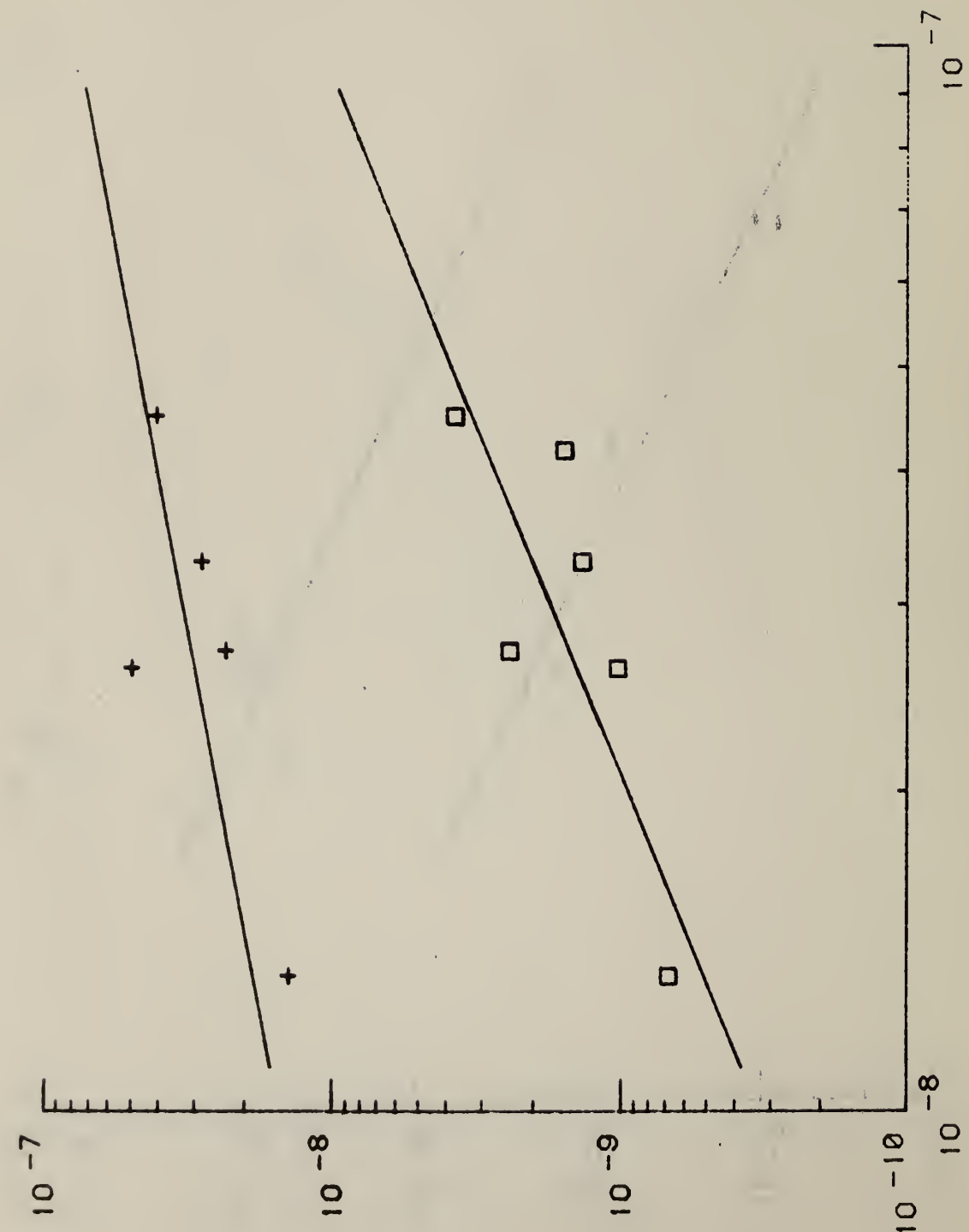

Figure IV-5. + Stereblock Polypropylene

□ Isotactic Polypropylene

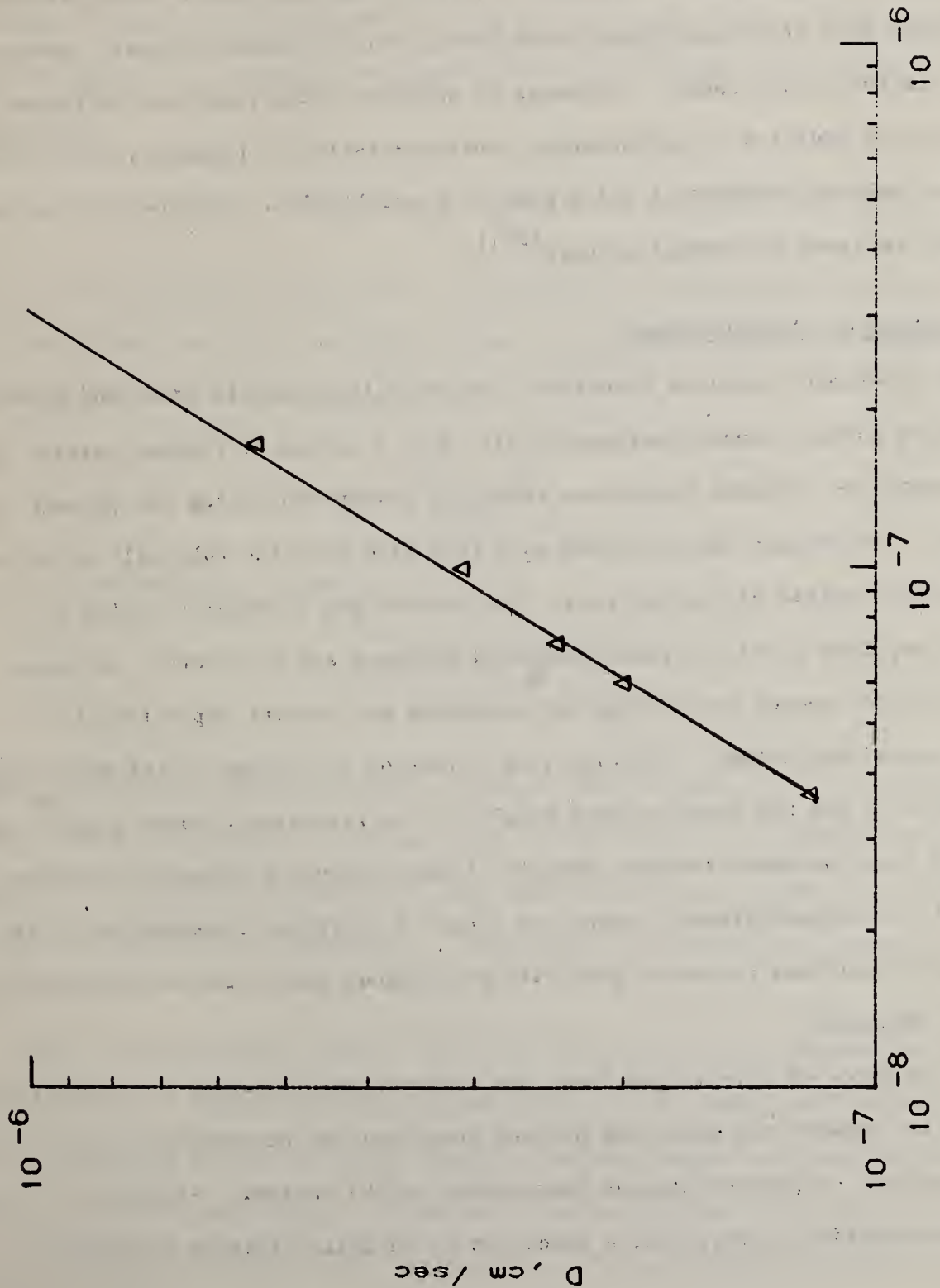

Figure IV-6. Hydrogenated Butadiene

V. Inverse Phase Gas Chromatography of Polymers

Inverse phase gas chromatography (IGC) was first reported by Guillet[1] less than ten years ago. The experiment differs from conventional gas chromatography (GC) in that the material of interest, a polymer with negligible vapor pressure, is employed as a stationary phase which sorbs various volatile organic species, often referred to as probes. Processes of solution, adsorption and diffusion can be studied in addition to morphological characteristics of polymers, such as the glass and melting temperature and degree of crystallinity. Studies of this nature have been reviewed by several authors[2-4].

A Description of the Experiment

The experiment involves injecting a pulse of the volatile probe and a non-interacting marker, usually methane or air, into a stream of flowing carrier gas which sweeps the injected substances through a column containing the polymer of interest. The polymer can be coated as a thin film onto the tube wall or on an inert support packed within the tube. The carrier gas is usually helium or nitrogen supplied at an accurately measured pressure and flow rate. An appropriate detector senses the elution of the marker and solvent vapor from the polymer-containing column. The time from injection to elution of the marker (t_M) and vapor (t_R) and the width at half height of the resulting chromatographic peaks are noted from the chart recorder output. Figure 1 gives a schematic representation of the chromatographic system and Figure 2 a typical chromatogram of the inert marker peak and the probe peak with the various quantities of experimental interest indicated.

At low rates of carrier gas flow, the vapor or probe reaches a steady-state distribution between the vapor and polymer phase and the thermodynamics of polymer-solvent or polymer-migrant interaction can be studied. Since the probe concentration is very low, a condition of infinite dilution is approxi-

mated and the interaction parameter χ^{∞} can be obtained. At high carrier gas flow rates, the equilibrium state is not approached and the kinetics of polymer-solvent interactions can be studied. The diffusion constant of the probe in the polymer can be determined at low probe concentrations.

The parameter directly measured in IGC experiments is the retention volume or the volume of carrier gas required to elute the injected probe. The adjusted retention volume, V_R', corrects for dead volume in the system and is given by the equation:

$$V_R' = (t_R - t_M)\dot{V} \tag{1}$$

where $\dot{V}$ is the volumetric flow rate. A correction for nonuniform flow velocity along the column length is required in order for the final specific retention volume (V_g) equation to be obtained:

$$V_g = \frac{273.2\ j\ V_R'}{T_c\ W_2} \tag{2}$$

where j is the velocity correction:

$$j = \frac{3}{2}\left[\frac{(p_i/p_o)^2 - 1}{(p_i/p_o)^3 - 1}\right] \tag{3}$$

p_i and p_o the column inlet and outlet pressure respectively, T_c the column temperature and W_2 the weight of polymer phase in the column. V_g should also be corrected for carrier gas nonideality and vapor-carrier gas interactions when very accurate results are required[5]. The symbol is denoted as V_g° when this is done.

Several considerations must be taken into account in the experimental determination of V_g. A sufficiently low concentration of the probe must be introduced to avoid operating in the nonlinear sorption isotherm range which can contribute to skewing of elution peaks and corresponding anomalous values of the net retention time as illustrated schematically in Figure 3. If the surface to volume ratio of

the supported polymer film is high, surface adsorption can make a significant contribution to the retention time. When both bulk and surface sorption mechanisms occur the measured net retention volume is given by the expression:

$$V_R = K_b W_2 + K_a A_2 \qquad (4)$$

where K_b and K_a are the bulk and surface partition coefficients and A_2 the total polymer surface area. The contribution of these concurrent retention mechanisms can be resolved by conducting experiments with several polymer films of differing surface to volume ratio. Carrier gas flow rate can also have an effect on V_g. If the flow rate is too rapid then partitioning of the probe molecules between the polymer and the vapor will be incomplete. A linear extrapolation of determinations at several flow rates to zero flow rate is often necessary to eliminate this influence. The capillary column studies of Lichtenthaler et al[6] suggest a relationship of the form:

$$V_g = a \cdot \exp(-b\dot{V}^2) \qquad (5)$$

a and b being temperature dependent constants characteristic of each polymer-solvent pair. Such a relationship was found to give a good fit to their data at low flow rates, however, its derivation has limited physical justification.

Generalized Semicrystalline Polymer Behavior

A retention diagram, a plot of log V_g vs. inverse temperature as shown in Figure 4, is constructed by determining V_g at a series of temperatures for a particular polymer-probe system. Several types of information about the polymer-probe system can be deduced from the retention diagram, as discussed in references 1-3, provided that the vapor pressure of the probe is accurately known as a function of temperature.

The retention diagram is usually linear below the glass transition temperature, as in region AB. This region generally corresponds to condensation and adsorption of the probe onto the polymer surface. The slope of the curve can be used to

give ΔH_a, the heat of adsorption, when the heat of vaporization of the probe and the surface area of the film are known, provided that a judicious choice of the probe molecule precludes penetration of the probe into the bulk polymer. Adsorption isotherms can be determined from analysis of the shape of the eluted probe pulse. A more common occurence is for both surface and bulk sorption to be operative in this region particularly for nonpolar systems. The contribution of each mechanism may be resolved by varying the polymer surface to volume ratio as described previously.

At point B on the diagram the polymer glass transition temperature is reached. The retention mechanism begins to shift from a predominantly surface mode at B to a largely bulk mode at C. Over this region the diffusion coefficient of the probe in the polymer increases by several orders of magnitude. IGC can be used to determine the glass transition temperature of a polymer by noting the first departure of a strongly adsorbed probe from the linear behavior exhibited below the glass transition.

As the temperature is increased, equilibrium absorption of the probe molecules in the amorphous phase will occur in region CD. Retention in this region is primarily attributed to solution in the bulk polymer but may also be caused by adsorption at the polymer-support, polymer-vapor or amorphous-crystalline interfaces and condensation on the polymer-vapor surface. If the portion of retention due to various modes of adsorption is evaluated experimentally, the enthalpy of mixing may be found from the slope of the retention diagram. Activity coefficients may also be calculated when the vapor pressure of the probe is known. From the activity coefficients and their temperature coefficients, the partial molal excess free energy, enthalpy and entropy of mixing and the polymer-solvent interaction parameter χ can be evaluated. The particular solution theory employed will determine the exact formulations of equations used to obtain these quantities. Operation at low flow rates and probe concentrations is preferable and the surface to volume ratio of the polymer film should be low. The utility

of GC in obtaining activity coefficients in low molecular weight systems has been demonstrated by the work of Tewari, Martire and Sheridan[7] who report results thought to be accurate to within 1% at four temperatures for sixty nine binary systems; eleven probes with n-tetracosane, n-triacontane and n-hexatriacontane as the sorbing phases.

Diffusion coefficients can also be determined above the glass transition temperature. Several conditions must be met in order to employ the van Deemter equation that allows calculation of the diffusion coefficient in the stationary phase. Polymer film thickness must be uniform, equilibration in the vapor phase must be instantaneous, and trans-column diffusion must be much faster than diffusion in the stationary phase. The experiments must be conducted at extremely low probe concentration, or extrapolated to infinite dilution, and peak broadening from other sources must be minimized. Under these conditions the flow rate dependence of the plate height yields the diffusion coefficient at the temperature of measurement.

Polymer melting begins at point D on the retention diagram. A perfectly ordered crystalline polymer would show a sharp increase in retention volume at the melting temperature but because of the distribution of crystal size and perfection normally present, melting occurs gradually as the temperature is increased to the final melting point. An increase in the amorphous content at the expense of crystalline regions impervious to penetration occurs as the melting region is traversed, giving rise to the gradual increase in V_g over region DF. Such information has been employed by Gray and Guillet[8] to obtain the degree of crystallinity at various temperatures in a study of LDPE and HDPE using a decane probe. In addition to melting and recrystallization as a function of temperature, isothermal crystallization of both materials was carried out. Crystallization half-times for LDPE agreed with previously reported studies conducted by dillatometric methods. The sharp discontinuity in slope at point F has been found to correspond to the complete disappearance of crystallinity and compares

favorably with the peak position of the melting endotherm determined by differential scanning calorimetry experiments.

The thermodynamic and kinetic parameters studied in region CD can also be determined for the polymer melt in region FG. The presence of polymer crystals in region CD reduces the retention volume by a constant amount over that predicted by extrapolation of line FG since the crystals present below T_m cannot be penetrated by the probe molecules.

Experimental Considerations

The use of IGC for the acquisition of physicochemical data requires a knowledge of some parameters that are unimportant in analytical GC, for example, the weight of polymer phase and the column outlet pressure. The many variables of the experiment must be controlled to ensure that the final V_g value calculated is sufficiently accurate. The studies of Wicarova and coworkers[9] on elution of hexane from a squalane column have shown that each experimental error can be considered to be random and independent of other error sources. They have treated the variance of V_g as a propagation of errors for the generalized function Q:

$$Q = a^m b^n \tag{6}$$

with the standard deviation of Q given by:

$$\sigma_Q = \left[\left(\frac{\partial Q}{\partial a} \right)_b^2 \sigma_a^2 + \left(\frac{\partial Q}{\partial b} \right)_a^2 \sigma_b^2 \right]^{1/2} \tag{7}$$

This relation can be applied to equation 2 and used to estimate the standard deviation of V_g as measured by the present IGC apparatus. Typical values of the measured variables, their estimated or calculated standard deviation and their contribution to the total variance of V_g are shown in Table 1 for a study of decane-SRM 1475 at 150°C carried out in our laboratory. The flow meter temperature, T_{fm}, and the vapor pressure of water at this temperature, p_w, are required

to correct the flow rate measured with a soap film flow meter downstream of the detector to the column temperature and outlet pressure. For an ideal gas the correction is of the form:

$$\dot{V} = \dot{V}_m \left(\frac{T_c}{T_{fm}}\right) \left(\frac{p-p_w}{p}\right) \tag{8}$$

where $\dot{V}_m$ is the experimentally measured volumetric flow rate and p the atmospheric pressure. The standard deviation of j is obtained by treating j, a function of the column inlet and outlet pressures as given by equation 3, in the same manner as the generalized function Q. Fluctuations in the column temperature have the greatest effect on the probe partition coefficient which in turn influences the retention time by the relation:

$$t_R = \frac{4\ell^2}{K} \eta \, (1 + k') \left[\frac{p_i^3 - p_o^3}{(p_i^2 - p_o^2)^2}\right] \tag{9}$$

where ℓ is the column length, K the packing permeability coefficient, η the carrier gas viscosity and k' the capacity factor, defined as:

$$k' = \frac{V_M}{V_L K_R} \tag{10}$$

where K_R is the partition coefficient and V_M and V_L the mobil and stationary phase volumes, repsectively. Equation 9 was developed by Guiochon[10] and has been employed by Goedert and Guiochon[11-13] in studies of the influence of pressure and temperature variations on the precision of measured retention times. Their findings show that the change in carrier gas viscosity with temperature is negligible compared with the variation of k'. The uncertainty of T_c is accounted for in the experimentally determined σ_{t_R} and is therefore not included as a separate source of variance in Table 1.

The overall standard deviation in V_g expected from contributions of random errors is found to be about 5%. The primary contributions to σ_{V_g} are the high

uncertatinty in determining the retention times and the column loading. As the concentration of polymer coated onto the glass beads is small, typically 0.5% by weight, precise determination of the polymer loading is critical for obtaining a reliable value of W_2. The most common methods reported in the literature are gravimetric in nature. Calcination or solvent refluxing are employed to remove the film from the beads and the weight of polymer deposited is obtained by difference. The accuracy of these methods has been evaluated for a SRM 1475 coated glass bead packing. Calcination in a 380°C oven gave a polymer weight fraction loading of 6.20×10^{-3} with standard deviation of ±3.5%. The weight change of a blank was less than 2% of the weight lost from destruction of the polymer. A loading of 6.97×10^{-3} with standard deviation of ±21% was found by solvent refluxing experiments. The weight change of the blank was sizeable in this instance, comparable to the weight lost from dissolution of the polymer. The calcination method gave more consistent results at these low loadings and was used for other determinations. A standard deviation as low as 0.5% has been achieved in one case. Retention times can be measured at higher precision by the use of a data handling system with a more rapid sampling rate or by employing a high chart speed recorder. A reduction in σ_{t_R} and σ_{t_M} to 0.2 s and σ_{w_2}/w_2 to 1% would allow the standard deviation of V_g to be reduced to 2%. Laub and Pecsok[14] suggest that the inherent precision in V_g is limited to about 0.5% by the determination of W_2.

Thermodynamic Studies

The specific retention volume is related to the polymer-probe interaction parameter, χ, through the activity coefficient of the probe molecule, a concept originally developed for GC by Porter, Deal and Stross[15]. Patterson and coworkers[16] have obtained an expression which relates the polymer-probe interaction parameter, χ^{∞}, derived from the Flory-Huggins lattice theory in the limit of vanishing probe concentration to V_g°

$$\chi^{\infty} = \ln \left[\frac{273.2\ R\ v_2}{V_g^{\circ} V_1 p_1^{\circ}} \right] - 1 - \frac{(B_{11}-V_1)p_1^{\circ}}{RT_c} \qquad (11)$$

where M_1 is the molecular weight, p_1° the pure liquid vapor pressure, V_1 the molar volume and B_{11} the gas phase second virial coefficient of the probe, v_2 the specific volume of the polymer and R the gas constant. These workers have derived a similar relation for the Flory equation of state theory which is given as:

$$\chi^{\infty} = \ln \left[\frac{273.2\ R\ v_2^*}{V_g^{\circ} V_1^* p_1^{\circ}} \right] - 1 - \frac{(B_{11}V_1)p_1^{\circ}}{RT_c} \qquad (12)$$

where the superscripted volumes correspond to the close-packed specific volumes of the hypothetical liquids at 0°K[16]. An equation of state treatment of polymer solutions based on the lattice fluid theory has been described by Sanchez and Lacombe[17-20]. The relation between χ^{∞} and V_g° is:

$$\chi^{\infty} = \ln \left[\frac{273.2\ R\ \rho_1^*}{V_g^{\circ} M_1 p_1^{\circ} \rho_2^*} \right] - 1 - \frac{(B_{11}-V_1)p_1^{\circ}}{RT_c} \qquad (13)$$

where ρ_1^* and ρ_2^* are the close-packed densities of probe and polymer. The theoretical relation for χ^{∞} is given by equation 73 of reference 20. The three theories yield an identical dependence of χ^{∞} on V_g°.

The interaction between a decane probe and NBS SRM 1475, a high density polyethylene, has been studied by IGC at this laboratory. The net retention time between a methane marker and the decane probe was determined from the flame ionization detector output as a function of decane concentration and carrier gas flow rate at 70 and 150°C. The net retention time was found to remain constant at 70°C for decane concentrations below about 2 ppm. Concentrations below this amount were employed in all subsequent measurements. A linear relationship between V_g and $\dot{V}$ and one of the form of equation 5 were used to extrapolate to zero flow rate and gave retention volumes identical within 3%. The range of flow rates examined is in-

sufficient to distinguish the preferable relation.

Two determinations of V_g were made at 70°C, one before and one after heating to 150°C. These are shown as 1 and 2 respectively in Figure 5. Different V_g values were obtained in each case, 234 and 258 cm^3/g respectively. Part of this 10% discrepancy could be due to a different percent crystallinity for each determination. Below the melting temperature, only the amorphous fraction contributes to bulk sorption and any change in the amount of amorphous material present will affect W_2, and in turn V_g, as can be seen from equation 2. The accuracy of the percent crystallinity determination probably limits the maximum reliability to which V_g may be determined below the polymer melting temperature. An IGC study of crystallization in Tenite 3310 high density polyethylene by Gray and Guillet[8] gives a V_g of 260 ml/g for decane at 70°C, in reasonable accord with the SRM 1475 results.

The limiting V_g at 150°C was found to be 70.2 cm^3/g. Previous studies by Braun et al[21] employed two linear polyethylenes, Marlex 50 and Marlex 6050, and decane at temperatures from 145 to 153°C. Schreiber and coworkers[22] have also studied Marlex 50 and decane over the same temperature region. These results are interpolated to 150°C and compared to SRM 1475-decane results in Table 2. The three sets of results for V_g differ from the average value of 72.5 cm^3/g by about 3.5%. The χ^∞ calculated from the Flory equation of state based theory of polymer solutions and the lattice fluid theory agree quite well, while the Flory-Huggins result is found to be somewhat lower. The agreement among the χ^∞ values calculated from various sources is about that expected based on other interlaboratory comparisons available in the literature[23,24]. These two studies also favorably compare IGC derived interaction parameters to those obtained by the classical method of vapor sorption for different rubbers above T_g with a variety of hydrocarbon probes.

Interaction parameters from IGC experiments on many polyethylene-probe combinations are given in the extensive study of Schreiber and coworkers[22]. For

these nonpolar systems, χ^{∞} values range between 0.2 and 0.4. When one component is polar the value of χ^{∞} is expected to be much larger in magnitude, for example, χ^{∞} values for PVC and ethanol, acetonitrile and hexane of 2.35, 1.85 and 1.76, respectively have been determined in IGC studies[25]. Large values of χ_p^{∞} can make a significant contribution to the partition coefficient calculated from the equation:

$$\ln K_o = \ln S + \chi_p^{\infty} + 1 \qquad (14)$$

derived in progress report NBSIR 79-1779.

Kinetic Studies

Diffusion coefficients can be determined from IGC experiments at high carrier gas flow rates where slow diffusion of the probe in the polymer phase can be studied. The affect of this diffusion process is to broaden the emerging chromatographic peaks. Other factors such as vapor transverse and longitudinal diffusion in the gas phase, non-instantaneous equilibration of the vapor with the stationary phase, chemical reaction at the interface and non-linearity of sorption isotherms can also cause peak broadening and must be minimized in a determination of the probe-polymer diffusion coefficient. These and other causes of broadening of elution peaks are reviewed by Littlewood[26]. When the primary mechanism is that of slow diffusion in the stationary phase, the diffusion coefficient is related to the height equivalent of the theoretical plate H by the van Deemter equation:

$$H = A + B/u + Cu \qquad (15)$$

where u is the linear flow velocity and A, B and C are constants having the following values:

$$A = 2\lambda d_p \qquad (16)$$

$$B = 2\gamma D_{gas} \tag{17}$$

$$C = \frac{8}{\pi^2} \frac{d_f^2}{D_{liq}} \frac{k'}{(1+k')^2} \tag{18}$$

where λ is a measure of packing irregularities, d_p is the average solid support particle diameter, γ a correction for the tortuosity of the gas flow in the column, D_{gas} the probe diffusivity in the gas phase, d_f the effective thickness of the polymer film, D_{liq} the diffusion coefficient of the probe in the polymer and k' the capacity factor. At high flow rates, a plot of H vs. u is linear and D_{liq} can be determined from the slope. Such a plot is illustrated schematically in Figure 6. Equation 18 is only applicable for a uniform carrier gas velocity profile. Several groups have derived a relation similar to equation 18 for the case of a parabolic velocity profile and a uniformly distributed film on a solid surface.

$$C = \frac{2}{3} \frac{d_f^2}{D_{liq}} \frac{k'}{(1+k')^2} \tag{19}$$

Purnell[27] gives an expression for the case of a thin continuous film on spherical particles obtained by approximating the packed column as a series of parallel capillaries:

$$C = \frac{1}{24k^2} \frac{d_p^2}{D_{liq}} \frac{(k')^3}{(1+k')^2} \tag{20}$$

This treatment eliminates the effective film thickness term. A non-equilibrium treatment of Giddings[28], taking into account peak dispersion from many sources, reduces to equation 19 for uniform film thickness but allows a distribution of film thickenss to be considered. Jones[29] has developed an extended van Deemter equation to take into account resistance to mass transfer in the gas phase, a distribution of carrier velocities, and a correlation between the two. These and other rate theories of chromatography have been discussed in several texts[27,28,30].

Several methods are available for determining the height equivalent to a theoretical plate. For a gaussian peak, any of the following expressions can be used:

$$H = \ell \left(\frac{w_i}{t_R}\right)^2 = \frac{\ell}{5.54}\left(\frac{w_{1/2}}{t_R}\right)^2 = \frac{\ell}{16}\left(\frac{w_b}{t_R}\right)^2 = \frac{\ell}{2\pi}\left(\frac{A}{ht_R}\right)^2 \qquad (21)$$

where ℓ is the column length, A the peak area and w the width at the inflection point, half height, and baseline as indicated in Figure 2.

We have made a preliminary determination of the diffusion coefficient of decane in SRM 1475 at 70°C by assuming a uniform polymer film thickness and applying equation 19. A diffusion coefficient of 2.2×10^{-8} cm^2/s is calculated. No other HDPE-decane IGC data are available, however Gray and Guillet[31] have studied LDPE-decane diffusion from 30 to 80°C. Interpolation of their results to 70°C gives a diffusion coefficient of 1.5×10^{-8} cm^2/s. Weight-loss gravimetric measurements on LDPE-decane from 30 to 50°C are available[32] and an extrapolation to 70°C gives $D = 1.6 \times 10^{-7}$ cm^2/s. The latter diffusion coefficient value is obtained at a much higher diffusant concentration than those present in the IGC determinations and as such is not strictly comparable to the IGC results. The result from the SRM 1475-decane determination are of an acceptable order of magnitude but further consideration is necessary to fully evaluate the technique. Rosolovskaya and Sal'vinski[33] have indicated that this method cannot be used for accurate measurements due to the difficulty in determining the effective thickness of the film. Scanning electron microscopy studies of solution coated polystyrene films used in IGC experiments have shown that the film thickness can be highly non-uniform at both low and high loadings[34]. These issues will be addressed in future IGC diffusion studies.

Few IGC studies of diffusion in polymers have been reported in the literature. Gray and Guillet[31] have studied decane and benzene diffusion in LDPE below the polymer melting point and LDPE-tetradecane in the melt. Braun and coworkers[35] studied diffusion of BHA, BHT, dodecane and three naphthalene

derivatives in molten LDPE. Millen and Hawkes[36] maintain that the results of the latter study should be calculated from equation 19 rather than equation 18 and present a table of corrected diffusion coefficients.

Gas Chromatography Determinations of the Purity of the Radiolabeled Alkanes

Radiolabeled alkanes employed in migration studies have been examined by GC using both a flame ionization detector for its extreme sensitivity and a thermal conductivity detector to allow for collection of the effluent peaks and subsequent determination of their radioactivity by liquid scintillation counting. This was accomplished by passing the TCD effluent through a heated transfer line to dry ice chilled counting vials containing heptane.

A mixture of labeled and unlabeled dodriacontane used in the preparation of samples for migration studies contains several impurities as can be seen from the chromatogram in Figure 7. The identity of these impurities can be determined from a plot of retention volume vs. carbon number as discussed in references 27 and 30. Several alkanes of known chain length were used to construct such a plot, as shown in Figure 8. This plot allows the identity of the impurity peaks to be estimated from their retention time. Such a procedure is best carried out with at least two stationary phases to insure unequivocal assignments, however, this was not done since the few stationary phases suitable for high temperature (>280°C) analysis of these nonvolatile materials are of similar selectivity. Assuming that the detector response to the impurities is the same as toward $C_{32}H_{66}$, the approximate concentration of the impurities are as follows: 0.2% $C_{31}H_{64}$, 0.05% $C_{28}H_{58}$, $C_{30}H_{62}$ and $C_{34}H_{70}$, 0.02% $C_{26}H_{54}$ and $C_{33}H_{68}$, and 0.01% $C_{29}H_{60}$. These impurities are also present in unlabeled dotriacontane obtained from two sources. Scintillation counting studies of fractions collected under the same chromatographic conditions but substituting a TCD for the FID indicates that about 2% of the total radioactivity arises from the more volatile alkanes which elute before $C_{32}H_{66}$ while another 2% is from the higher chain length impurities.

A similar analysis has shown that undiluted radiolabeled octadecane contains about 0.25% of $C_{17}H_{36}$ as the primary impurity with small amounts of less volatile impurities, about 0.01% $C_{20}H_{42}$ and 0.04% of an unidentified material. Only about 0.02% of the total radioactivity originates from the heptadecane.

The presence of radiolabeled alkane impurities may have to be taken into account in interpreting results from future migration experiments.

References

1. J. E. Guillet, Macromolecules, 4, 1669 (1970).

2. J. E. Guillet in Adv. in Analyt. Chem. and Inst., Vol. 11, H. Purnell, ed., John Wiley, New York (1973) p. 187.

3. J.-M. Braun and J. E. Guillet in Adv. in Polym. Sci., Vol. 21, Springer-Verlag, Berlin (1976) p. 107.

4. D. G. Gray in Prog. Polym. Sci., Vol. 5, Pergamon Press, London (1977) p. 1.

5. C. L. Young, Chromatogr. Revs., 10, 129 (1968).

6. R. N. Lichtenthaler, D. D. Liu and J. M. Prausnitz, Macromolecules, 7, 563 (1974).

7. Y. B. Tewari, D. E. Martire and J. P. Sheridan, J. Phys. Chem., 74, 2345 (1970).

8. D. G. Gray and J. E. Guillet, Macromolecules, 4, 129 (1971).

9. O. Wicarova, J. Novak and J. Janak, J. Chromatogr., 51, 3 (1970).

10. G. Guiochon, Chromatogr. Rev., 8, 1 (1967).

11. M. Goedert and G. Guiochon, Analyt. Chem., 42, 962 (1970).

12. M. Goedert and G. Guiochon, Analyt. Chem., 45, 1180 (1973).

13. M. Goedert and G. Guiochon, Analyt. Chem., 45, 1188 (1973).

14. R. J. Laub and R. L. Pecsok, Physicochemical Applications of Gas Chromatography, John Wiley, New York (1978) p. 55.

15. P. E. Porter, C. H. Deal and F. H. Stross, J. Amer. Chem. Soc., 78, 2999 (1956).

16. D. Patterson, Y. B. Tewari, H. P. Schreiber and J. E. Guillet, Macromolecules, 4, 356 (1971).

17. I. C. Sanchez and R. H. Lacombe, J. Phys. Chem., 80, 2352 (1976).

18. I. C. Sanchez and R. H. Lacombe, J. Polym. Sci., Letters, 15, 71 (1977).

19. R. H. Lacombe and I. C. Sanchez, J. Phys. Chem., 80, 2568 (1976).

20. I. C. Sanchez and R. H. Lacombe, Macromolecules, 11, 1145 (1978).

21. J.-M. Braun, M. Cutajar, J. E. Guillet, H. P. Schreiber, and D. Patterson, Macromolecules, 10, 864 (1977).

22. H. P. Schreiber, Y. B. Tewari and D. Patterson, J. Polym. Sci., Phys., 11, 15 (1973).

23. W. E. Hammers and C. L. DeLigny, J. Polym. Sci., Phys., 12, 2065 (1974).

24. Y.-K. Leung and B. E. Eichinger, J. Phys. Chem., 78, 60 (1974).

25. O. Olabisi, Macromolecules, 8, 316 (1975).

26. A. B. Littlewood, Gas Chromatography, 2nd ed., Academic Press, New York, 1970, ch. 6.

27. H. Purnell, Gas Chromatography, John Wiley, New York, 1962, ch. 8.

28. J. C. Giddings, Dynamics of Chromatography, Part 1, Marcel Dekker, New York, 1965.

29. W. L. Jones, Analyt. Chem., 33, 829 (1961).

30. S. DalNogare and R. S. Juvet, Gas-Liquid Chromatography, John Wiley, New York, 1962, ch. 5.

31. D. G. Gray and J. E. Guillet, Macromolecules, 6, 223 (1973).

32. D. W. McCall and W. P. Slichter, J. Amer. Chem. Soc., 80, 1861 (1958).

33. Y. N. Rosolovskaya and Y. Sal'vinski, Polym. Sci. USSR, 18, 1638 (1976).

34. G. J. Courval and D. G. Gray, Can. J. Chem., 54, 3496 (1976).

35. J. M. Braun, S. Poos and J. E. Guillet, J. Polym. Sci., Letters, 14, 257 (1976).

36. W. Millen and S. J. Hawkes, J. Polym. Sci., Letters, 15, 463 (1977).

Table 1

Standard deviation of variables for the elution of decane from a HDPE column at 150°C

Variable	Nominal Value, X	σ_X	$\frac{100\sigma_X}{X}$	$\left(\frac{dV_g}{dX}\right)^2 \sigma_X^2$
T_c	150°C	±0.3	0.1	a
W_2	100 mg	±2.0	2.0	2.00
t_R	40 s	±0.6	1.5	4.89
t_M	21 s	±0.6	2.9	4.89
$\dot{V}_m$	0.5 ml/s	$\pm 2.5 \times 10^{-3}$	0.5	0.13
T_{fm}	25°C	±0.2	0.1	3×10^{-4}
p	101 kPa	±0.7	0.7	3×10^{-4}
p_w	3.3 kPa	±0.03	0.8	4×10^{-4}
p_i	148 kPa	±0.3	0.2	b
p_o	107 kPa	±0.3	0.3	b
j	0.831	±0.009	1.0	0.55
V_g	70.8 ml/g	±3.5	5.0	$\Sigma = 12.4$

a) contributes to σ_{t_R}

b) used to calculate σ_j

Table 2

HDPE-decane Results at 150°C

Polymer	V_g, cm^3/g	χ^∞		
		FH	FES	LF
SRM 1475	70.2	0.24	0.38	0.37
Marlex 50	69.9[a]			
Marlex 50	74.6[b]	0.18	0.32	0.30
Marlex 6050	75.1[b]			

a) interpolated from data of reference 22.

b) interpolated from data of reference 21.

Figure V-1

Schematic Drawing of a Gas Chromatoraphic System

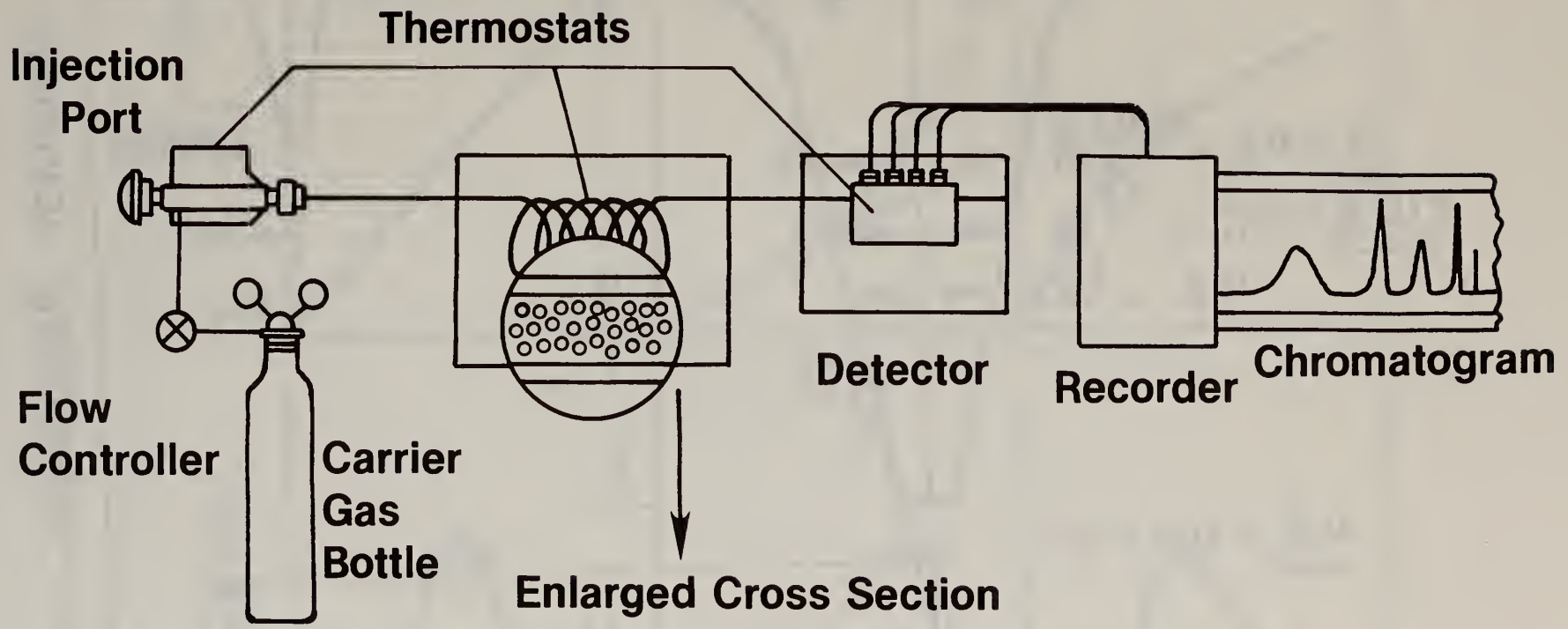

Elution chromatogram showing a marker peak at t_M and a probe peak at t_R

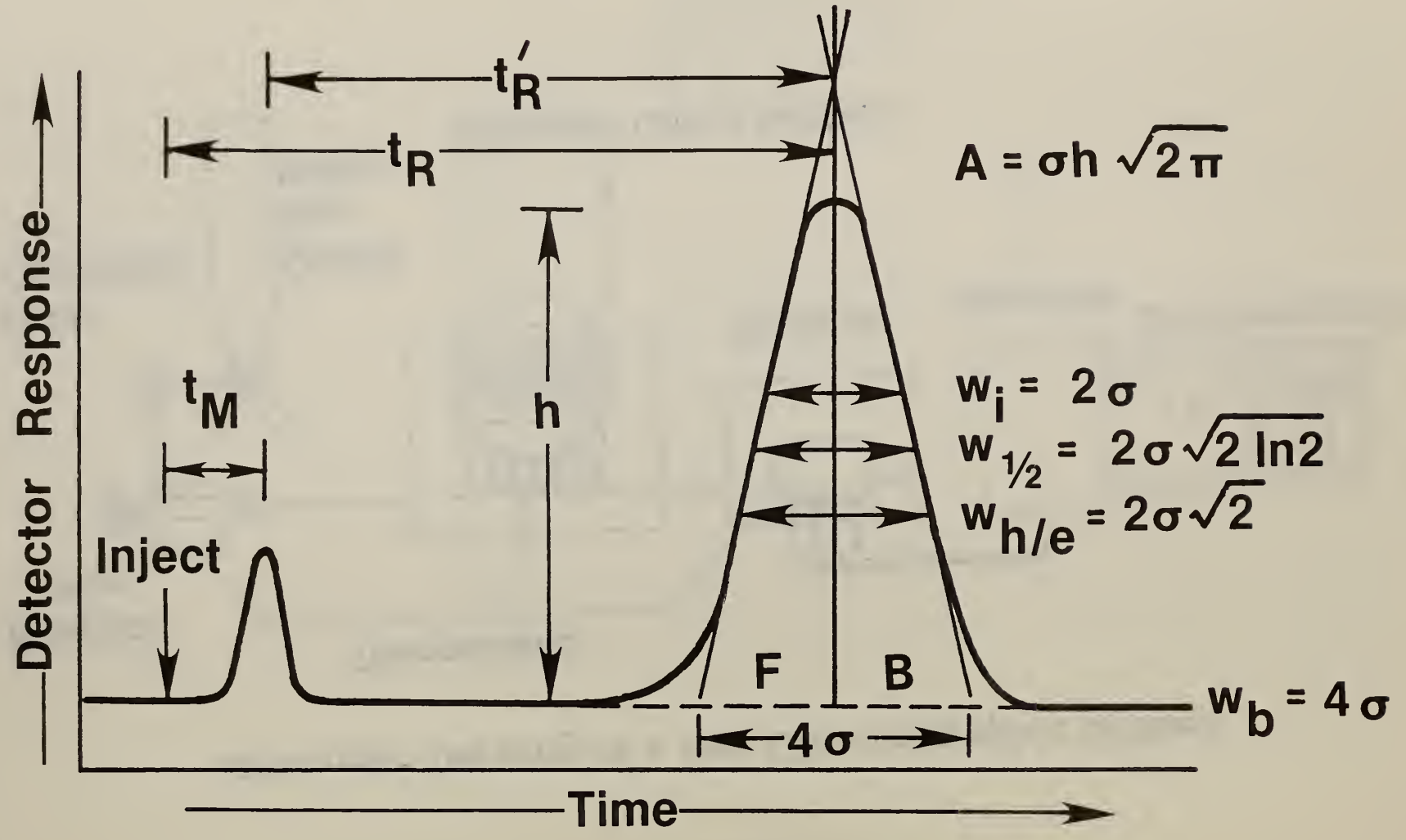

Figure V-3

Shape of isotherms and resulting peaks

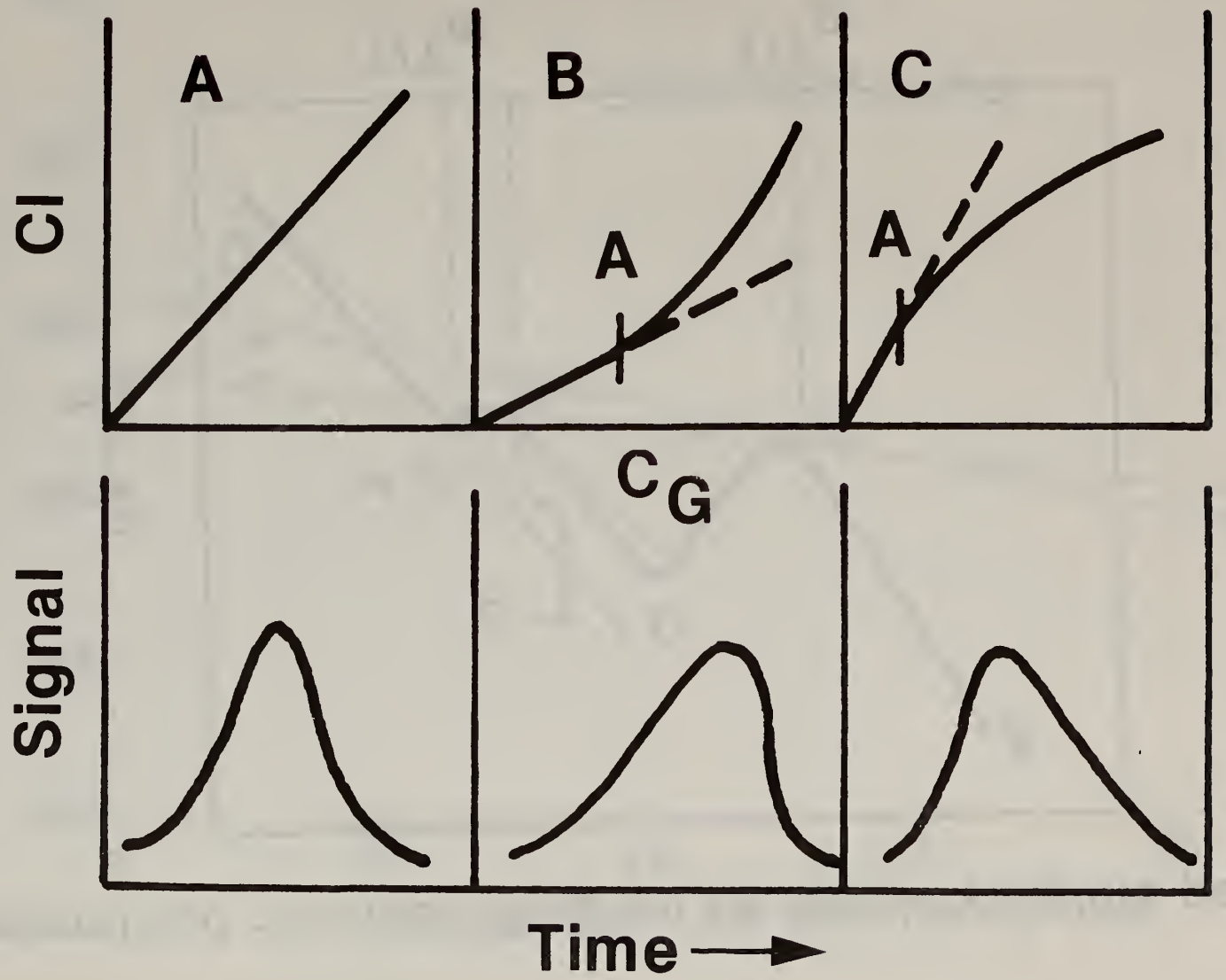

Figure V-4

Generalized retention diagram for semicrystalline polymer

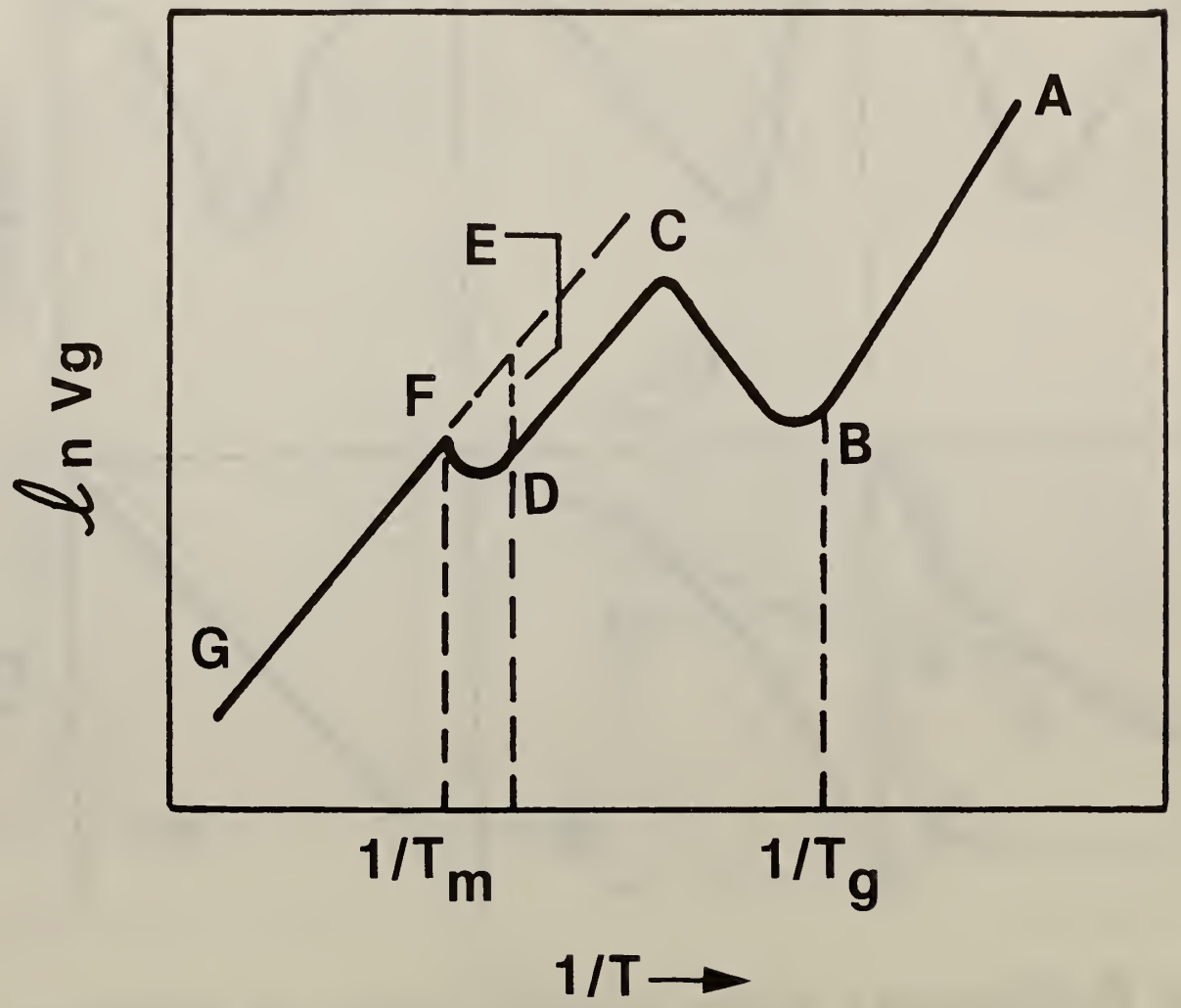

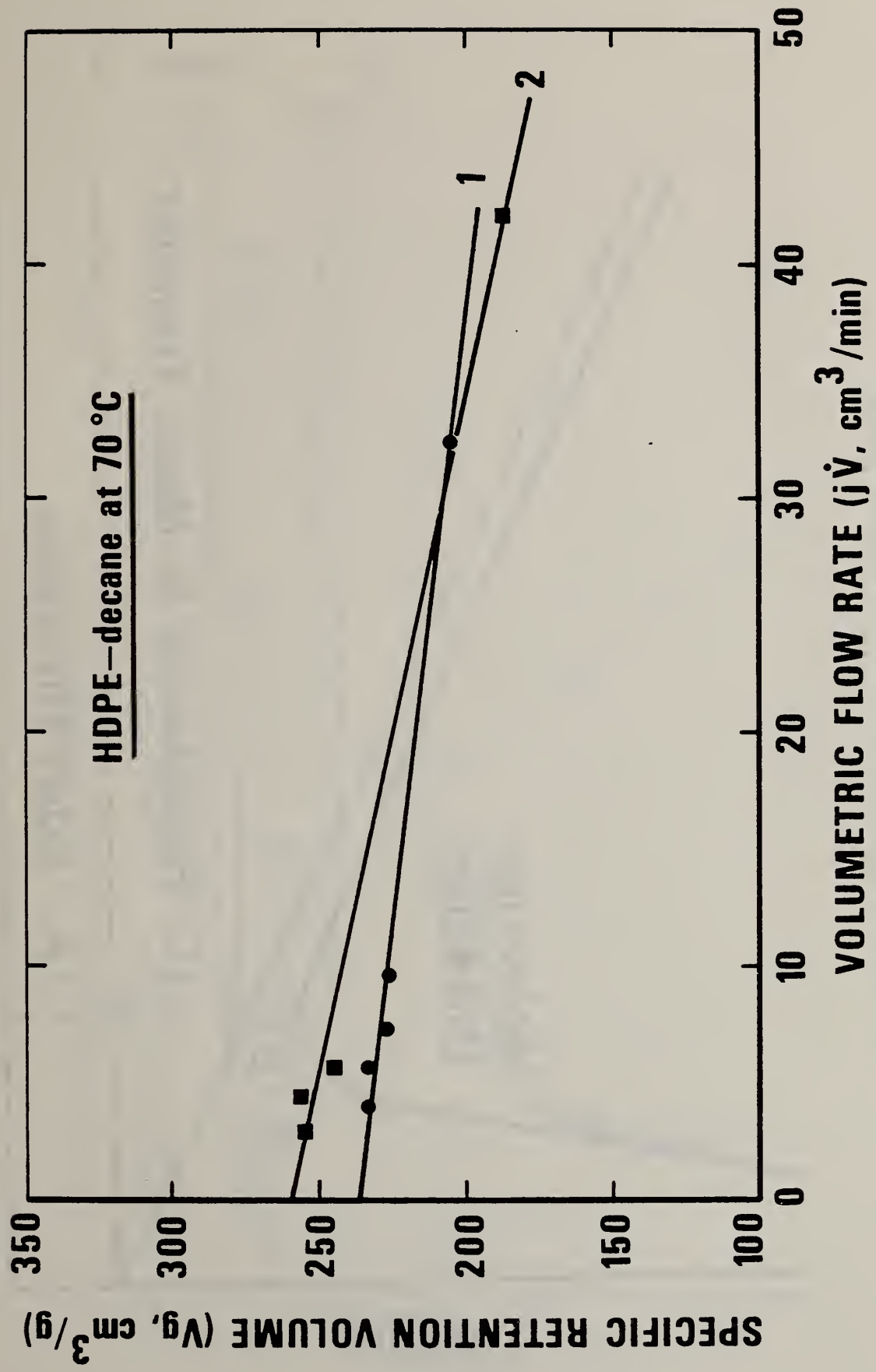
HDPE—decane at 70 °C
1
2
SPECIFIC RETENTION VOLUME (V_g, cm^3/g)
VOLUMETRIC FLOW RATE ($j\dot{V}$, cm^3/min)
350
300
250
200
150
100
0
10
20
30
40
50

Figure V-5

HETP Against Gas Velocity

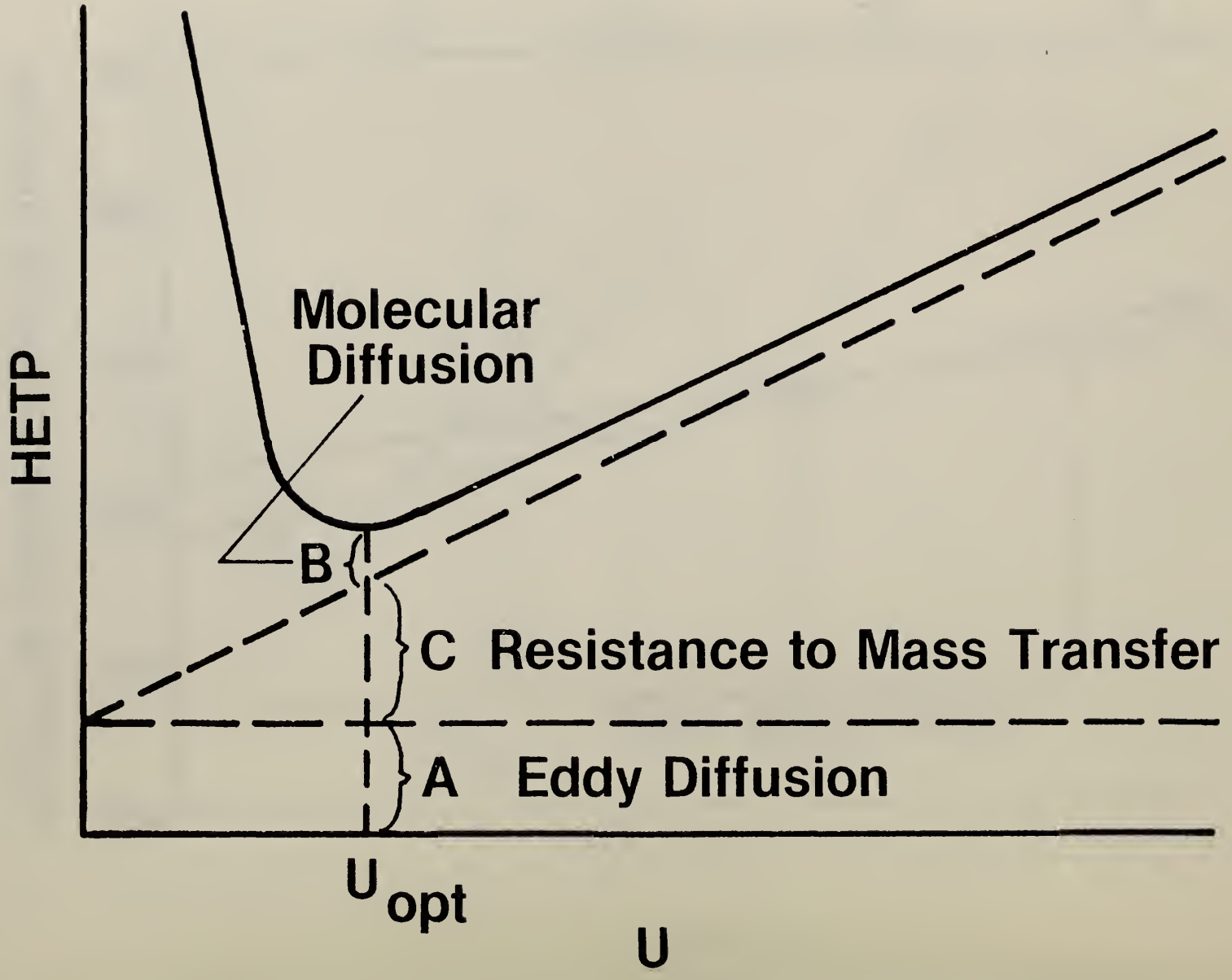

Figure V-6

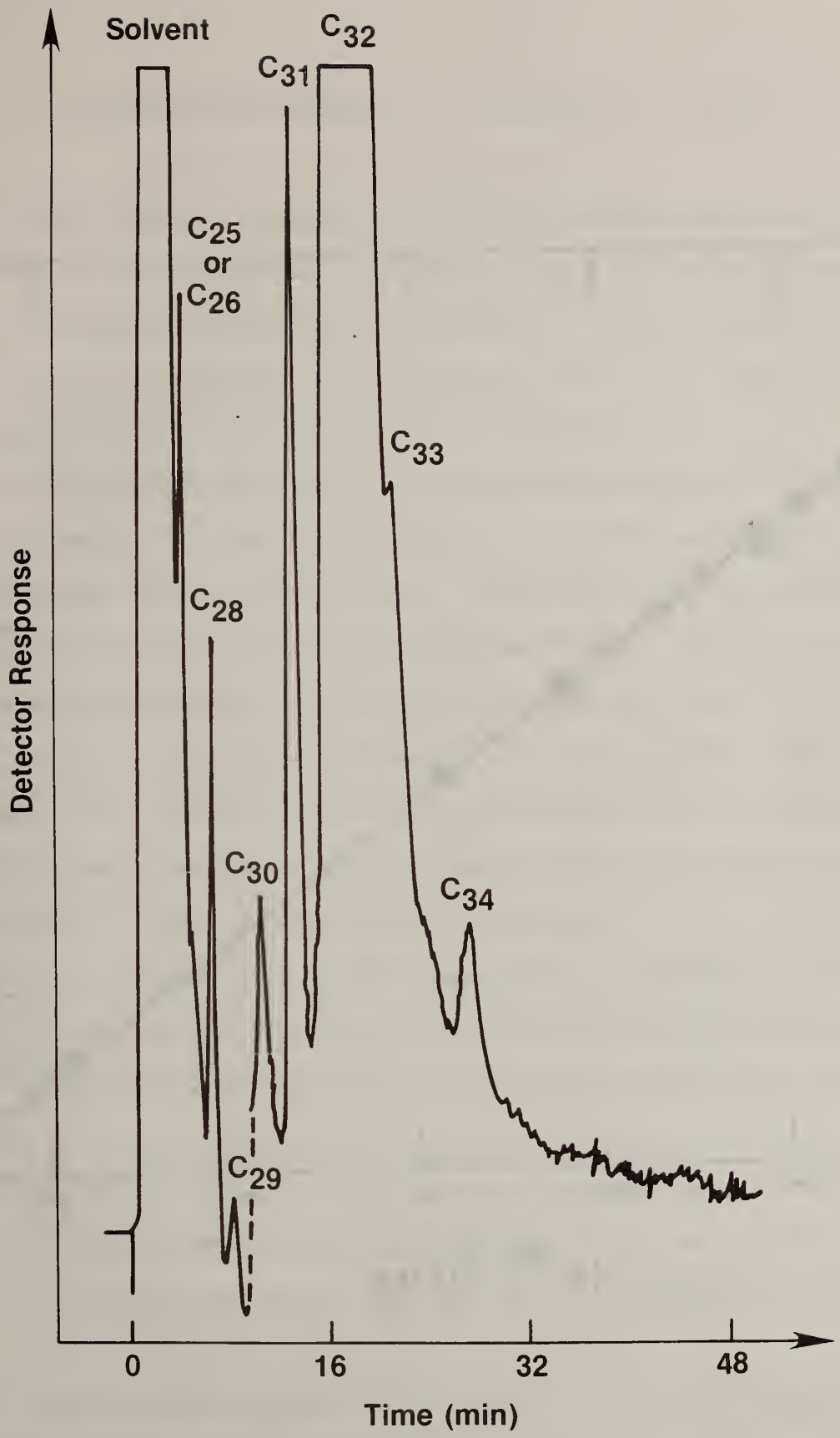
Solvent
C32
C31
C25
or
C26
C33
C28
C30
C34
C29
Detector Response
0
16
32
48
Time (min)

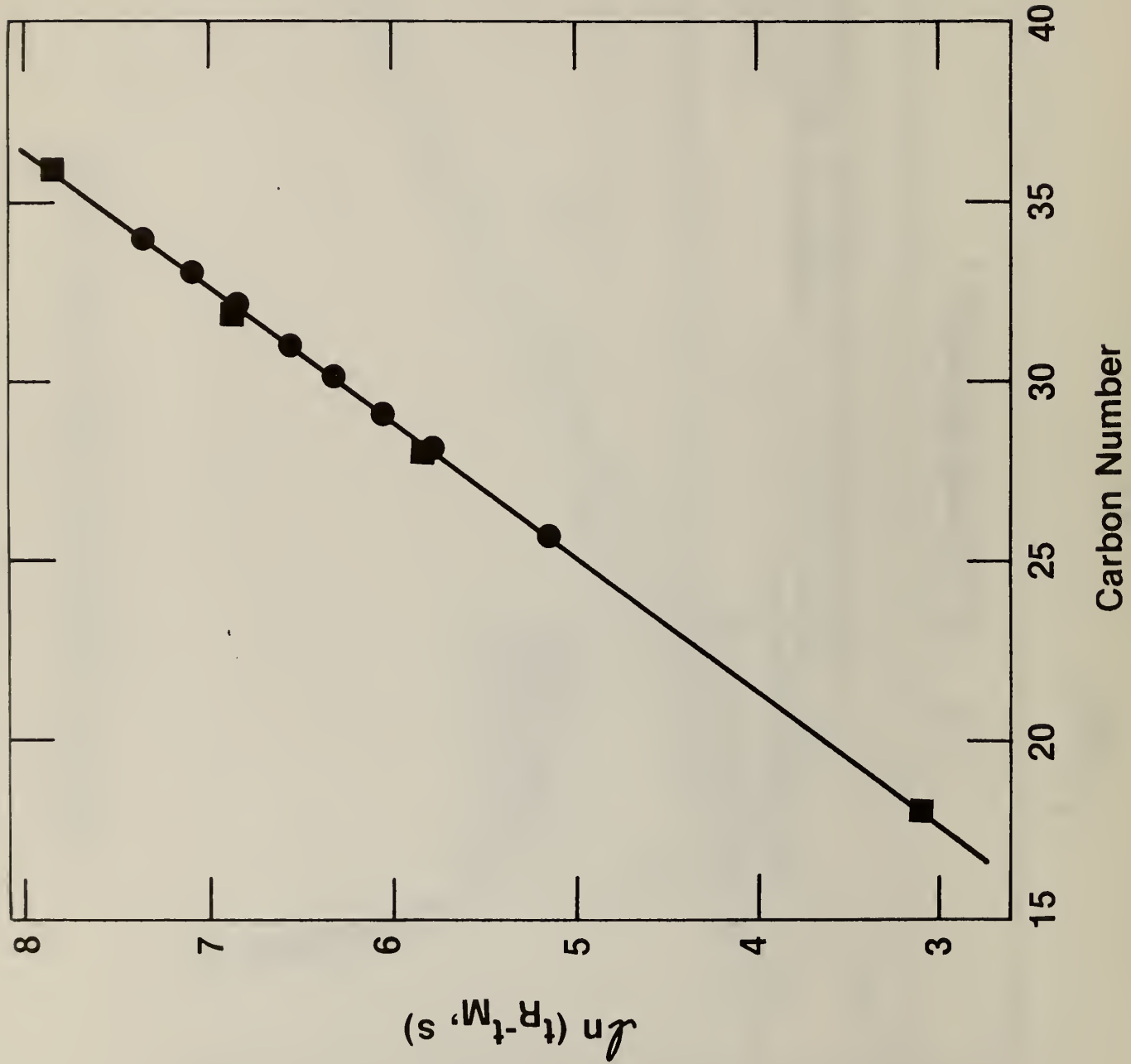
8
7
6
5
4
3
15
20
25
30
35
40
Carbon Number
ln (tR-tM, s)

VI. Experimental Measurements of Migration by Extraction

Of the four important branching points in the Decision Making Tree (DMT) -- M_0, C_s, K and D -- we are attempting to study at least the latter two parameters, partition coefficient K and diffusion coefficient D. The third parameter, solubility C_s, may also be studied, as it is closely related to K. The original amount of migrant present in the polymer is considered known.

We have studied the migration of oligomers and antioxidants from two base polymers -- branched (low density) or linear (high density) polyethylene. Three migrants are under study -- two oligomers: n-octadecane and n-dotriacotane, and an antioxidant: BHT (3,5-di-tert-butyl-4-hydroxytoluene). Five pure solvents are used -- two non-polar solvents: n-heptane and n-octadecane, and three polar solvents: corn oil, ethanol and trioctanoin. One mixed solvent system, ethanol-water, is also used. The migration studies are carried out at two temperatures, 60 and 30°C, to show temperature effect. Sample plaques of different thicknesses are also studied to show the correlation of thickness.

Only a few of the n-$C_{32}H_{66}$ and BHT observations are completed at this time, therefore, the details of these observations are not given here in this report.

The following highlights are related to n-$C_{18}H_{38}$ migration from polyethylene only.

Fickian behavior, i.e., the amount migrated is proportional to $t^{1/2}$ for up to $M_t/M_\infty=0.6$, is only observed in the following cases: (a) from polyethylene samples saturated with n-$C_{18}H_{38}$ into C_7H_{16} or $C_{18}H_{38}$, (b) from branched polyethylene into ethanol.

Near Fickian behavior is observed for ethanol, oil and trioctanoin extractions at high temperatures or for absorption experiments.

In poor solvents, near linear t behavior is observed.

Solvent absorption or swelling tends to increase the migration.

Migration kinetics in corn oil, ethanol and trioctanoin are practically identical.

Solubility of n-$C_{18}H_{38}$ in ethanol-water varies over a range covering six orders of magnitude.

Partitioning of migrant in polymer and the surrounding solvent has been observed.

Partition coefficients may also be estimated from solubilities.

At low partition coefficients, absorption of migrant into polymer from the surrounding media is possible.

Besides the effect of migrant, polymer and solvent, rate of migration depends on the level or concentration of the initial migrant in polymer, temperature as well as crystallinity.

Effect of crystallinity is minimized either in the case of saturated migrant or in the case of poor solvent.

Materials

(a) Polymeric Materials

The base polymers used in this report are the two National Bureau of Standards Standard Reference Materials (NBS-SRM) 1475 and 1476 for linear and branched polyethylene (whole polymers), respectively. These two SRMs have been well characterized*. The essential characteristics of these two materials are listed in Table E-1.

(b) Radioactive Tracers

Two n-paraffins, octadecane and dotriacontane, are used to spike the oligomer level of the polyethylene samples for oligomer migration studies. A commonly used antioxidant, BHT or 3,5-di-tert-butyl-4-hydroxy toluene, are used for the study of

*cf. NBS Special Publication 260-42, September 1972, and Certificates for National Bureau of Standards Standard Reference Material 1475 and 1476, November, 1969.

TABLE E-1

Characteristics of Polyethylene

		Linear SRM 1475	Branched SRM 1476
Gel Permeation Chromatography	M_n	18,310	
	M_w	53,070	
Light Scattering	M_w	52,000	
[η]	CN	0.890	0.8132
130°C	TCB	1.010	0.9024
dl/g	DHN	1.180	1.042
Melt Flow Rate, g/10 min.		2.07	1.19
ρ g/cm^3		0.97844	0.9312

CN -- 1-chloronaphthalene

TCB -- 1,2,4-trichlorobenzene

DHN -- decahydronaphthalene

Melt Index by Procedure A, ASTM Method D 1238-65T, Test Condition D, 190°C, load 325 g for SRM 1475 and 2160 g for SRM 1476.

Density by ASTM Method D 1505-67; sample prepared by Procedure A, ASTM Method D 1928-68.

additive migration. The characteristics of these tracers are shown in Table E-2 for their specific activities and the minimum detection levels.

(c) Sample Plaque Preparation

The following procedure for the mixing of additives to the polymer stock and the molding of the sample plaques was chosen. A large quantity of polyethylene powder stock was prepared from either NBS-SRM 1475 or 1476 pellets first by dissolution in hot toluene or xylene. Most of the polyethylene precipitates out upon cooling. The precipitate, together with the residue obtained by evaporating the solvent, was dried in a vacuum oven to remove the last trace of solvent.

To a quantity of the polyethylene powder stock, a specific amount of labeled additive dissolved in a highly volatile solvent is mixed. The mixture is then evaporated to dryness in a rotary evaporator, together with a number of glass beads to act as a ball mill, under reduced pressures at relatively low temperatures and further dried in a vacuum oven.

The mixture is then compression molded in a hydraulic press operated at about 180°C. Plaques of 125 mm x 125 mm or less are molded with brass or stainless steel shim stocks of appropriate thickness sandwiched between two sheets of teflon or teflon coated plates. The teflon surfaces are used for the easy removal of the sample plaques without the aid or contamination of mold release agents.

Sample Coding Scheme and Sample Plaque Designations

Only a small modification of the coding scheme detailed in the Semi-Annual Report for the period (October 1, 1978 - March 31, 1979) was required, such that the fractional notation for the composition of solvent mixture was replaced by the percentage notation. This change was necessary in order that the coding scheme is compatible with the code for file and element names that are acceptable by our central computing system.

The code sequence is

TABLE E-2

Characteristics of Radioactive Tracers

	μC_i/mg	ng/25 dpm
n-$C_{18}H_{38}$-1-^{14}C	86.0	0.13
	13.3	0.83
n-$C_{32}H_{66}$-16,17-^{14}C	45.5	0.25
3,5-di-tert-butyl-4-hydroxytoluene-7-^{14}C (BHT)	57.9	0.19

(1) First Character -- Solvent Type

C: Corn Oil

E: Ethanol (the numeral following the letter E denotes the percentage ethanol content of the composition of aqueous ethanol mixtures)

H: n-Heptane

O: n-Octadecane

T: Trioctanoin

(2) Second Character -- Sample Plaque Designation

Refer to Table E-3

(3) Extraction temperature in °C follows the second character

(4) Third Character -- Condition of Extraction

No third character: simulated infinite bath or unlimited volume extraction

L: Limited volume extraction

R: Reverse of extraction -- absorption

(5) Additional experiments with identical experimental conditions are distinguished by a dashed line followed by a number.

For example, E50M60R indicates an absorption experiment on a branched polyethylene sample M, which contains no labeled octadecane additive, carried out in 50% aqueous ethanol at 60°C.

Experimental Methods

Two extraction methods were used, i.e., (1) continuous extraction into limited solvent volume and (2) discrete extraction into simulated infinite solvent volume.

In method (1) an extraction vial of 25 ml in volume with a teflon valved cap is used. The solvent in the vial will only meet glass walls and the teflon surfaces during normal experimental processes. A silicone plug is situated above the valve. A small area of the silicon rubber, less than 1 mm in diameter

TABLE E-3

Sample Plaque Designations

		% $C_{18}H_{38}$					% $C_{32}H_{66}$		% BHT
		0	0.01	1	5	10	0	1	0.01
	ℓ, cm								
Linear Polyethylene (SRM 1475)	0.02		D	B	F				
	0.07	N	C	A,L	E		S	T	U
	0.26		K						
Branched Polyethylene (SRM 1476)	0.02							Q	
	0.07	M		G,I,J		H	R	P	V

and used as a septum for the hypodermic needle, may be exposed to the solvent vapor. The polymer sample may sometimes be surrounded by a nichrome or stainless steel screen to prevent it from sticking to the walls or another sample if more than one piece is being extracted in the same vial or if the sample has lower density than the solvent.

The total amount extracted, M_t, at time t is

$$M_t = C_{st}W_{st} + \sum_{i=1}^{t-1} C_{si}W_{ai}$$

where C_s, W_s and W_a represent the concentration of the migrant, total weight of the solution (including that of the aliquot) and the weight of the aliquot, respectively. At equilibrium the partition coefficient is estimated as

$$k = \frac{C_{s\infty}}{C_{p\infty}} = \frac{C_{s\infty}}{M_0 - M_\infty} = \frac{C_{s\infty}W_p}{M_0 - M_\infty}$$

where M_0 is the amount of migrant originally present in the polymer of weight W_p, and M_∞ is the total amount extracted at long times calculated from the concentration, aliquot weights and solution weights as mentioned above.

In method (2), the polymer sample is immersed in about 10 ml of extracting solvent in a typical 20 ml liquid scintillation counting vial. At specific times the sample is removed from the solvent, rinsed and palced in another vial with fresh solvent to repeat the extraction process. The total amount extracted at time t is simply the sum of all extracts:

$$M_t = \sum_{i=1}^{t} M_i$$

Method (1) is able to yield information about the equilibrium partition coefficient at infinite extraction time. However, it suffers from rigid requirements of knowing accurately the ratio of aliquot versus total solution and of keeping track of materials lost during the sampling process for material balance

purposes. As extraction time increases, there is only very small change in the concentration of extracted material in the solution, whereas the weighing or ratio error may persist. Therefore, the results at long time or high degree of extraction will show considerable degree of scatter.

Method (2) is much simpler in operation, but simulates a condition of migration into infinite media, and is relatively free from aforementioned experimental difficulties. However, it cannot be used to generate partitioning information nor migration kinetics for migrant that is sparingly soluble in the solvent. It should only be used for convenience when the migrant is highly soluble or miscible with the solvent.

An absorption experiment, the reversal of extraction, can be performed similar to that of the limited volume extraction by starting with unlabeled polymer and labeled migrant in solution.

For all the methods mentioned the extraction vials are shaken inside a temperature controlled aluminum block on a shaking table at a rate of about 200 reciprocations per minute.

When the extraction process is ended, the residual radioactivity remaining in the polyethylene sample is extracted by dissolving the sample in toluene at high temperatures. We found that the single crystals or precipitates of polyethylene in the counting vial does not interfere with the counting efficiency beyond the normal scattering of the counting results.

Presentation of Results

The results of completed experiments on the extraction, as well as absorption, of octadecane into and from polyethylene are presented in the Appendix and summarized in Table E-4. Several slow experiments involving the extraction of octadecane are still in process, it may take another 3-6 months before leveling off occurs.

Only a few of the experiments on the extraction of $C_{32}H_{66}$ and BHT are com-

TABLE E--4A

Characteristics and Summary of Heptane and Octadecane Extractions

Sample Designation	Polymer	Density g/cm^3	Migrant Content %	Thickness cm	Specific Activity μ Ci/g	Sample Weight g	Exposed Area cm^2	Apparent $D_{max} \times 10^{-8}$ cm^2/s	Total Solvent Absorption %
HA24	L	.968	1	0.070	2.3	0.165	5.8	1.1	5.1
HA24L	L	.968	1	0.068	2.3	0.449	14.0	1.5	4.5
HA30	L	.968	1	0.071	2.1	0.149	4.8	1.5	4.5
HA60-1	L	.968	1	0.067	2.3	0.138	4.8	9.0	4.4
HA60-2	L	.968	1	0.069	2.3	0.150	5.3	9.5	5.2
HB24	L	.969	1	0.019	2.2	0.043	5.2	1.8	3.5
HB30	L	.969	1	0.019	2.1	0.034	4.0	2.0	3.3
HC24	L	.965	0.01	0.070	1.6	0.160	5.2	0.2	3.6
HC30	L	.965	0.01	0.069	1.7	0.141	4.9	0.3	4.0
HC60	L	.965	0.01	0.069	1.6	0.140	4.8	7.0	4.3
HD24	L	.969	0.01	0.023	1.0	0.054		0.2	1.9
HE30	L	.966	5	0.084	0.14	0.305	8.5	18.0	5.4
HG30	B	.928	1	0.062	0.018	0.213		4.3	7.1
HG60	B	.928	1	0.066	0.019	0.241	8.7	46.0	14.4
HH30	B		10	0.066	0.23	0.124		16.0	8.0
OA30	L	.968	1	0.072	2.1	0.138	4.7	0.2	5.4
OB60	L	.969	1	0.018	2.3	0.035	4.6	(3.0)	5.0
OC30	L	.965	0.01	0.069	1.7	0.182	6.2	0.2	5.4
OC60	L	.965	0.01	0.069	1.3	0.157	5.3	2.8	5.1
OE30	L	.966	5	0.089	0.12	0.310	8.3	4.5	4.8
OE60	L	.966	5	0.085	0.11	0.325	9.0	9.6	4.4
OF60	L	.966	5	0.027	0.13	0.146	11.7	17.0	5.2
OH30	B		10	0.065	0.24	0.098	3.6	3.9	10.5
OH60	B		10	0.065	0.23	0.099	3.7	22.0	10.0
OI30	B	.930	1	0.056	0.17	0.156	6.5	0.4	7.0
OI60	B	.930	1	0.056	0.17	0.152	6.4	8.4	7.3

TABLE E-4B

Characteristics and Summary of Corn Oil, Ethanol and Trioctanoin Extractions

Sample Designation	Polymer	Density g/cm^3	Migrant Content %	Thickness cm	Specific Activity μ Ci/g	Sample Weight g	Exposed Area cm^2	Apparent $D_{max} \times 10^{-8}$ cm^2/s	Total Solvent Absorption %
CA60L	L	.968	1	0.075	2.0	0.119	3.9	0.48	3.2
CC60L	L	.965	0.01	0.072	1.4	0.172	5.7	0.08	2.3
CG60	B	.928	1	0.067	0.021	0.209	7.4	3.5	1.5
EA60L	L	.968	1	0.073	1.9	0.152	5.0	0.43	1.0
EB24	L	.969	1	0.018	2.3	0.041	4.9	0.012	0.9
EB24L	L	.969	1	0.019	2.3	0.075	8.5	0.03	0.9
EB30L	L	.969	1	0.019	2.1	0.036	4.1	0.016	0.9
EB60	L	.969	1	0.019	1.8	0.051	6.1	0.8	1.7
EB60L	L	.969	1	0.019	2.1	0.059	6.9	0.4	
EC60L	L	.965	0.01	0.069	1.4	0.157	5.3	0.11	0.6
EG30	B	.928	1	0.062	0.017	0.190	7.3	0.055	0.5
EG60	B	.928	1	0.064	0.019	0.190	5.2	3.8	0.6
TA60L	L	.968	1	0.075	2.1	0.125	4.0	0.6	2.9
TC60L	L	.965	0.01	0.071	1.6	0.160	5.4	0.12	2.7
TG60	B	.928	1	0.064	0.022	0.171	3.5	4.0	2.2

TABLE E-4C

Characteristics and Summary of Ethanol/Water Mixture Extractions

Sample Designation	Polymer	Density g/cm^3	Migrant Content %	Thickness cm	Specific Activity μ Ci/g	Sample Weight g	Exposed Area cm^2	Apparent D_{max} X 10^{-8} cm^2/s	Total Solvent Absorption %	K C_s/C_p
E10C60L	L	.965	1	0.071	0.7	0.204	6.7	(2.0)	0.0	0.00003
E30C60L	L	.965	1	0.071	1.1	0.200	6.7	(0.4)	0.1	0.00006
E50A60L	L	.968	1	0.071	2.0	0.151	5.3	2.0	0.1	0.001
E50B60	L	.969	1	0.019	1.8	0.061	7.3	0.1	1.0	-----
E50B60L	L	.969	1	0.020	1.7	0.054	6.1	0.7	0.3	0.001
E50C60L	L	.965	0.01	0.071	1.7	0.122	4.1	2.0	0.2	0.0005
E50I30L	B	.930	1	0.057	0.17	0.154	6.5	0.8	0.1	0.0002
E50I60L	B	.930	1	0.056	0.17	0.154	6.3	3.0	0.1	0.0009
E50M60R	B	.929	0	0.064	0.0	0.204	7.5	4.5	0.2	0.0008
E50M60L	B	.929	(0.5)	0.064	2.7	0.204	7.5	4.0	0.0	0.0008
E50N60R	L	.965	0	0.064	0.0	0.204	8.0	6.0	0.1	-----
E50N60L	L	.965	(0.5)	0.064	2.4	0.204	8.0	3.7	0.0	0.0009
E70A60L	L	.965	1	0.074	1.9	0.236	7.4	1.0	0.3	0.027
E90A60L	L	.965	1	0.076	2.1	0.234	7.4	0.6	0.6	0.3
E90B60	L	.969	1	0.019	1.9	0.054	6.9	0.9	0.9	-----

TABLE E-4B

Characteristics and Summary of Corn Oil, Ethanol and Trioctanoin Extractions

Sample Designation	Polymer	Density g/cm^3	Migrant Content %	Thickness cm	Specific Activity μ Ci/g	Sample Weight g	Exposed Area cm^2	Apparent D_{max} X 10^{-8} cm^2/s	Total Solvent Absorption %
CA60L	L	.968	1	0.075	2.0	0.119	3.9	0.48	3.2
CC60L	L	.965	0.01	0.072	1.4	0.172	5.7	0.08	2.3
CG60	B	.928	1	0.067	0.021	0.209	7.4	3.5	1.5
EA60L	L	.968	1	0.073	1.9	0.152	5.0	0.43	1.0
EB24	L	.969	1	0.018	2.3	0.041	4.9	0.012	0.9
EB24L	L	.969	1	0.019	2.3	0.075	8.5	0.03	0.9
EB30L	L	.969	1	0.019	2.1	0.036	4.1	0.016	0.9
EB60	L	.969	1	0.019	1.8	0.051	6.1	0.8	1.7
EB60L	L	.969	1	0.019	2.1	0.059	6.9	0.4	
EC60L	L	.965	0.01	0.069	1.4	0.157	5.3	0.11	0.6
EG30	B	.928	1	0.062	0.017	0.190	7.3	0.055	0.5
EG60	B	.928	1	0.064	0.019	0.190	5.2	3.8	0.6
TA60L	L	.968	1	0.075	2.1	0.125	4.0	0.6	2.9
TC60L	L	.965	0.01	0.071	1.6	0.160	5.4	0.12	2.7
TG60	B	.928	1	0.064	0.022	0.171	3.5	4.0	2.2

TABLE E-4C

Characteristics and Summary of Ethanol/Water Mixture Extractions

Sample Designation	Polymer	Density g/cm^3	Migrant Content %	Thickness cm	Specific Activity μ Ci/g	Sample Weight g	Exposed Area cm^2	Apparent D_{max} X 10^{-8} cm^2/s	Total Solvent Absorption %	K C_s/C_p
E10C60L	L	.965	1	0.071	0.7	0.204	6.7	(2.0)	0.0	0.00003
E30C60L	L	.965	1	0.071	1.1	0.200	6.7	(0.4)	0.1	0.00006
E50A60L	L	.968	1	0.071	2.0	0.151	5.3	2.0	0.1	0.001
E50B60	L	.969	1	0.019	1.8	0.061	7.3	0.1	1.0	-----
E50B60L	L	.969	1	0.020	1.7	0.054	6.1	0.7	0.3	0.001
E50C60L	L	.965	0.01	0.071	1.7	0.122	4.1	2.0	0.2	0.0005
E50I30L	B	.930	1	0.057	0.17	0.154	6.5	0.8	0.1	0.0002
E50I60L	B	.930	1	0.056	0.17	0.154	6.3	3.0	0.1	0.0009
E50M60R	B	.929	0	0.064	0.0	0.204	7.5	4.5	0.2	0.0008
E50M60L	B	.929	(0.5)	0.064	2.7	0.204	7.5	4.0	0.0	0.0008
E50N60R	L	.965	0	0.064	0.0	0.204	8.0	6.0	0.1	-----
E50N60L	L	.965	(0.5)	0.064	2.4	0.204	8.0	3.7	0.0	0.0009
E70A60L	L	.965	1	0.074	1.9	0.236	7.4	1.0	0.3	0.027
E90A60L	L	.965	1	0.076	2.1	0.234	7.4	0.6	0.6	0.3
E90B60	L	.969	1	0.019	1.9	0.054	6.9	0.9	0.9	-----

pleted, therefore it would be more desirable to discuss them when more information is available. Some preliminary information indicates that the migration of $C_{32}H_{66}$ into corn oil is about 20 times as slow in comparison with the migration of $C_{18}H_{38}$ at 60°C, and having a much greater temperature coefficient. The rate of migration of BHT into corn oil is at similar magnitudes as that of the $C_{32}H_{66}$.

In the tables of experimental results given in the Appendix, the fractional migrant migrated, M_t/M_0, was listed as a function of time. Other units of concern, for example, M_t/A may be calculated as (M_t/M_0) (C_0W_p/A) from the various parameters listed in Table E-3.

The results are generally shown as graphs of M_t/M_∞ versus t/L^2 to allow easier identification of other parameters. In cases $M_\infty \sim M_0$, M_t/M_0 is used in place of M_t/M_∞ for simplicity. Thickness scaling is generally observed except for a couple of isolated cases. The long dash lines or the dotted lines in the graphs denote the linear $t^{1/2}$ or t behavior, or a slope of 0.5 or 1 in the log M_t/M_∞ vs. log (t/L^2) plots, respectively.

In many cases, especially when a large amount of solvent swelling occurs, a pronounced enhancement from the normal linear $t^{1/2}$ behavior is seen. For semi-quantitative or trend analysis purposes, a D_{max} may be estimated from the maximum slope of a tangential line that passes through the origin in a M_t/M_∞ versus $t^{1/2}$ plot, or from the highest tangential line having a slope of 0.5 in a log (M_t/M_∞) versus log t/L^2 plot. Often in the extraction of octadecane by heptane, D_{max} is reached around $M_t/M_\infty \sim 0.8$. This is a much higher fraction than the linear $t^{1/2}$ region of a Fickian type diffusion behavior. Since most of the original migrant has now been removed from the polymer, the D_{max} so estimated represents the minimum of the diffusion coefficient under the equilibrium swollen condition. On the other hand, when a long initial linear $t^{1/2}$ behavior is observed, the D_i so estimated may represent the maximum diffusion coefficient for the original unswollen polymer. Since D and t are inversely proportional, the interpretation in

the following section may use either the change in D or t, the fastness or slowness, in describing the experiments.

The interpretation of the extraction results from Sample C and D requires special caution. The added amount of 0.01% labeled octadecane is probably not very far from the concentration of the original oligomer fraction of octadecane in polyethylene. The original oligomer fractions near the molecular weight of octadecane may also contribute to the total migration and having effects on the solubility.

The samples loaded with 1% of octadecane seem to lose some 10-20% of their activities in 6 mo. - 1 year period to the surroundings. No significant change in the efficiency of the liquid scintillation counter was detected over the same period.

The amount of solvent intake listed in Table E-4 is generally obtained from gravimetric method, and includes the amount of solvent absorbed to compensate for the loss of migrant. In the case of extraction or exchange of pre-saturated samples by unlabeled octadecane, the amount absorbed by the polymer may be checked both by the radioactivity as well as by gravimetric weightings.

Migration of n-Octadecane $C_{18}H_{38}$ into n-Heptane C_7H_{16}

Heptane has long been used as a fat-simulating solvent in a large number of studies for migration of indirect food additives. The study reported here focuses on the migratory behavior of an oligomer, n-octadecane, of polyethylene into n-heptane. The results are summarized in Table E-4A, listed in the Appendix and are shown in Figures E-1A, B and C for 24°C, 30°C and 60°C extractions, respectively. The following conclusions may be deduced from the results.

In general, thickness may be scaled as $M_t/M_0 \propto 1/\ell$, as seen by comparing (HA24, HA24L, HB24), (HC24, HD24) and (HA30, HB30). For high solubility or complete miscibility of the migrant in the solvent, there is no difference in the

results of the two methods of extraction, namely finite bath vs. infinite bath (HA24L, HA24).

The only experiment in this series that can be subjected to simple theoretical treatment is HE30, where the linear polyethylene sample has been saturated with the oligomer octadecane to about 5% weight content prior to the extraction experiment. The extraction or exchange of octadecane by heptane in this case behaves as a normal Fickian diffusion. The final content of heptane in the sample is also about 5%.

The migratory behavior is strongly dependent upon the initial oligomer content (HE30, HB30, HA30) since the oligomer may behave as a plasticizer or a swelling agent to the polymer. At lower oligomer content and lower temperatures, the initial extraction behavior seems to be linear with $t^{1/2}$. However, soon the migration rate increases due to the absorption of the solvent. Maximum extraction rate is reached when the solvent intake has reached its maximum. However as most of the migrant in the polymer has now been removed by the solvent, the apparent maximum rate is far below that of a pre-swollen sample. Therefore the apparent maximum diffusion coefficient is not a true characteristic of the migratory behavior but is an indication of the minimum diffusion coefficient under the combined swollen condition caused by the migrant and the solvent.

The influence of temperature and crystallinity of the polymer may also include the effects due to the more rapid absorption of solvent at higher temperature or at higher amorphous content if the polymer has not been fully saturated with low molecular weight hydrocarbons.

Migration of Labeled Octadecane into Unlabeled Octadecane

In order to gain more insight of the migratory behavior of oligomers of polyethylene into light hydrocarbons, the migration of octadecane in the polymer into octadecane as solvent was studied (Figures E-2A and B).

Similar conclusions may be drawn as that discussed in the section concerning

heptane as the solvent. When the polymer samples have been pre-saturated with 5% octadecane for linear polyethylene (OE30, OE60, OF60) and 10% for branched polyethylene (OH30, OH60), the subsequent extraction or exchange of octadecane follows a Fickian behavior. Deviations from a Fickian behavior become more pronounced at lower temperatures and at lower initial octadecane content. Judging from the results of the experiment OE60, it might have been performed on a sample not yet fully saturated with octadecane. The amount of labeled octadecane intake is estimated from the activities, which compares favorably with the gravimetrically determined amount of unlabeled species moved in later on.

A decrease in the diffusion coefficient by a factor of 2 to 4 from that of octadecane into heptane is observed. However, the crystallinity of the polymer seems to have no effect on the migration of octadecane into octadecane.

By increasing the temperature from 30 to 60°C, an increase of diffusion coefficient by a factor of about 5 is observed. Thus the effects from changing of good solvent and from changing of temperature could be viewed as having a common cause, changing in the viscosity of the solvent. Such a view may be tested by measuring the viscosity concerned, in the future.

The literature values* for the diffusion coefficient of octadecane in low density polyethylene are 4×10^{-8} and 16×10^{-8} cm^2/s at 40 and 60°C, respectively. These values are in good agreement with our findings of 4×10^{-8} and 22×10^{-8} at 30 and 60°C, respectively.

Migration of Octadecane into Corn Oil, Ethanol and Trioctanoin

By comparing the results of corn oil extractions (CA60L, CC60L, CG60) with that of heptane extractions (HA60, HC60, HG60), it appears that at an initial loading of 1% octadecane the diffusion constant changes by a factor of about 15. Much greater differences are seen at lower initial loading. It seems that even

*I. Auerbach, W. R. Miller, W. C. Kuryla and S. D. Gehman, J. Polym. Sci., 28, 129 (1958).

though both solvents may extract almost all of the migrant added to the polymer, the kinetic behavior is vastly different. Hence heptane should not be considered as a fat simulating solvent if migration kinetics may be involved. The estimated diffusion coefficients along with that for heptane extractions are listed in Table E-5.

In working with corn oil extractions, caution must be exercised to minimize or compensate for the effect of chemiluminescence during the liquid scintillation counting process. This is achieved by keeping the extract sample vial in the refrigerated counter overnite before counting data are accepted, and also by using the random coincidence monitor feature to detect and correct for the remaining single photon events.

Trioctanoin, a pure triglyceride, was selected as a fat-simulant, while it was rather readily available. Along with the results of corn oil and trioctanoin extractions, corresponding results of ethanol extractions on two linear and one branched polyethylene samples are compared together in Figure E-3. It is obvious that all three corresponding sets of extractions behave practically identical to each other, even the small irregularity at short times and low extraction level for Sample A and C shows up in each of the extractions. At 60°C, all the results at M_t/M_0 above 0.02 behave rather Fickian-like, especially for the cases of branched polyethylene samples.

Unlike the results of migration of octadecane into octadecane, there is an eight-fold increase in diffusion coefficient from linear to branched polyethylene. There appears also an five-fold increase in D when the initial octadecane loading changes from 0.01 to 1%.

It seems that, at least for the case of octadecane, anhydrous ethanol could act as a fat-simulant in a much more rational way than the use of heptane. One shall reserve the comments about general suitability until the results on $C_{32}H_{66}$ and BHT migrations, as well as results from 30°C extraction, are completed.

TABLE E-5

Diffusion Coefficients

$D_{max} \times 10^{-8}$ cm^2/s

Sample	Corn Oil	Ethanol	Trioctanoin	Heptane*
A, LPE 1%	0.48	0.43	0.6	9
C, LPE 0.01%	0.08	0.11	0.12	7
G, BPE 1%	3.5	3.8	4.0	46

Octadecane is miscible with corn oil and trioctanoin at temperatures above the melting point of n-$C_{18}H_{38}$. The solubilities rise sharply in a narrow temperature range just below the melting point of n-$C_{18}H_{38}$.

Migration of Octadecane into Ethanol

Results of extraction of octadecane by the more readily available anhydrous ethanol are represented in Fig. E-4A for 24 and 30°C and Fig. E-4B for 60°C. The results of extraction by 90% aqueous ethanol is also shown in Fig. E-4. Kinetically, the difference between the finite bath and infinite bath extractions, e.g., (EB24, EB24L) and (EB60, EB60L), are rather small. This is, however, a borderline case where the convenience of a infinite bath experiment should be abandoned in favor of a definitive finite bath experiment for kinetic as well as equilibrium studies. The solubilities of octadecane in the solvent now is finite. At 60°C the solubility of octadecane in anhydrous ethanol remained high at 23%. However, the solubilities in 90% ethanol at 60°C and in anhydrous ethanol at 30°C have dropped to about 3% and 11% respectively.

Therefore, at long times, indications of reaching an equilibrium partitioning of octadecane in the solvent and in the polymer may be seen from these two latter cases and from the lower temperature and aqueous ethanol experiments. There is definitely an influence of the original migrant level (EA60L, EC60L) and influence of the crystallinity of the base polymer (EA60L, EB60) to the diffusion coefficient. The magnitude of solvent intake and the subsequent enhancement of the migration rate are far less pronounced in ethanol than that in heptane. Fickian behavior is observed for the extraction of octadecane from branched polyethylene. Near Fickian behavior may be seen in other ethanol extractions. A greater temperature dependency is seen for ethanol than for heptane.

Migration of Octadecane into Ethanol/Water Mixtures

(a) Solubility and the Mixed Solvent System

One of the most important factors to consider, in order to determine the

amount of migration, is the solubility of the migrant in the solvent. The solubility of n-octadecane in ethanol-water system spans over a range of more than six orders of magnitude (Table E-6, Figure E-5). These results were first obtained by gravimetric observations and were later more precisely determined by means of ^{14}C-labeled octadecane. The reproducibilities of the data at low ethanol content are rather poor, partly due to evaporation of the solvent mixture and partly due to contamination problems. Any contamination during the sampling process by minute amount of undissolved suspension may cause an error in the orders of magnitude above that of the solution itself.

It was thought that the wide-range of solubilities of the ethanol-water system may be used to simulate a wide variety of solvents of interest. However, as we may conclude from the following that, unless meticulous care is taken, the extraction results may be somewhat difficult to interpret using ethanol-water mixtures as solvents. For extraction experiments lasting a long time, it is difficult to keep the evaporation through the sample container seals to a very low figure or to prevent the removal of some of the vapor phase during sampling process. Since the vapor phase is ethanol-rich, the remaining liquid composition drifts toward lower ethanol composition than the original composition. This results to a drastic change in the solubility as well as the partition coefficient. A better mixed solvent system should be rather non-volatile. Perhaps the system ethylene glycol-water would perform much better in this respect. In any event, the absorption of the more compatible component of the solvent system by the polymer may also change the composition of mixed solvent.

(b) Extraction Results

The results of migration of octadecane into a number of the ethanol-water mixtures are shown in Figure E-6A, where the amount migrated is normalized by the original amount of migrant in the polymer, M_0, and in Figure E-6B, where the amount migrated is normalized by the final amount migrated, M_∞. In certain

TABLE E-6

Solubility of n-$C_{18}H_{38}$ in Ethanol/Water System

Weight Fraction of $C_{18}H_{38}$

% C_2H_5OH	11°C	30°C	60°C
0	1.2×10^{-5}	1.5×10^{-7}	1.7×10^{-7}
5		5×10^{-6}	6×10^{-6}
10	1.5×10^{-6}	1×10^{-6}	8×10^{-6}
30		1.9×10^{-5}	2.5×10^{-5}
50	1.9×10^{-5}	1.1×10^{-4}	1.3×10^{-4}
75	3.7×10^{-4}	0.0018	0.004
90	0.00183	0.0156	0.0316
95	0.0036	0.0387	0.0736
100	0.0089	0.113	0.226

cases, where the loss of solvent is serious, the migrated amount or the solution activity starts to drop drastically after a maximum value was reached, due to the change in solubility and partition coefficient. This maximum amount of extraction is the lower bound corresponding to the equilibrium concentration value as dictated by the partition coefficient.

The migration behavior is Fickian-like at high ethanol content but changes toward a linear time dependency at lower ethanol content. When the polymer is only loaded with 0.01% of octadecane, the estimated partition coefficient may be lower than the actual value, since there is an undetermined amount of octadecane present in the original polymer at comparable levels. At such a low additive level, even the dissolution or extraction of species other than octadecane from the original polymer may also effect the observation of the partition coefficient for octadecane alone.

Some of the 50% aqueous ethanol extractions were subject to renewed extractions after each apparent equilibrium condition has been reached. Aside from the experimental result from E50B60L, all the results on 50% aqueous ethanol extractions at 60°C (Figure E-7A and B) seem to behave in similar fashion and magnitude, regardless of the crystallinity of the original polymer.

Figure E-8A and B show the results of 50% aqueous ethanol extraction on branched polyethylene samples at two different temperatures. The 30°C extraction seems to be about 4 times slower.

At low ethanol content, the solubility is low, therefore, a local partition equilibrium may easily be established by only a very small amount of migrant. The extraction of the migrant may depend more on the surface characteristics, mass transport kinetics similar to that of dissolution, as well as agitation. Although the eventual partition of the migrant is still determined by the partition coefficient.

(c) Partition Coefficient

Figure E-5 shows the observed partition coefficient from the experiments shown in E-6A and B. The partition coefficient, K, is defined, at equilibrium, as

$$K = \frac{C_s}{C_p} = \frac{M_s}{W_s + M_s} \cdot \frac{W_p + M_p}{M_p} \sim \frac{M_s}{W_s} \cdot \frac{W_p}{M_p}$$

where C and M represent the concentration and the weight of the migrant in either the solvent, s, or the polymer, p. W_p and W_s represent the weights of polymer or solvent, respectively.

As a first approximation, one may estimate a reasonable partition coefficient from the more readily available or more easily obtainable solubility data, such that

$$K \sim \frac{C_{s,sat}}{C_{p,sat}}$$

where $C_{s,sat}$ and $C_{p,sat}$ represent the independent saturation solubilities of the migrant concerned in the solvent and the polymer, respectively. The maximum level of swelling of the migrant in the polymer is taken as the saturation solubility of the migrant in the polymer. For octadecane in linear and branched polyethylene $C_{p,sat}$ is about 0.05 and 0.1, respectively. If the solubility is further normalized to the amorphous content of the polymer, then $C_{pa,sat}=0.25$, or $K_a=4C_{s,sat}$, where the subscript denotes the amorphous region of the polymer.

The lattice theories yield a relationship

$$\ln K = \ln C_s + \chi^{\infty} + 1$$

Since the parameter χ^{∞}, which characterizes the thermodynamic interaction at infinite dilution of the migrant with the polymer, usually falls in the range

$$0 < \chi^{\infty} < 2$$

It follows

$$2.7\ C_s < K < 20\ C_s$$

The observed partition coefficients are listed in Table E-7. These values compare favorably with the assumption of $K \sim C_{s,sat}/C_{p,sat}$ and are also within the range as predicted by lattice theories.

Migration of n-Octadecane into/from Polyethylene and 50/50 Ethanol/Water Mixture

When the distribution or partition coefficient is strongly in favor of the polymer, the absorption of a migrant from the solution into the polymer will cause a substantial change in the solution activity. Thus it is possible to study the migration phenomenon via absorption into the polymer, in addition to the commonly employed technique of extraction of the migrant out of the polymer. Let the parameter α be defined as

$$\alpha = K \frac{W_s}{W_p}$$

Therefore,

$$\frac{M_s}{M_0} = \frac{\alpha}{1+\alpha} \quad ,$$

where the total amount of migrant M_0 is defined as

$$M_0 = M_s + M_p$$

For extraction and absorption experiments, it is common to have

$$\frac{W_s}{W_p} \sim 100 \quad \text{or} \quad \alpha \sim 100\ k \ .$$

Under this condition, and neglecting the amount of aliquot removed for analysis (the weight of solvent W_s and the total amount of migrant available for redistribution will change slightly from the original amount), the following values

TABLE E-7

Partition Coefficients

of n-Octadecane in Aqueous Ethanol/Polyethylene

Sample	% Ethanol	$K = C_s/C_p$	Solubility, Weight Fraction $C_{18}H_{38}$
	30°C		
I, BPE	50	2×10^{-4}	1×10^{-4}
	60°C		
C, LPE	10	3×10^{-5}	8×10^{-6}
C, LPE	30	6×10^{-5}	2.5×10^{-5}
C, LPE	50	5×10^{-4}	1.3×10^{-4}
A, LPE	50	0.001	1.3×10^{-4}
B, LPE	50	0.001	1.3×10^{-4}
I, BPE	50	0.0009	1.3×10^{-4}
M, BPE	50	0.0008	1.3×10^{-4}
N, LPE	50	0.009	1.3×10^{-4}
A, LPE	70	0.027	0.002
A, LPE	90	(0.3)	0.032

may be estimated for equilibrium conditions:

K	M_s/M_0
1	0.99
0.1	0.90
0.01	0.50
0.001	0.091
0.0001	0.0099
0.00001	0.0010

Therefore, in an experiment where the solvent weight is 100 times that of the polymer weight, more than 90% of the migrant will be extracted if K is greater than 0.1. Alternatively, more than 90% of a migrant in the solution will be absorbed by the polymer if K is less than 0.001. If the migration kinetics are to be followed experimentally, it is quite possible to produce reliable data from extraction aliquots even at relatively low solution concentrations or small values of K, limited mainly by the background and the instrumental sensitivity. In absorption experiments, however, the important parameter is the change in the solution concentration from a relatively large C_s value. When the total change in C_s is small, the data will be imprecise. Therefore, the value of α should be less than 1 or K less than 0.01 at $W_s/W_p \sim 100$ for a substantial solution concentration change to occur during an absorption experiment.

Results from experiments involving absorption (immigration) of the migrant octadecane into branched and linear polyethylene samples (E50M60R, E50N60R) from a 2.5 ppm octadecane solution in 50% aqueous ethanol, and the subsequent extraction (emigration) experiments (E50M60L, E50N60L) are shown in Figure E-9A, where the solution activity is normalized by the total activity of the system, M_0, and in Figure E-9B, where the absorbed or extracted activity is normalized by the equilibrium amount migrated, M_∞, across the polymer/solvent interface. The partition coefficients for all four experiments reach a value about 0.001. The estimated maximum diffusion coefficients based on M_t/M_∞ are all about 4×10^{-8} cm^{-2}/s. Both of these figures compare favorably with the results of separate

extraction experiments (E50I60L, E50A60L, E50B60L). The two absorption and extraction experiments behave almost identical to each other, in spite of the differences in the crystallinity of the base polymer. Similar observations were noted as that for other experiments using 50% aqueous ethanol as solvent, therefore same comments will apply here. However, the absorption experiments show a quite Fickian-like behavior rather than the behavior of close to a linear time dependence as noted in the extraction experiments.

Figure E-1A

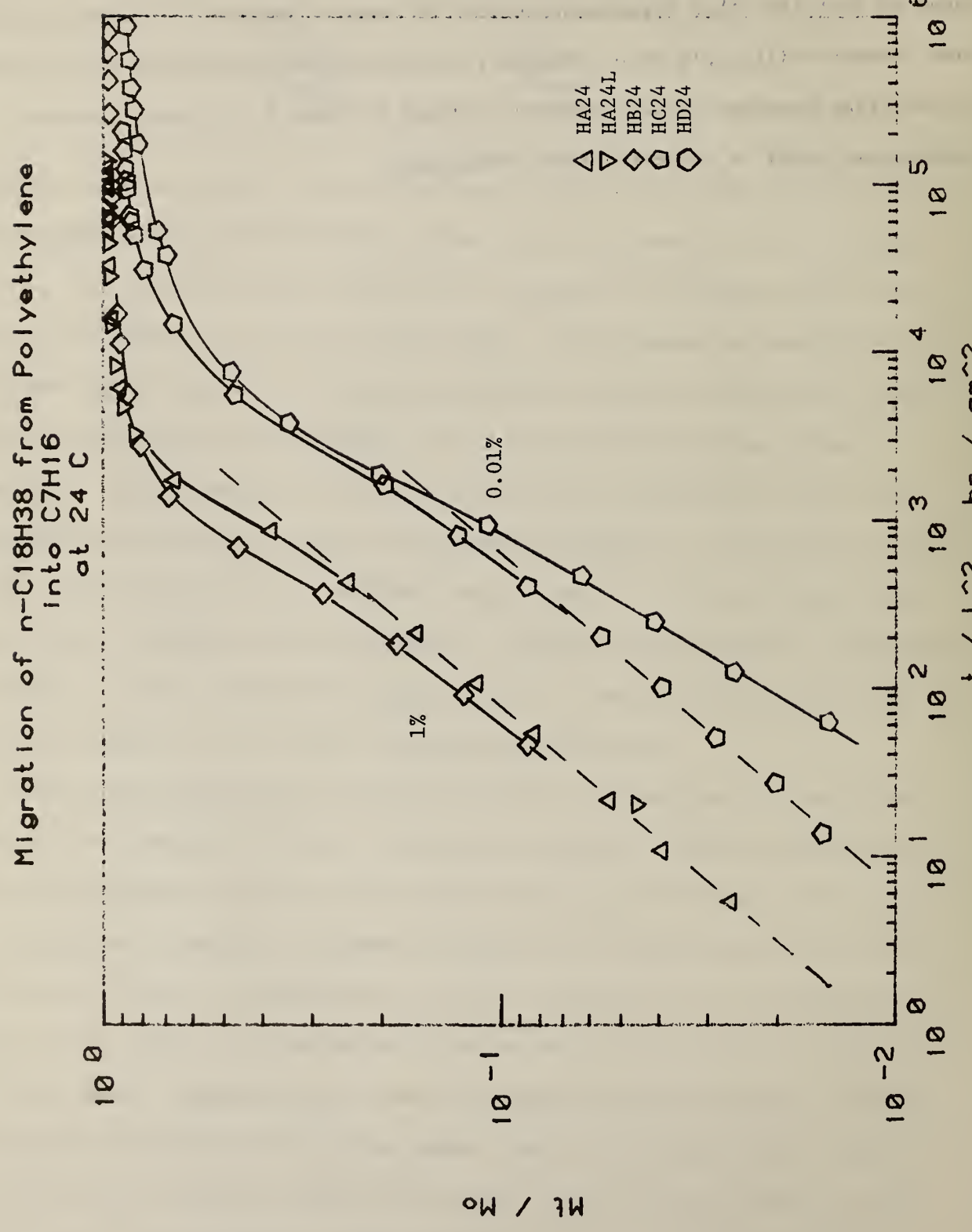
Migration of n-C18H38 from Polyethylene
into C7H16
at 24 C
HA24
HA24L
HB24
HC24
HD24
0.01%
1%
Mt / Mo
t / L^2 , hr / cm^2
10 0
10 -1
10 -2
10 0
10 1
10 2
10 3
10 4
10 5
10 6

Figure E-1B

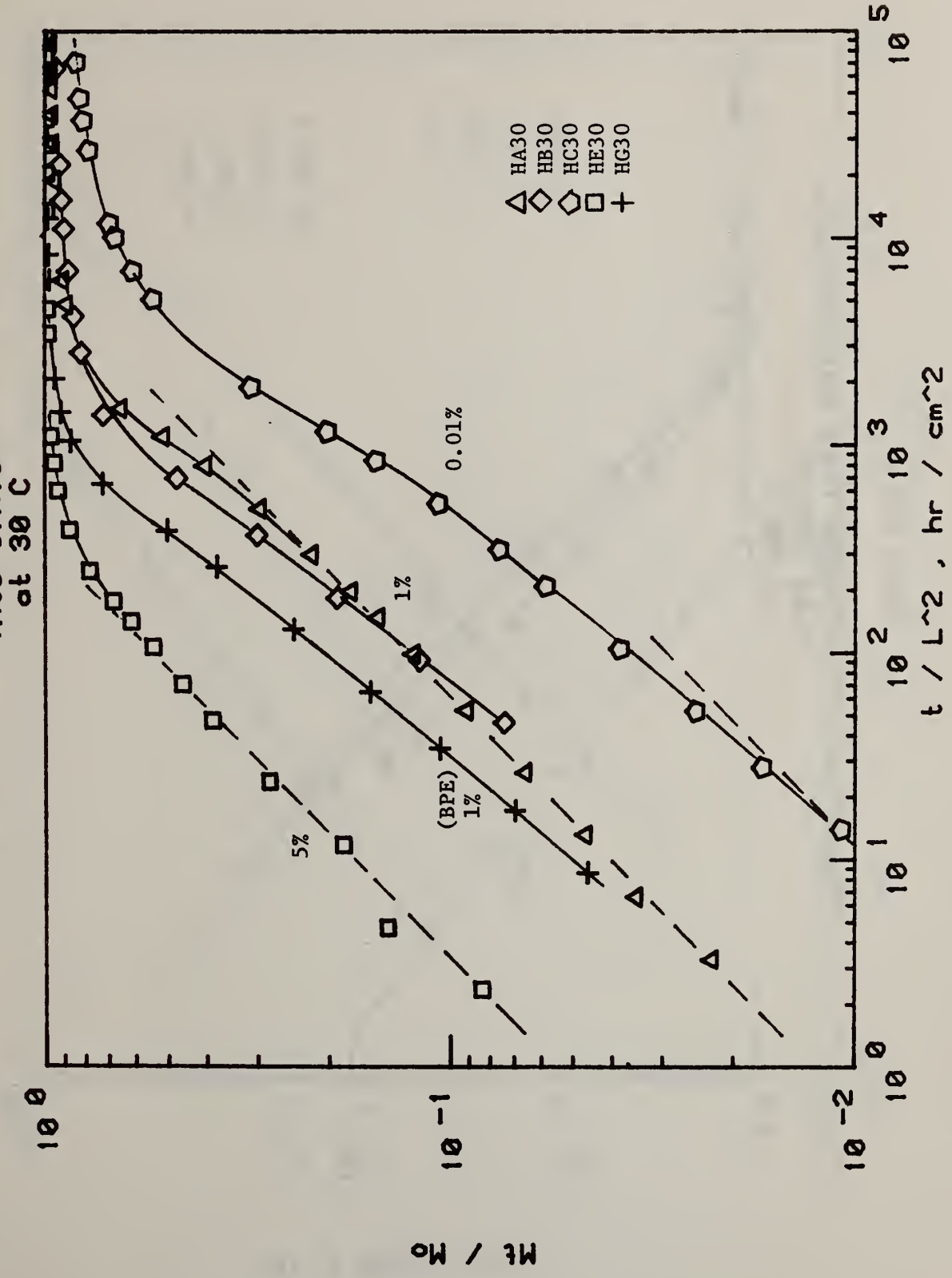
Migration of n-C18H38 from Polyethylene
into C7H16
at 30 C
HA30
HB30
HC30
HE30
HG30
0.01%
1%
(BPE)
1%
5%
Mt / Mo
t / L^2 , hr / cm^2
10 0
10 -1
10 -2
10 0
10 1
10 2
10 3
10 4
10 5

Figure E-1C

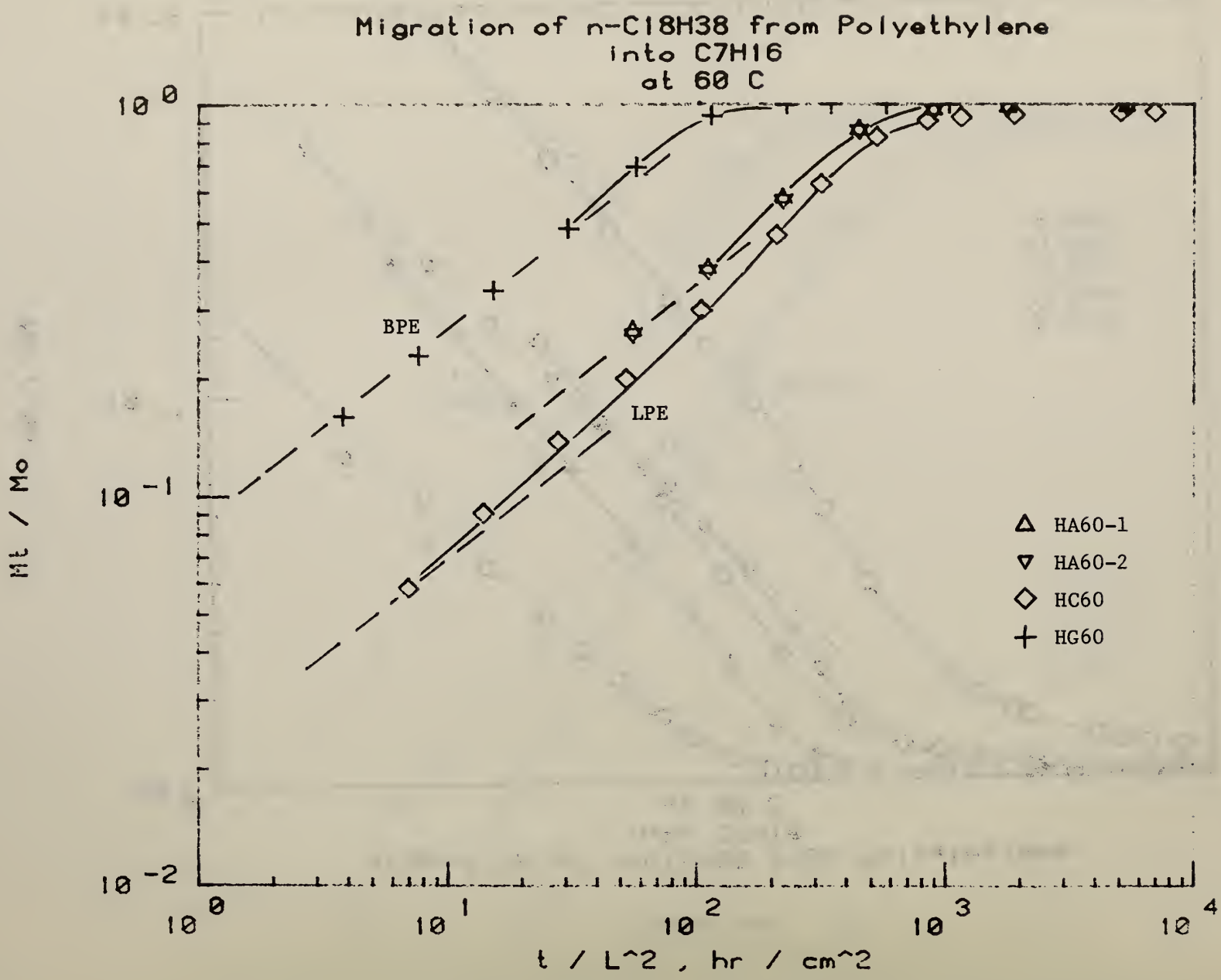
Migration of n-C18H38 from Polyethylene
into C7H16
at 60 C
Mt / Mo
10 0
10 -1
10 -2
BPE
LPE
HA60-1
HA60-2
HC60
HG60
10 0
10 1
10 2
10 3
10 4
t / L^2 , hr / cm^2

Figure E-2A

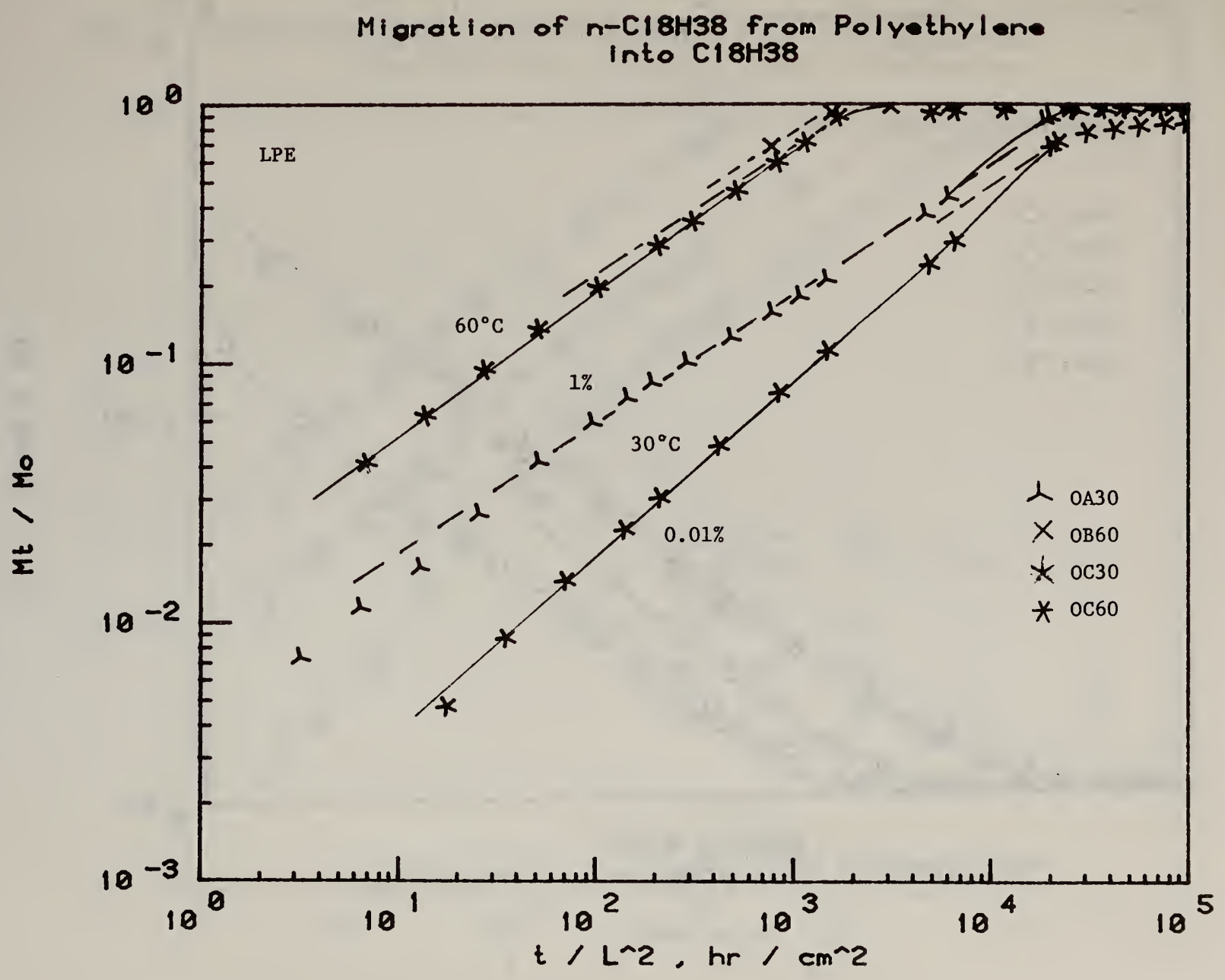
Migration of n-C18H38 from Polyethylene into C18H38
LPE
60°C
1%
30°C
0.01%
OA30
OB60
OC30
OC60
Mt / Mo
t / L^2 , hr / cm^2
10 0
10 -1
10 -2
10 -3
10 0
10 1
10 2
10 3
10 4
10 5

Figure E-2B

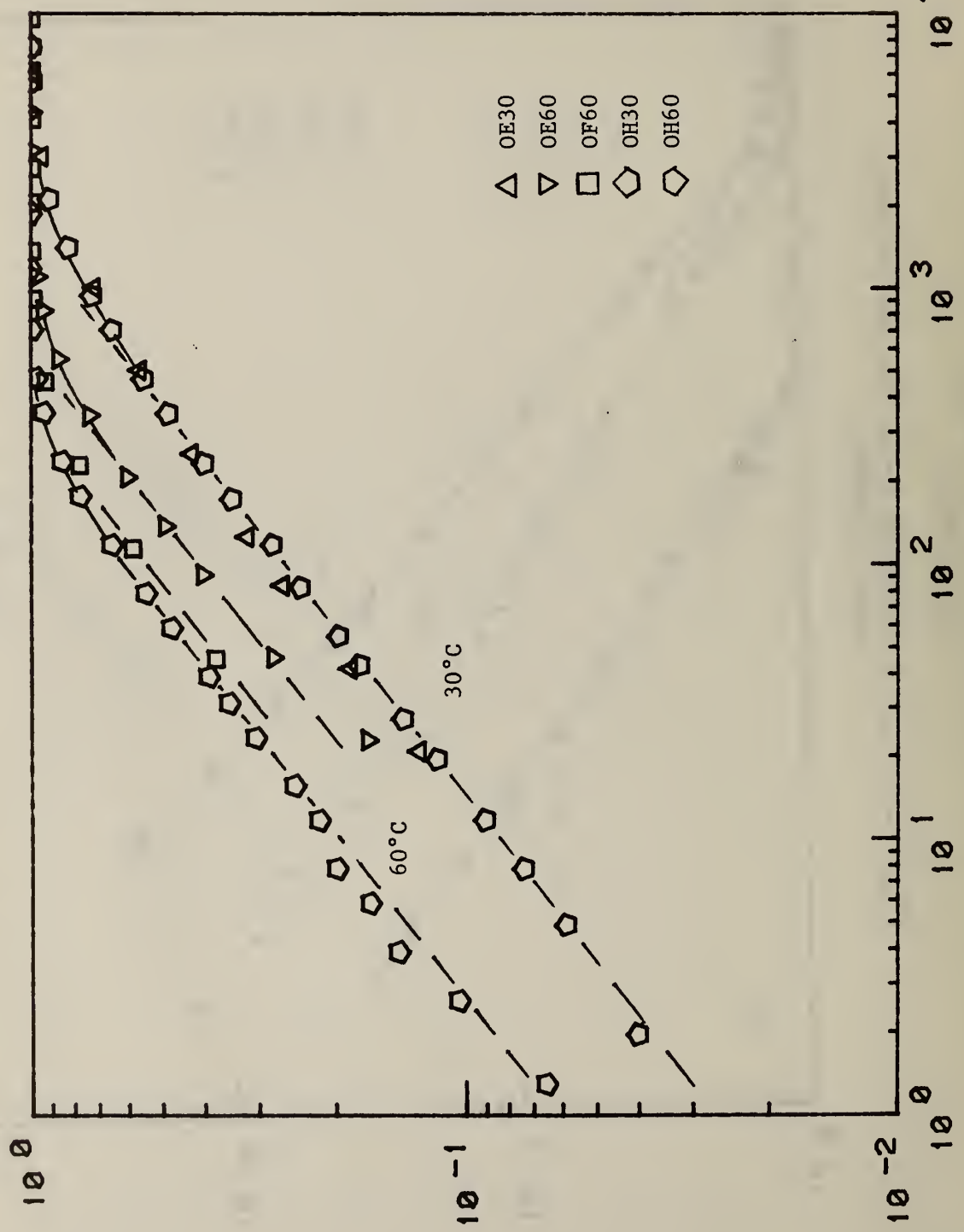
Migration of n-C18H38 from Polyethylene into C18H38
Mt / Mo
t / L^2 , hr / cm^2
10^0
10^-1
10^-2
10^0
10^1
10^2
10^3
10^4
30°C
60°C
OE30
OE60
OF60
OH30
OH60

Figure E-3

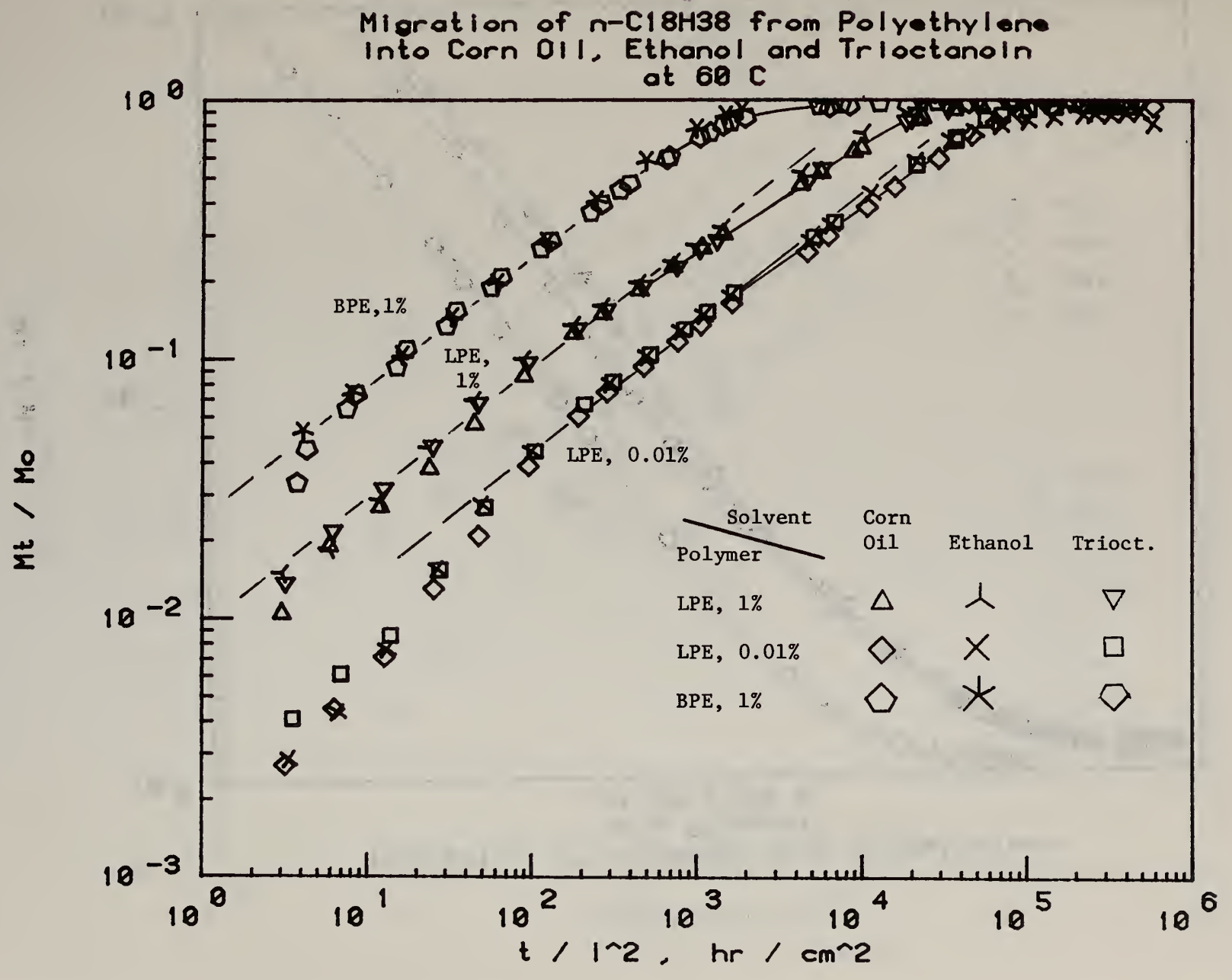
Migration of n-C18H38 from Polyethylene
Into Corn Oil, Ethanol and Trioctanoin
at 60 C
Mt / Mo
10 0
10 -1
10 -2
10 -3
BPE,1%
LPE,
1%
LPE, 0.01%
Solvent
Polymer
Corn
Oil
Ethanol
Trioct.
LPE, 1%
LPE, 0.01%
BPE, 1%
10 0
10 1
10 2
10 3
10 4
10 5
10 6
t / l^2 , hr / cm^2

Figure E-4A

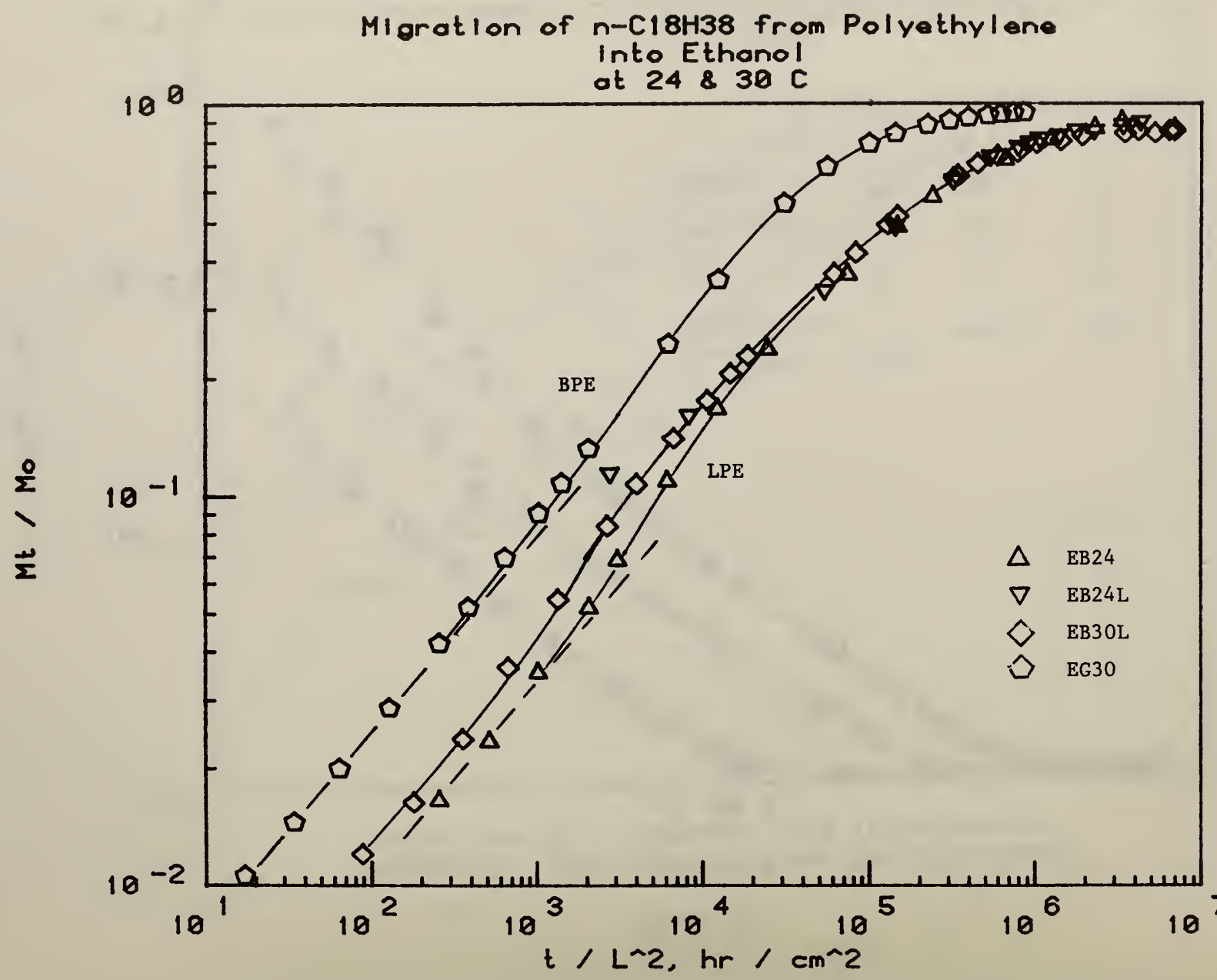
Migration of n-C18H38 from Polyethylene
into Ethanol
at 24 & 30 C
Mt / Mo
10 0
10 -1
10 -2
BPE
LPE
EB24
EB24L
EB30L
EG30
10 1
10 2
10 3
10 4
10 5
10 6
10 7
t / L^2, hr / cm^2

Figure E-4 B

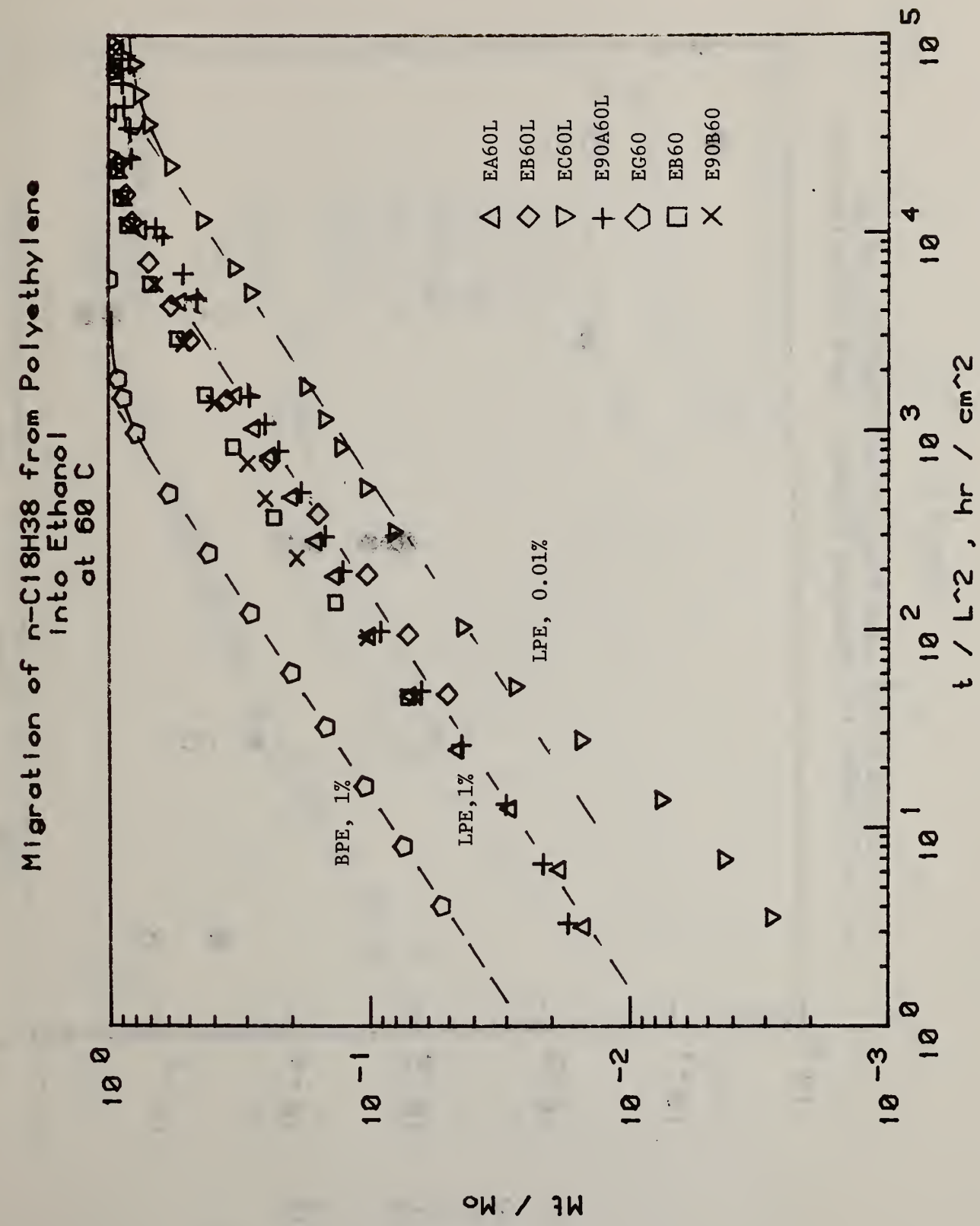
Migration of n-C18H38 from Polyethylene
into Ethanol
at 60 C
Mt / Mo
t / L^2 , hr / cm^2
EA60L
EB60L
EC60L
E90A60L
EG60
EB60
E90B60
BPE, 1%
LPE,1%
LPE, 0.01%

Figure E-5

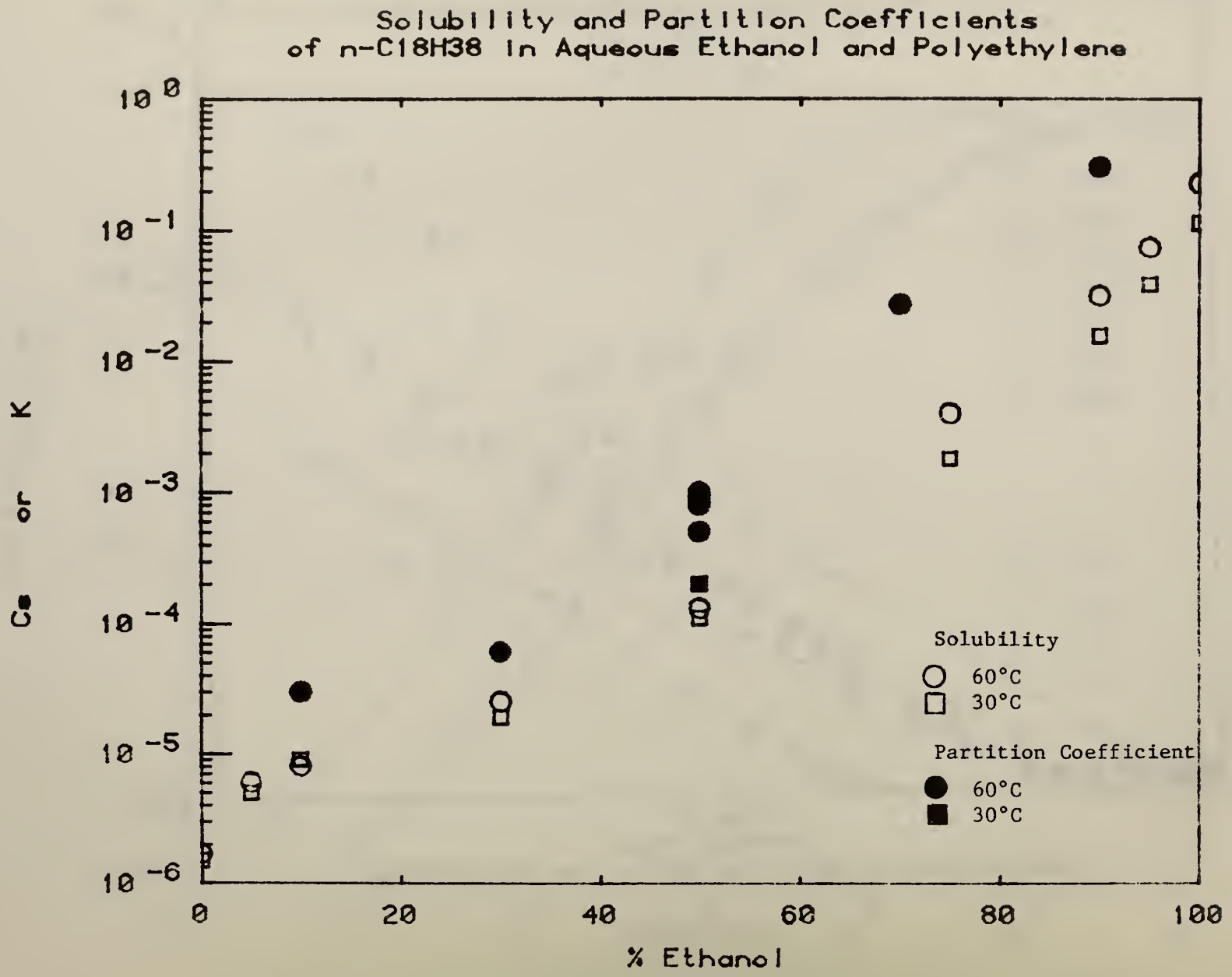
Solubility and Partition Coefficients
of n-C18H38 in Aqueous Ethanol and Polyethylene
10 0
10 -1
10 -2
10 -3
10 -4
10 -5
10 -6
Cs or K
0
20
40
60
80
100
% Ethanol
Solubility
60°C
30°C
Partition Coefficient
60°C
30°C

Figure E-6A

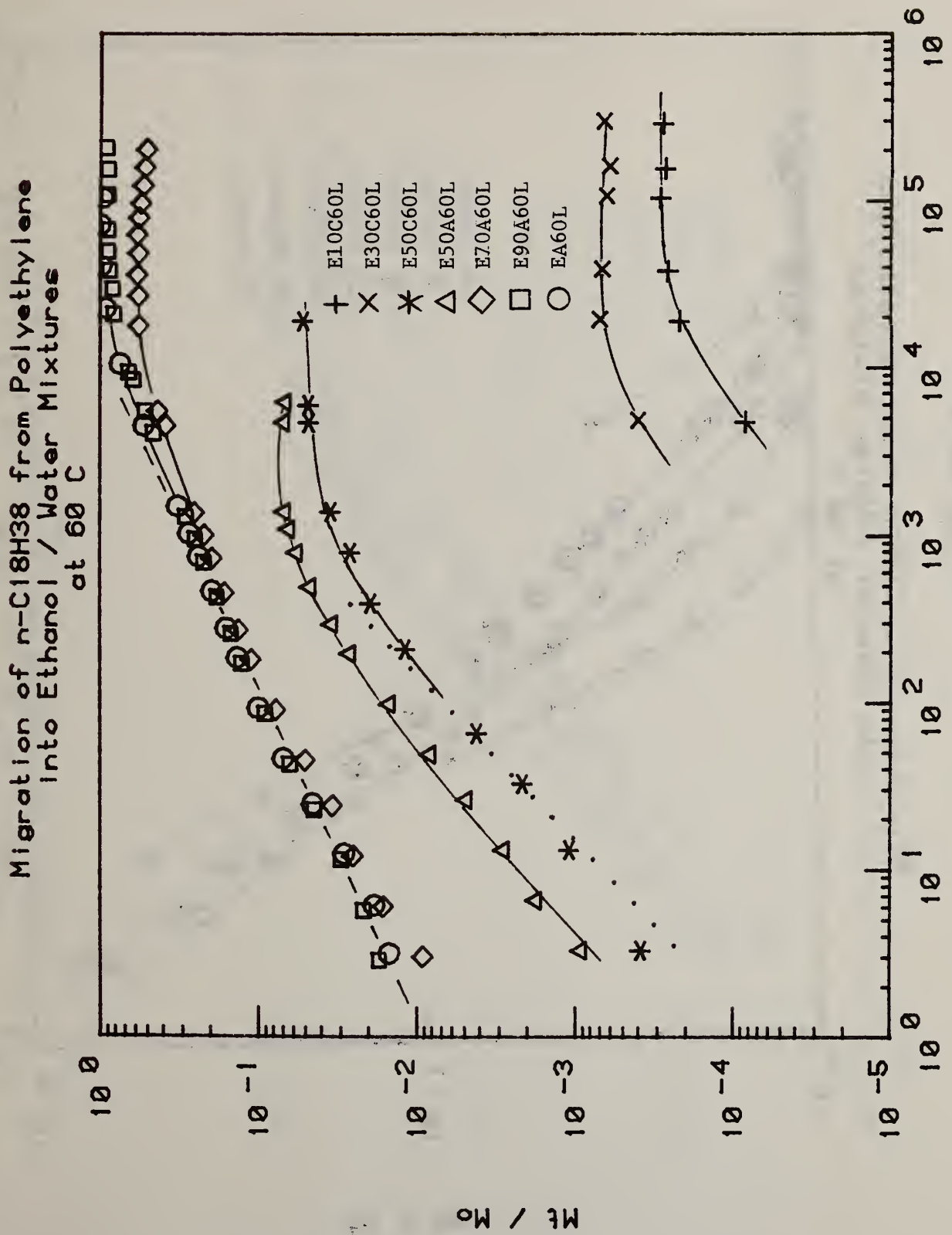
Migration of n-C18H38 from Polyethylene
Into Ethanol / Water Mixtures
at 60 C
E10C60L
E30C60L
E50C60L
E50A60L
E70A60L
E90A60L
EA60L
Mt / Mo
t / L^2 , hr / cm^2
10 0
10 -1
10 -2
10 -3
10 -4
10 -5
10 0
10 1
10 2
10 3
10 4
10 5
10 6

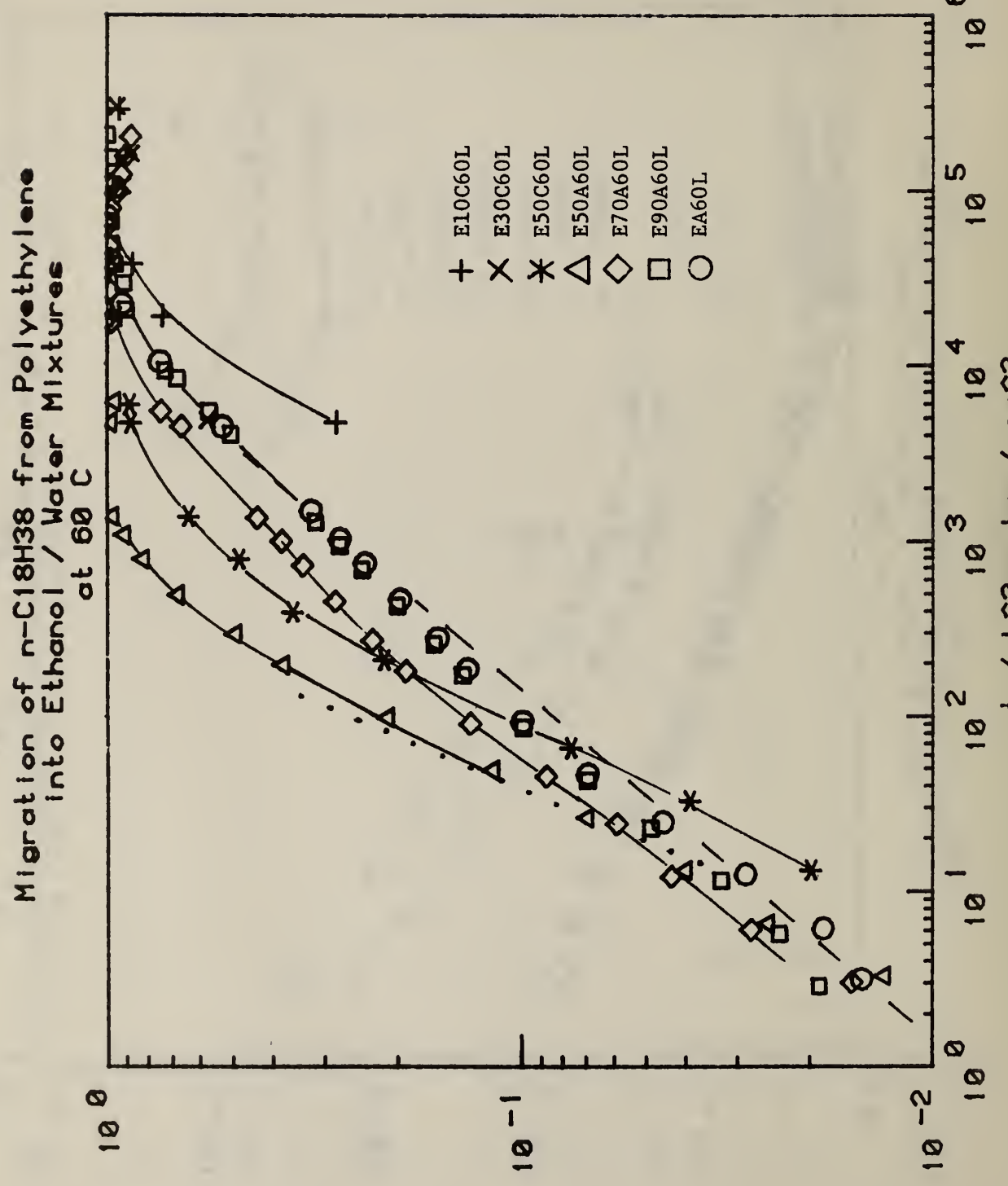
Migration of n-C18H38 from Polyethylene
into Ethanol / Water Mixtures
at 60 C
E10C60L
E30C60L
E50C60L
E50A60L
E70A60L
E90A60L
EA60L
Mt / Mo
t / L^2 , hr / cm^2
10 0
10 -1
10 -2
10 0
10 1
10 2
10 3
10 4
10 5
10 6

Figure E-6B

Figure E-7A

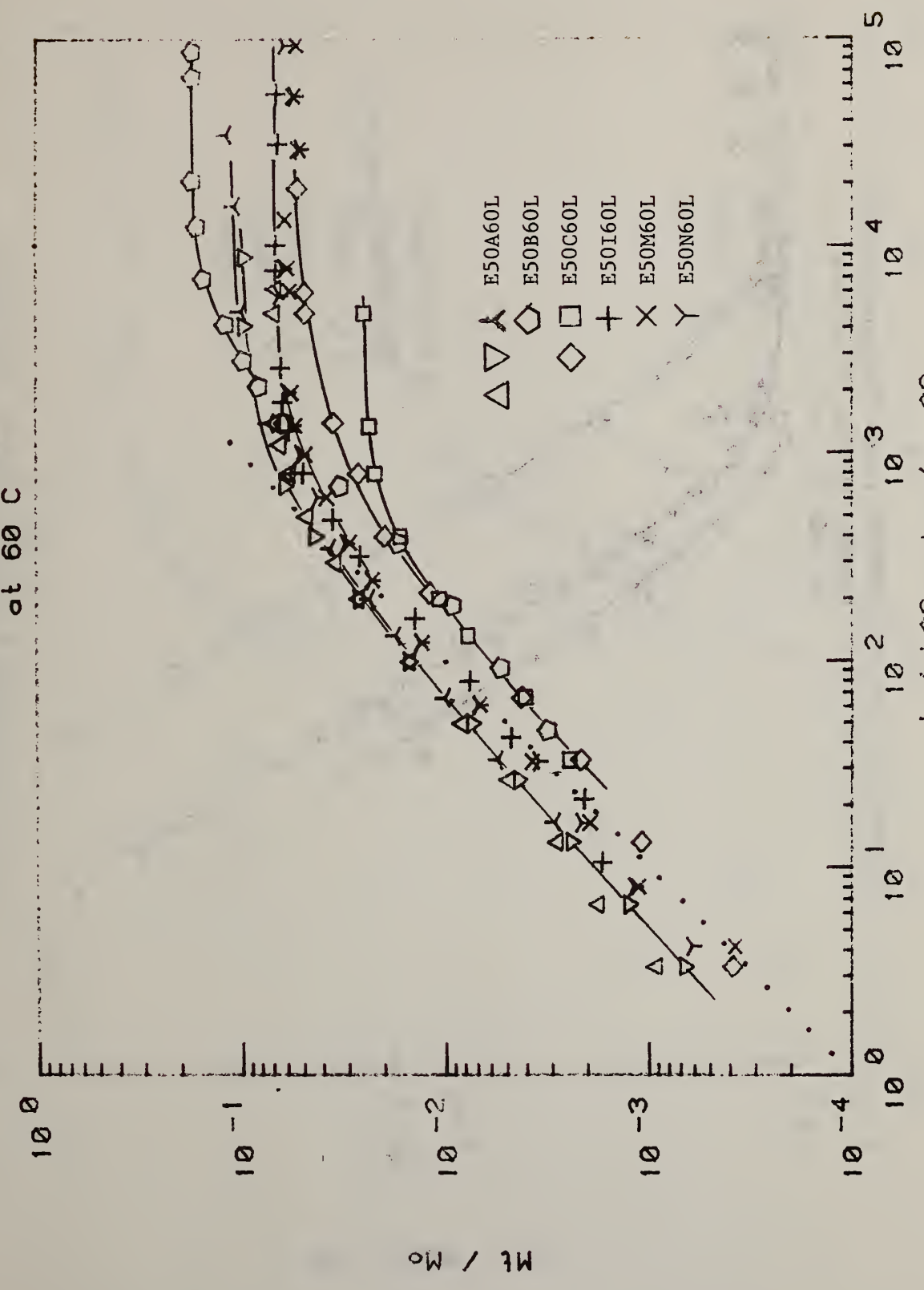
Migration of n-C18H38 from Polyethylene
into 50/50 Ethanol/Water Mixture
at 60 C
E50A60L
E50B60L
E50C60L
E50I60L
E50M60L
E50N60L
Mt / Mo
t / L^2 , hr / cm^2
10 0
10 -1
10 -2
10 -3
10 -4
10 0
10 1
10 2
10 3
10 4
10 5

Figure E-7B

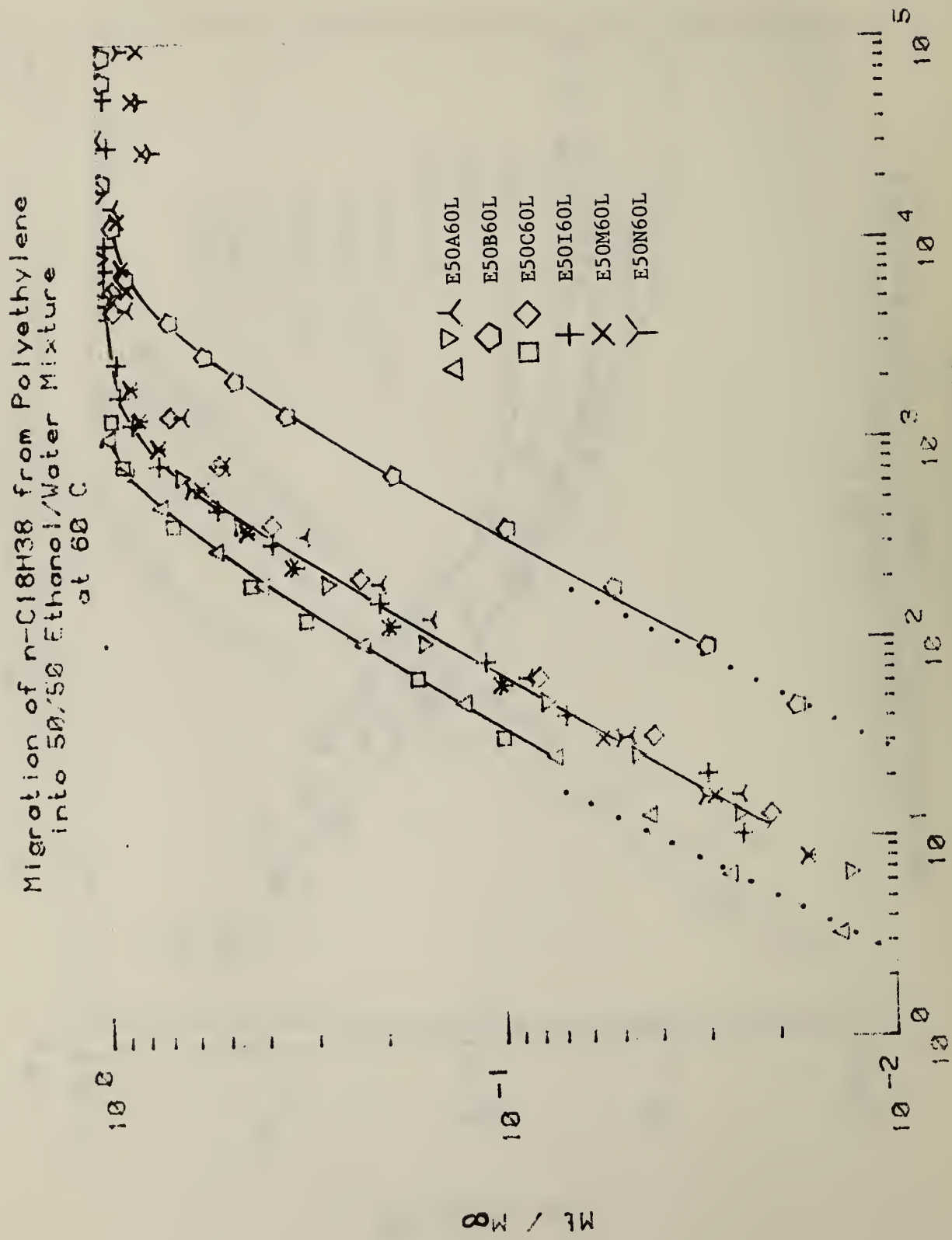
Migration of n-C18H38 from Polyethylene
into 50/50 Ethanol/Water Mixture
at 60 C
E50A60L
E50B60L
E50C60L
E50I60L
E50M60L
E50N60L
Mt / M∞

Figure E-8A

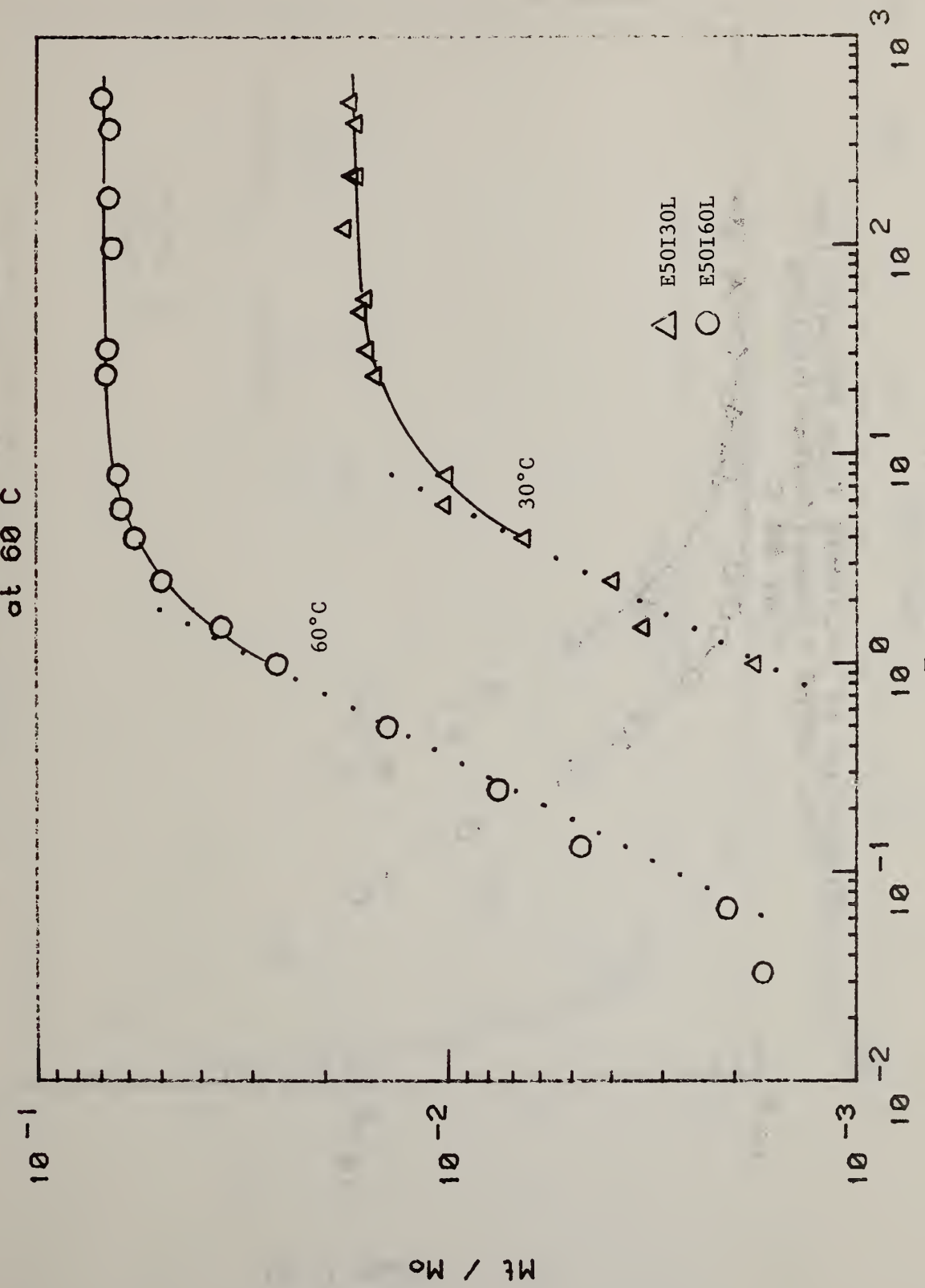
Migration of n-C18H38 from Polyethylene
into 50/50 Ethanol/Water Mixture
at 60 C
Mt / Mo
Time, Hours
60°C
30°C
E50I30L
E50I60L
10 -1
10 -2
10 -3
10 -2
10 -1
10 0
10 1
10 2
10 3

Figure E-8B

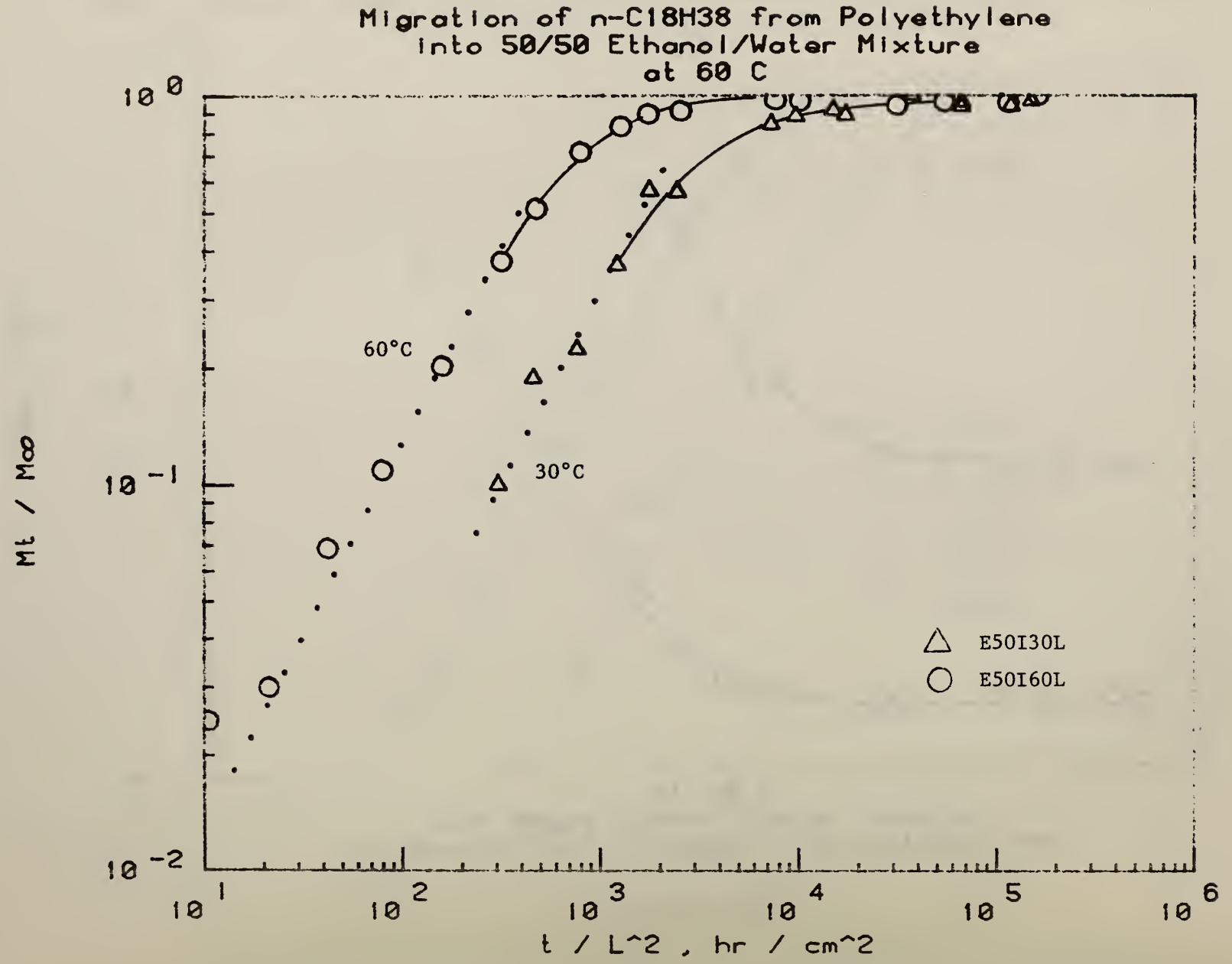
Migration of n-C18H38 from Polyethylene
into 50/50 Ethanol/Water Mixture
at 60 C
10 0
10 -1
10 -2
Mt / M∞
60°C
30°C
E50I30L
E50I60L
10 1
10 2
10 3
10 4
10 5
10 6
t / L^2 , hr / cm^2

Figure E-9A

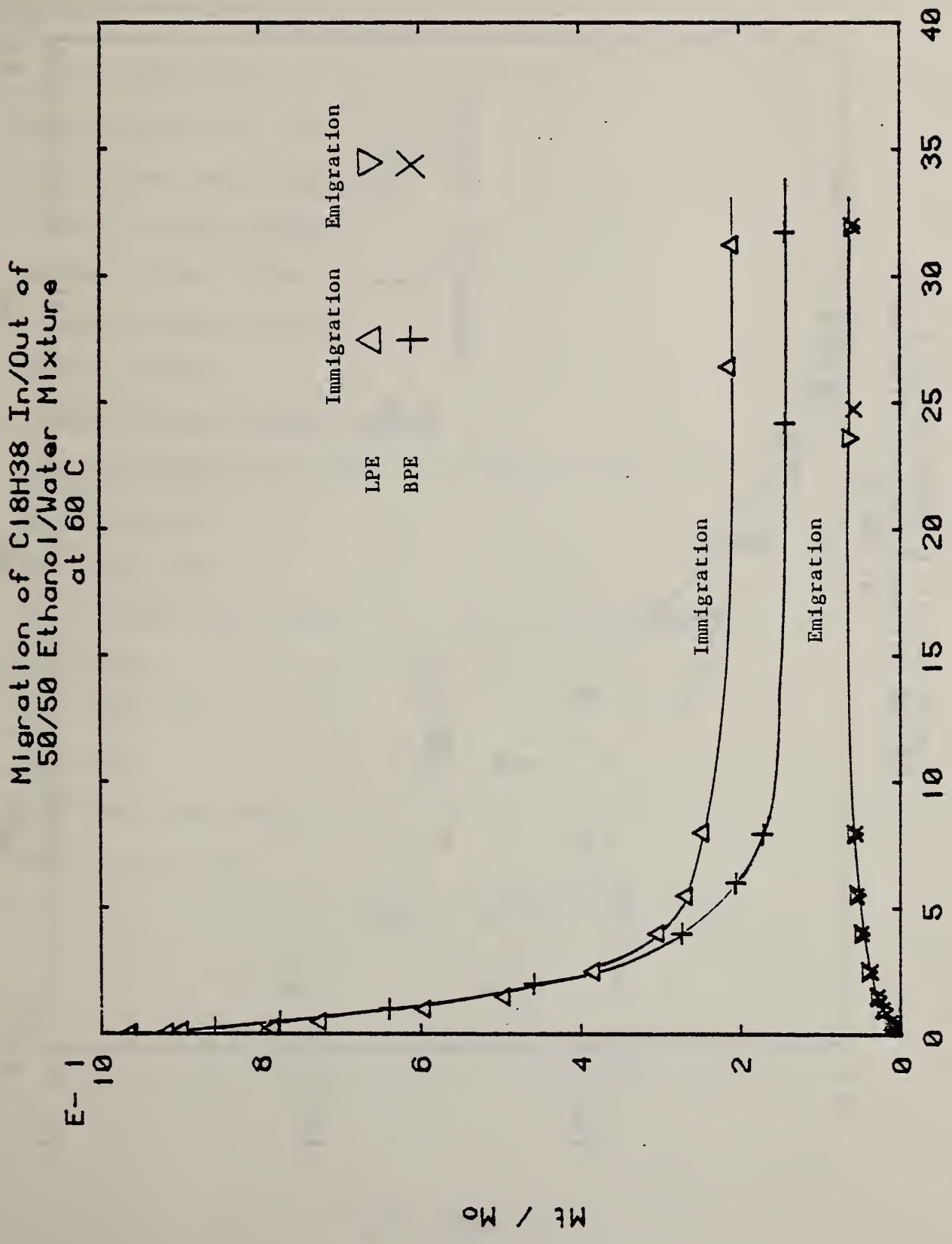
Migration of C18H38 In/Out of
50/50 Ethanol/Water Mixture
at 60 C
Immigration
Emigration
LPE
BPE
Immigration
Emigration
E- 1
10
8
6
4
2
0
0
5
10
15
20
25
30
35
40
Time, Hours
Mt / Mo

Figure E-9B

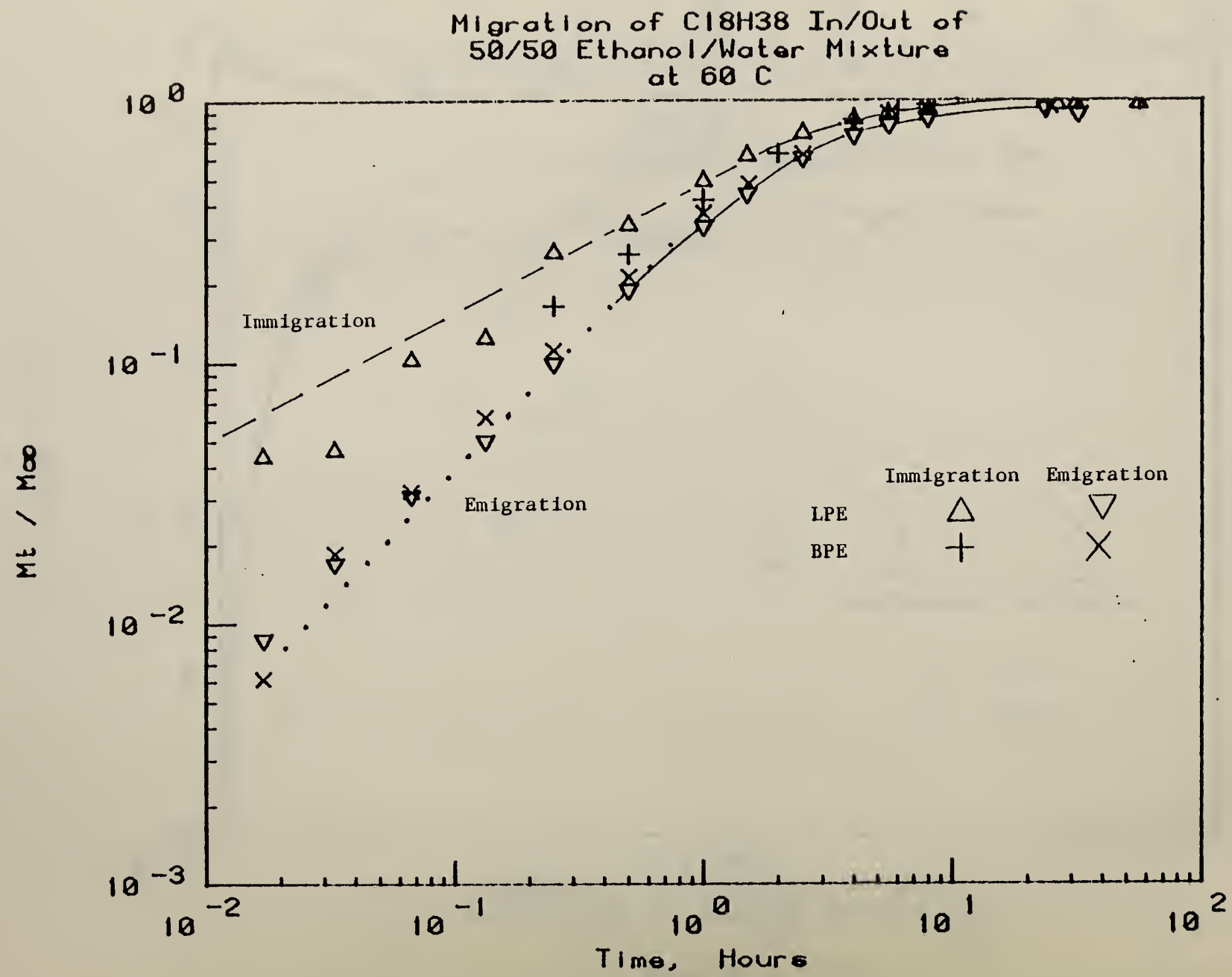
Migration of C18H38 In/Out of
50/50 Ethanol/Water Mixture
at 60 C
Mt / M∞
Time, Hours
Immigration
Emigration
Immigration
Emigration
LPE
BPE

APPENDIX A

List of Experimental Data

CA60L, CC60L, CG60

EB24, EB24L, EB30L, EG30

EA60L, EB60, EB60L, EC60L, EG60

E50A60L, E70A60L, E90A60L

E50B60L, E50B60, E90B60

E10C60L, E30C60L, E50C60L

E50I30L, E50I60L

E50M60R, E50M60L, E50N60R, E50N60L

HA24L, HA24, HB24, HC24, HD24

HA30, HB30, HC30

HE30, HG30, HH30

HA60-1, HA60-2, HC60, HG60

OA30, OC30

OE30, OH30, OI30

OB60, OC60

OE60, OF60, OH60, OI60

TA60L, TC60L, TG60

CA60L

t (hours)	M_t/M_0
0.017	0.010
0.033	0.019
0.067	0.027
0.133	0.038
0.25	0.056
0.5	0.085
1.0	0.125
1.5	0.150
2.5	0.185
4.0	0.227
6.0	0.268
8.0	0.304
23.5	0.470
31.0	0.524
48.5	0.631
54.0	0.651
120.2	0.834
127.5	0.850
198.0	0.914
288.6	0.959
456.8	0.985
725.2	0.996
965.0	0.981

CC60L

t (hours)	M_t/M_0
.017	.0027
.033	.0045
.067	.0071
.133	.013
.25	.021
.5	.039
1.0	.060
1.5	.074
2.5	.094
4.0	.117
5.5	.136
8.5	.165
24.0	.259
32.0	.299
55.0	.385
81.0	.460
150.0	.592
240.0	.730
337.0	.815
488.0	.883
720.6	.935
1153.9	.966
1399.5	.949
1583.7	.971
1919.8	.966
2403.6	.983
3030.4	.942

CG60

t (hours)	M_t/M_0
0.017	0.033
0.033	0.064
0.067	0.093
0.133	0.134
0.25	0.188
0.5	0.267
1.0	0.368
1.5	0.447
3.0	0.597
5.25	0.738
7.0	0.819
24.0	0.945
32.0	0.958
55.0	0.970
124.25	0.980
364.25	0.989
1157.0	0.999

EB24L

$\frac{t}{\text{hours}}$	$\frac{M_t}{M_0}$
1.0	0.114
3.0	0.16
19.5	0.335
51.5	0.487
116.0	0.639
195.0	0.735
288.0	0.778
337.0	0.799
287.0	0.816
505.0	0.832
648.0	0.857
820.0	0.855
1220.0	0.883
1556.0	0.900

EB24

$\frac{t}{\text{hours}}$	$\frac{M_t}{M_0}$
0.083	0.016
0.167	0.023
0.33	0.035
0.67	0.052
1.0	0.069
2.0	0.109
4.0	0.166
8.0	0.237
24.0	0.367
48.0	0.485
78.0	0.578
216.0	0.720
409.0	0.809
745.0	0.865
1081.0	0.902

EB30L

$\frac{t}{\text{hours}}$	$\frac{M_t}{M_0}$
0.017	.0074
0.033	.0127
0.067	.0173
0.133	.0252
0.25	.038
0.5	.058
1.0	.089
1.5	.114
2.5	.145
4.0	.186
5.5	.217
7.0	.241
23.03	.390
31.0	.441
48.0	.520
55.0	.547
120.0	.683
128.0	.696
168.0	.744
223.0	.780
294.0	.797
384.0	.838
535.0	.854
720.0	.878
1290.0	.893
1560.0	.904
1966.0	.890
2403.0	.902
2572.0	.912

EG30

$\frac{t}{\text{hours}}$	$\frac{M_t}{M_0}$
0.033	0.008
0.067	0.011
0.133	0.015
0.25	0.020
0.5	0.029
1.0	0.042
1.5	0.052
2.5	0.069
4.0	0.090
5.5	0.108
8.0	0.132
24.17	0.244
48.25	0.356
120.0	0.556
216.0	0.689
385.1	0.789
554.6	0.838
865.5	0.881
1181.0	0.904
1537.0	0.919
2022.0	0.932
2401.0	0.939
2881.0	0.945
3339.0	0.950

EA60L

$\frac{t}{\text{hours}}$	$\frac{M_t}{M_0}$
0.017	.015
0.033	.019
0.067	.029
0.133	.046
0.25	.069
0.5	.100
1.0	.135
1.5	.159
2.5	.197
4.0	.239
5.5	.275
8.0	.323
24.0	.527
55.83	.745
119.9	.920
216.3	.980
384.4	.997
558.0	.961

EB60

$\frac{t}{\text{hours}}$	$\frac{M_t}{M_0}$
0.012	0.071
0.05	0.135
0.13	0.232
0.3	0.331
0.55	0.423
1.05	0.543
2.0	0.688
4.0	0.840
5.5	0.890
7.5	0.924
24.0	0.971
55.5	0.980
72.0	0.981
144.5	0.983
246.5	0.986
318.6	0.986
414.0	0.987
534.0	0.988

EB60L

$\frac{t}{\text{hours}}$	$\frac{M_t}{M_0}$
0.017	.050
0.033	.071
0.067	.102
0.133	.157
0.25	.239
0.5	.350
1.0	.483
1.5	.573
2.5	.698
4.0	.808
5.52	.854
7.92	.911
23.60	.968
31.0	.966
55.82	.968
121.9	.966
220.1	.929
383.7	.971
626.3	.968
721.1	.970

EC60L

$\frac{t}{\text{hours}}$	$\frac{M_t}{M_0}$
0.017	.0028
0.033	.0043
0.067	.0076
0.133	.0155
0.25	.0275
0.5	.044
1.5	.080
2.5	.102
4.0	.129
5.5	.148
8.0	.175
24.0	.286
32.0	.329
56.0	.437
105.0	.580
170.0	.701
241.0	.762
344.0	.798
505.0	.831
720.3	.852
1086.0	.873
1273.0	.879
1583.0	.872
1945.0	.886
2400.0	.891
2883.0	.809

EG60

$\frac{t}{\text{hours}}$	$\frac{M_t}{M_0}$
0.017	.053
0.033	.074
0.067	.104
0.133	.146
0.25	.198
0.5	.286
1.0	.411
2.0	.582
4.0	.779
6.0	.877
7.5	.917
24.0	.990
98.25	.998
508.8	.999
1277.0	.999

E50A60L

	$\frac{t}{\text{hours}}$	$\frac{M_t}{M_0}$
(1)	0.017	0.0009
	0.033	0.0018
	0.067	0.0028
	0.133	0.0049
	0.25	0.0082
	0.5	0.0147
	1.0	0.0263
	1.5	0.0343
	2.5	0.0471
	4.0	0.0572
	5.5	0.0635
	7.0	0.0677
	23.75	0.0684
(2)	0.017	0.0007
	0.033	0.0012
	0.067	0.0024
	0.133	0.0043
	0.25	0.0073
	0.5	0.0147
	1.0	0.0268
	2.0	0.0426
	3.5	0.0597
	20.5	0.0946
(3)	0.083	0.0029
	0.167	0.0056
	0.333	0.0101
	0.667	0.0176
	1.00	0.0235
	1.75	0.0366
	4.0	0.0578
	7.0	0.0729
	24.25	0.100
	78.75	0.108
	173.7	0.118

E70A60L

$\frac{t}{\text{hours}}$	$\frac{M_t}{M_0}$
0.017	0.0091
0.033	0.016
0.067	0.025
0.133	0.034
0.25	0.051
0.5	0.077
1.0	0.110
1.5	0.133
2.5	0.163
4.0	0.196
5.5	0.220
7.5	0.252
24.5	0.383
30.0	0.429
96.5	0.565
146.5	0.569
196.2	0.578
264.4	0.569
343.7	0.577

E90A60L

$\frac{t}{\text{hours}}$	$\frac{M_t}{M_0}$
0.016	0.017
0.033	0.021
0.066	0.030
0.133	0.044
0.25	0.063
0.50	0.090
1.0	0.126
1.5	0.148
2.5	0.182
4.0	0.221
5.5	0.250
7.5	0.286
23.5	0.456
31.5	0.515
48.5	0.616
54.0	0.658
120.5	0.818
170.5	0.829
220.2	0.870
288.5	0.885
385.5	0.886
624.7	0.893
892.9	0.890
1204.0	0.905

E50B60L

$\frac{t}{\text{hours}}$	$\frac{M_t}{M_0}$
0.01660	0.0031
0.03333	0.0053
0.06665	0.0091
0.1333	0.017
0.25	0.033
0.50	0.060
0.75	0.081
1.0	0.097
1.5	0.110
2.5	0.152
4.5	0.164
7.5	0.173
23.67	0.172
31.5	0.172
54.5	0.174
168.0	0.176
343.5	0.178

E10C60L

$\frac{t}{\text{hours}}$	$\frac{M_t}{M_0}$
24.0	0.000084
96.0	0.00022
192.0	0.00026
528.0	0.00029
792.0	0.00027
1464.0	0.00028

E30C60L

$\frac{t}{\text{hours}}$	$\frac{M_t}{M_0}$
24.0	0.00040
96.0	0.00070
192.0	0.00068
528.0	0.00064
792.0	0.00061
1464.0	0.00066

E50C60L

	$\frac{t}{\text{hours}}$	$\frac{M_t}{M_0}$
a)	0.017	0.0004
	0.067	0.0011
	0.167	0.0022
	0.333	0.0042
	1.067	0.0118
	2.0	0.0196
	4.0	0.0264
	7.0	0.0349
	23.67	0.0481
	30.0	0.0484
	95.75	0.0533
b)	0.167	0.0027
	0.333	0.0043
	0.667	0.0083
	1.0	0.0114
	2.0	0.0178
	4.0	0.0236
	6.75	0.0252
	23.75	0.0267

E50I30L

$\frac{t}{\text{hours}}$	$\frac{M_t}{M_0}$
1.0	.002
1.5	.003
2.5	.004
4.0	.007
5.783	.010
8.0	.010
23.63	.015
31.5	.016
48.08	.016
55.72	.016
121.52	.018
216.25	.017
384.07	.017
486.25	.017

E50I60L

$\frac{t}{\text{hours}}$	$\frac{M_t}{M_0}$
0.033	.0017
0.067	.0021
0.133	.0048
0.25	.0076
0.5	.0141
1.0	.0263
1.5	.0359
2.5	.0501
4.0	.0582
5.5	.0626
8.0	.0637
23.92	.0681
31.80	.0675
97.67	.0659
169.9	.0623
359.9	.0669
508.6	.0700

E50M60R

$\frac{t}{\text{hours}}$	$\frac{M_t}{M_0}$
0.25	0.858
0.5	0.776
1.0	0.639
2.0	0.458
4.0	0.273
6.0	0.206
7.9	0.172
24.2	0.143
31.75	0.143
55.92	0.140
216.2	0.133
240.2	0.138
314.3	0.135
360.0	0.137

E50N60R

$\frac{t}{\text{hours}}$	$\frac{M_t}{M_0}$
0.017	0.964
0.033	0.962
0.067	0.916
0.133	0.898
0.25	0.784
0.5	0.725
1.0	0.594
1.5	0.494
2.5	0.383
4.0	0.302
5.5	0.267
8.0	0.246
26.42	0.212
31.25	0.208
55.85	0.203
102.5	0.199
200.0	0.189
360.4	0.186
551.7	0.179

E50M60L

$\frac{t}{\text{hours}}$	$\frac{M_t}{M_0}$
0.017	0.004
0.033	0.0011
0.067	0.0019
0.133	0.0036
0.25	0.0064
0.5	0.0123
1.0	0.0216
1.5	0.0278
2.5	0.0360
4.0	0.0459
5.5	0.0514
7.95	0.0538
24.73	0.0546
31.98	0.0563
55.0	0.0575
119.7	0.0493
215.7	0.0523
383.7	0.0505
458.2	0.0555
528.5	0.0574

E50N60L

$\frac{t}{\text{hours}}$	$\frac{M_t}{M_0}$
0.017	0.006
0.033	0.0012
0.067	0.0022
0.133	0.0036
0.25	0.0070
0.5	0.0135
1.0	0.0237
1.5	0.0314
2.5	0.0430
4.0	0.0522
5.53	0.0574
7.93	0.0609
23.6	0.0662
31.9	0.0634
119.7	0.0522
216.3	0.0556
383.9	0.0627
458.0	0.0662

HA24L

t hours	M_t/M_0
0.1	0.046
16.0	0.836
23.0	0.891
40.0	0.932
70.0	0.955
136.0	0.964
216.0	0.969
308.5	0.972
375.5	0.975
665.5	0.974

HA24

t hours	M_t/M_0
0.025	0.026
0.05	0.039
0.10	0.053
0.25	0.083
0.5	0.115
1.0	0.163
2.0	0.242
4.0	0.378
8.0	0.662
28.0	0.902
72.0	0.947
151.0	0.962
244.5	0.968
293.5	0.970
437.5	0.970
462.0	0.974
511.5	0.974
578.5	0.975

HB24

t hours	M_t/M_0
0.017	0.086
0.033	0.124
0.067	0.183
0.133	0.280
0.25	0.458
0.5	0.683
1.0	0.804
2.0	0.866
4.0	0.904
6.0	0.919
22.0	0.950
30.0	0.955
94.0	0.968
148.0	0.972
216.0	0.974
286.5	0.975

HC24

t hours	M_t/M_0
0.033	0.008
0.067	0.015
0.133	0.020
0.25	0.029
0.5	0.039
1.0	0.056
2.0	0.086
4.0	0.128
8.0	0.196
27.25	0.467
71.25	0.663
150.50	0.787
243.75	0.834
292.75	0.848
316.75	0.853
460.75	0.869
510.75	0.873
603.75	0.878
775.0	0.887
1008.0	0.894

HD24

t hours	M_t/M_0
0.033	0.015
0.067	0.026
0.133	0.041
0.25	0.063
0.5	0.108
1.0	0.202
2.0	0.342
4.0	0.477
20.0	0.693
28.0	0.732
92.0	0.817
146.0	0.838
196.0	0.850
289.0	0.861
460.0	0.873
692.5	0.885

HA30

$\frac{t}{\text{hours}}$	$\frac{M_t}{M_0}$
0.017	0.023
0.033	0.035
0.067	0.046
0.133	0.065
0.267	0.091
0.50	0.123
0.75	0.151
1.0	0.176
1.5	0.219
2.5	0.295
4.0	0.402
5.5	0.500
7.5	0.648
24.0	0.883
31.5	0.903
96.0	0.946
144.25	0.954
198.5	0.959
264.3	0.962
319.5	0.964
438.5	0.967
533.5	0.968
672.0	0.970
1033.0	0.972
1269.0	0.974
1464.0	0.974

HB30

$\frac{t}{\text{hours}}$	$\frac{M_t}{M_0}$
0.017	.074
0.033	.119
0.067	.190
0.133	.300
0.25	.472
0.5	.715
1.0	.812
1.5	.844
2.5	.874
4.0	.895
5.5	.906
8.13	.917
23.82	.939
47.80	.949
79.88	.954
144.0	.959
217.4	.962
384.2	.966
577.5	.968
655.2	.969

HC30

$\frac{t}{\text{hours}}$	$\frac{M_t}{M_0}$
0.033	0.0073
0.067	0.010
0.133	0.017
0.25	0.025
0.5	0.038
1.0	0.050
1.5	0.076
2.5	0.107
4.0	0.153
5.5	0.201
9.0	0.310
24.0	0.542
33.0	0.607
48.0	0.671
56.0	0.694
126.0	0.780
175.0	0.804
224.35	0.819
336.7	0.838
488.5	0.853
720.0	0.866
870.5	0.872
1203.75	0.882
1536.0	0.888
1909.0	0.893
2407.0	0.898
2905.0	0.902
3409.0	0.905
3894.0	0.908
4517.0	0.910

HE30

$\frac{t}{\text{hours}}$	$\frac{M_t}{M_0}$
0.017	.083
0.033	.143
0.083	.184
0.167	.279
0.333	.385
0.50	.458
0.75	.542
1.00	.612
1.25	.678
1.75	.772
2.75	.867
4.25	.925
5.75	.947
7.75	.960
24.25	.979
31.75	.981
96.00	.987
144.50	.988
198.75	.989
264.68	.990
438.75	.991
533.75	.991
652.25	.991

HG30

$\frac{t}{\text{hours}}$	$\frac{M_t}{M_0}$
0.033	.046
0.067	.069
0.133	.106
0.25	.157
0.5	.243
1.0	.376
1.5	.499
2.5	.720
4.0	.862
5.5	.912
8.0	.942
24.0	.974
32.0	.977
48.0	.980
119.4	.986
215.3	.988
383.2	.989
628.4	.990

HH30

$\frac{t}{\text{hours}}$	$\frac{M_t}{M_0}$
0.0055	0.045
0.0083	0.057
0.0167	0.086
0.0333	0.129
0.067	0.187
0.133	0.274
0.25	0.388
0.5	0.582
1.0	0.814
1.5	0.901
2.5	0.955
4.0	0.976
5.667	0.982
6.5	0.984
23.83	0.990
31.25	0.991
48.00	0.992
74.92	0.993
172.5	0.994

HA60-1

t, hours	M_t/M_0
0.25	0.265
0.5	0.382
1.0	0.576
2.0	0.860
4.0	0.968
8.0	0.982
24.0	0.986
48.0	0.988
120.0	0.990
168.0	0.991

HA60-2

t, hours	M_t/M_0
0.25	0.260
0.5	0.378
1.0	0.572
2.0	0.859
4.0	0.968
8.0	0.982
24.0	0.986
48.0	0.988
120.0	0.990
168.0	0.991

HC60

t, hours	M_t/M_0
0.033	.058
0.067	.091
0.133	.139
0.25	.200
0.5	.300
1.0	.464
1.5	.626
2.5	.826
4.0	.908
5.5	.927
9.0	.940
24.0	.952
33.0	.956
55.0	.960
97.0	.964
104.0	.965
175.0	.968
242.0	.970
337.6	.972
536.6	.975
720.0	.976
918.6	.977
1200.0	.978
1536.0	.980
1564.0	.980

HG60

t, hours	M_t/M_0
0.017	0.160
0.033	0.229
0.067	0.336
0.133	0.484
0.25	0.693
0.5	0.932
1.0	0.9969
1.5	0.9987
2.5	0.9991
4.5	0.9995
23.5	0.9998
95.75	0.9998
267.25	0.9998

0A30

$\frac{t}{\text{hours}}$	$\frac{M_t}{M_0}$
0.017	0.0073
0.033	0.0114
0.067	0.0163
0.133	0.0263
0.267	0.042
0.50	0.059
0.75	0.073
1.0	0.084
1.5	0.102
2.5	0.126
4.0	0.157
5.5	0.182
7.5	0.210
24.0	0.376
31.5	0.437
96.0	0.865
102.5	0.885
103.0	0.887
144.5	0.936
198.5	0.949
264.3	0.955
319.5	0.958
438.5	0.962
533.5	0.964
672.0	0.967
1033.0	0.971
1372.0	0.974
1561.0	0.974

0C30

$\frac{t}{\text{hours}}$	$\frac{M_t}{M_0}$
0.083	0.0047
0.167	0.0087
0.333	0.015
0.667	0.023
1.0	0.030
2.0	0.048
4.0	0.077
7.0	0.112
23.0	0.241
31.0	0.295
96.0	0.689
103.0	0.715
144.0	0.774
199.0	0.801
267.0	0.819
360.0	0.834
456.0	0.844
696.0	0.861
1272.0	0.882
1613.0	0.889
1942.0	0.894
2380.0	0.900
2886.0	0.905
3507.0	0.910

OE30

$\frac{t}{\text{hours}}$	$\frac{M_t}{M_0}$
0.17	0.133
0.33	0.189
0.67	0.267
1.0	0.321
2.0	0.427
4.0	0.560
8.0	0.710
24.0	0.934
48.0	0.983
79.5	0.989
168.0	0.991
217.0	0.992
271.0	0.992
389.0	0.993

OH30

$\frac{t}{\text{hours}}$	$\frac{M_t}{M_0}$
0.0042	0.023
0.0083	0.040
0.021	0.059
0.033	0.074
0.05	0.091
0.083	0.117
0.117	0.140
0.183	0.176
0.233	0.197
0.35	0.240
0.5	0.280
0.733	0.345
0.983	0.400
1.483	0.484
1.983	0.550
2.983	0.649
3.983	0.721
5.983	0.820
8.983	0.904
23.817	0.987
31.983	0.991
48.233	0.993
56.417	0.993
72.317	0.994
168.05	0.995

OI30

$\frac{t}{\text{hours}}$	$\frac{M_t}{M_0}$
0.017	.013
0.033	.020
0.067	.029
0.117	.040
0.183	.051
0.25	.060
0.5	.088
0.75	.111
1.0	.130
1.5	.162
2.0	.190
2.5	.214
4.0	.277
5.5	.329
8.0	.404
24.0	.706
23.67	.860
48.0	.941
56.17	.956
72.25	.966
98.57	.972
171.8	.978

0B60

$\frac{t}{\text{hours}}$	$\frac{M_t}{M_0}$
0.25	0.687
0.5	0.922
1.0	0.978
2.0	0.984
4.0	0.987
8.0	0.990
24.0	0.992
48.0	0.993
127.0	0.994
168.0	0.995

0C60

$\frac{t}{\text{hours}}$	$\frac{M_t}{M_0}$
0.033	0.041
0.067	0.063
0.133	0.094
0.25	0.136
0.5	0.196
1.0	0.285
1.5	0.352
2.5	0.463
4.0	0.595
5.5	0.708
8.0	0.889
24.0	0.923
32.033	0.933
57.0	0.943
122.0	0.954
176.0	0.958
225.0	0.960
343.917	0.964
480.65	0.967
720.25	0.970
1038.31	0.972
1302.0	0.974
1559.6	0.975
1899.8	0.977
2405.3	0.979

0E60

t (hours)	M_t/M_0
0.083	0.177
0.17	0.260
0.33	0.357
0.67	0.468
1.0	0.548
1.5	0.644
2.5	0.762
4.0	0.878
6.0	0.943
8.0	0.973
23.0	0.994
31.5	0.994
120.0	0.995
169.0	0.995
223.0	0.996
319.0	0.996

0F60

t (hours)	M_t/M_0
0.033	0.393
0.083	0.600
0.17	0.771
0.33	0.923
0.67	0.981
1.0	0.990
1.5	0.992
2.0	0.993
3.0	0.993
4.5	0.994
7.0	0.994
24.0	0.995
48.0	0.994
102.5	0.996
198.5	0.997

0H60

t (hours)	M_t/M_0
0.0055	0.065
0.011	0.104
0.017	0.143
0.025	0.166
0.033	0.198
0.050	0.218
0.067	0.248
0.100	0.305
0.133	0.350
0.167	0.391
0.250	0.476
0.333	0.544
0.50	0.652
0.75	0.770
1.0	0.848
1.5	0.932
2.0	0.969
3.0	0.992
5.0	0.9978
8.0	0.9982
24.0	0.9987
32.0	0.9987
48.0	0.9988
55.97	0.9988
143.7	0.9990
149.6	0.9990

0I60

t (hours)	M_t/M_0
0.017	0.077
0.033	0.110
0.067	0.164
0.117	0.222
0.183	0.283
0.25	0.334
0.5	0.480
0.75	0.598
1.0	0.700
1.5	0.844
2.0	0.927
2.5	0.967
4.0	0.9947
5.75	0.9972
8.0	0.9976
23.88	0.9983
32.08	0.9984
48.17	0.9985
107.7	0.9985

TA60L

$\frac{t}{\text{hours}}$	$\frac{M_t}{M_0}$
0.017	0.014
0.033	0.022
0.067	0.032
0.133	0.046
0.25	0.068
0.5	0.097
1.0	0.131
1.5	0.155
2.5	0.193
4.0	0.228
5.5	0.266
7.0	0.288
24.5	0.488
30.03	0.543
96.33	0.827
103.5	0.841
174.0	0.924
264.5	0.966
433.0	0.978
701.3	0.988
964.7	0.978

TC60L

$\frac{t}{\text{hours}}$	$\frac{M_t}{M_0}$
.017	.0041
.033	.0061
.067	.0086
.133	.015
.25	.027
.5	.044
1.0	.067
1.5	.082
2.5	.104
4.0	.131
5.5	.153
8.0	.181
24.0	.296
32.0	.339
101.0	.563
176.0	.720
269.0	.838
338.0	.876
487.0	.918
704.5	.940
1105.9	.949
1351.6	.949
1535.8	.944
2021.0	.942

TG60

$\frac{t}{\text{hours}}$	$\frac{M_t}{M_0}$
0.017	0.045
0.033	0.073
0.067	0.109
0.133	0.154
0.25	0.208
0.5	0.286
1.017	0.397
1.5	0.475
2.5	0.592
4.0	0.716
5.5	0.793
7.5	0.856
24.0	0.934
31.5	0.946
71.25	0.960
169.0	0.972
748.25	0.984
1536.9	0.997

APPENDIX B

Here we briefly outline the Laplace transform solution to the diffusion problem posed in Section I [Eqs. (22)-(28)].

The Laplace transform of the diffusion Eqs. (22) and (23) [subject to the initial conditions in Eq. (24)] are

$$\frac{d^2\bar{C}}{dx^2} - q^2\bar{C} + C_o/D = 0 \tag{B.1}$$

and

$$\frac{d^2\bar{C}_s}{dx^2} - q_s^2\bar{C}_s = 0 \tag{B.2}$$

where

$$q^2 \equiv p/D \quad \text{and} \quad q_s^2 = p/D_s \tag{B.3}$$

Bars over a variable denote the transform of that variable and p is the transform variable.

Equations (B.1) and (B.2) are ordinary, second-order differential equations whose general solutions are well-known:

$$\bar{C} = a_1 e^{qx} + a_2 e^{-qx} + C_o/p \tag{B.4}$$

$$\bar{C}_s = b_1 e^{q_s x} + b_2 e^{-q_s x} \tag{B.5}$$

where a_1, a_2, b_1, and b_2 are constants of integration. These constants are determined from the transformed boundary conditions, Eqs. (25)-(28):

$$\bar{C}_s(0,p) = K\bar{C}(0,p) \tag{B.6}$$

$$\bar{J}(0,p) = D\frac{d\bar{C}}{dx} = D_s\frac{d\bar{C}_s}{dx} \tag{B.7}$$

$$\left.\frac{d\bar{C}}{dx}\right|_{x\to-\infty} = 0 \tag{B.8}$$

$$p\bar{C}_s(\ell_s,p) = -\frac{2A}{V_s}\bar{J}(0,p) \tag{B.9}$$

Boundary condition (B.8) implies that

$$a_2 = 0 \tag{B.10}$$

The other 3 boundary conditions yield 3 simultaneous linear equations in the 3 unknowns a_1, b_1, and b_2. These equations are easily solved by Cramer's rule.

From (B.4), (B.7) and (B.10), we have

$$\bar{J}(0,p) = (Dp)^{1/2}a_1 \tag{B.11}$$

where

$$-a_1 = \frac{\alpha C_o \cosh(t_s p)^{1/2}}{2(Dp)^{1/2} + \alpha\ell p[\cosh(t_s p)^{1/2} + \mu^{-1}\sinh(t_s p)^{1/2}]} \tag{B.12}$$

Combining (B.11) and (B.12) and using Eq. (I.18) for C_o, we obtain Eq. (I.29).

NBS-114A (REV. 9-78)

U.S. DEPT. OF COMM. BIBLIOGRAPHIC DATA SHEET	1. PUBLICATION OR REPORT NO. NBSIR 80-1999	2. Gov't. Accession No.	3. Recipient's Accession No.

4. TITLE AND SUBTITLE

Models for the Migration of Additives in Polyolefins

5. Publication Date: August 1980

6. Performing Organization Code

7. AUTHOR(S) L. E. Smith, S. S. Chang, F. L. McCrackin, I. C. Sanchez and G. A. Senich

8. Performing Organ. Report No.

9. PERFORMING ORGANIZATION NAME AND ADDRESS

NATIONAL BUREAU OF STANDARDS
DEPARTMENT OF COMMERCE
WASHINGTON, DC 20234

10. Project/Task/Work Unit No.

11. Contract/Grant No.

12. SPONSORING ORGANIZATION NAME AND COMPLETE ADDRESS *(Street, City, State, ZIP)*

Bureau of Foods
Food and Drug Administration
Washington, D.C. 20201

13. Type of Report & Period Covered

14. Sponsoring Agency Code

15. SUPPLEMENTARY NOTES

☐ Document describes a computer program; SF-185, FIPS Software Summary, is attached.

16. ABSTRACT *(A 200-word or less factual summary of most significant information. If document includes a significant bibliography or literature survey, mention it here.)*

In addition to continuing our experimental and theoretical program as previously described during the past quarter we have considered methods of organization and classification which could facilitate the understanding and use of our program outputs. We have also considered a number of specific technical questions that have been raised by FDA staff. Our program has focused initially on the class of polymers best described as polyolefins. These polymers represent the majority of plastics used in packaging applications and we feel that models of migration developed for the principal members of the class will be applicable to most members with only minor modifications. The technical requirement that the polymers be equilibrium fluids rather than glasses can be established by a glass transition temperature well below the use temperature or by evidence of some crystallinity at use temperatures. Using these criteria, a preliminary classification of polymers based on chemical structure has been developed. We have found a formal decision tree to be a useful device to focus attention on the specific technical decisions involved in amking regulatory judgments on indirect additive questions. A simple example of such a decision tree is given. The general form of this tree is, of course, independent of the polymer-migrant system involved but the functional forms used in the calculations of partition coefficients and diffusion constants are specific for the class of polymer involved. The determination of the appropriate functions for decisions is a principal objective of our work along with an assessment of the experimental data and methods needed as inputs.

17. KEY WORDS *(six to twelve entries; alphabetical order; capitalize only the first letter of the first key word unless a proper name; separated by semicolons)*

Additives; diffusion; food additives; indirect additives; migration; models; regulations.

18. AVAILABILITY	19. SECURITY CLASS (THIS REPORT)	21. NO. OF PRINTED PAGES
☒ Unlimited	UNCLASSIFIED	134
☐ For Official Distribution. Do Not Release to NTIS		
☐ Order From Sup. of Doc., U.S. Government Printing Office, Washington, DC 20402, SD Stock No. SN003-003-	20. SECURITY CLASS (THIS PAGE)	22. Price
☒ Order From National Technical Information Service (NTIS), Springfield, VA. 22161	UNCLASSIFIED	$10.00

USCOMM-DC